

UNCLASSIFIED

AD 268 286

*Reproduced
by the*

**ARMED SERVICES TECHNICAL INFORMATION AGENCY
ARLINGTON HALL STATION
ARLINGTON 12, VIRGINIA**



UNCLASSIFIED

NOTICE: When government or other drawings, specifications or other data are used for any purpose other than in connection with a definitely related government procurement operation, the U. S. Government thereby incurs no responsibility, nor any obligation whatsoever; and the fact that the Government may have formulated, furnished, or in any way supplied the said drawings, specifications, or other data is not to be regarded by implication or otherwise as in any manner licensing the holder or any other person or corporation, or conveying any rights or permission to manufacture, use or sell any patented invention that may in any way be related thereto.

268 286

Interim Scientific Report No. 2

Contract AF 33(616)-8262

HEAT DIODE CONVERTER

Period Covered:

August 1, 1961 to October 31, 1961

62-1-5

November 20, 1961

944 500



WESTINGHOUSE RESEARCH LABORATORIES
PITTSBURGH • PENNSYLVANIA

Interim Scientific Report No. 2

Contract AF 33(616)-8262

HEAT DIODE CONVERTER

Period Covered:

August 1, 1961 to October 31, 1961

November 20, 1961

Westinghouse Research Laboratories
Beulah Road, Churchill Borough
Pittsburgh 35, Pennsylvania

Table of Contents

	Page
I. Thermionic Diode Currents in Transverse Magnetic Fields R. J. Zollweg, M. Gottlieb	1
II. Fabrication of Electron Beam Heated Button-Cathode Cell R. J. Zollweg, M. Gottlieb, C. R. Taylor	15
III. The Lifetime and Efficiency of a Thermionic Energy Converter. L. S. Richardson, A. E. Fein, M. Gottlieb, G. A. Kemeny R. J. Zollweg.	21
IV. The Calculation of the Efficiency of Energy Conversion by Thermionic Emission. A. E. Fein, L. S. Richardson	55

Section I

THERMIONIC DIODE CURRENTS IN TRANSVERSE MAGNETIC FIELDS

by

R. J. Zollweg, M. Gottlieb

THERMIONIC DIODE CURRENTS IN TRANSVERSE MAGNETIC FIELDS*

R. J. Zollweg and M. Gottlieb

Introduction

The transport of electrons from cathode to anode of a thermionic diode is impeded by the presence of a transverse magnetic field. If the electron flow is in a vacuum the well-known magnetron effect takes place. In a gas the electron diffusion and mobility are not reduced as greatly by the transverse magnetic field because the scattering of electrons by gas atoms randomizes the direction of electron motion with each collision.

For thermionic power converter diodes it has been recognized that the magnetic field induced by the diode current itself can be sufficient to seriously reduce cell current thus producing a practical upper limit to diode current-carrying capacity. Schock¹ has made extensive calculations on the effects of self-induced magnetic fields for thermionic diode currents in a vacuum. Houston² has made a few measurements in cesium vapor. More extensive and precise data are needed for converter design calculations. When this work was undertaken it also appeared that it might be possible to obtain information about the collision frequency and elastic scattering cross section of electrons in neutral cesium since on the basis of relations derived by Langmuir³ and Cobine⁴, the measurement of cell current in a gas should give a measure

*This work was sponsored by Aeronautical Systems Division, Air Force Systems Command, United States Air Force, in part.

1. A. Schock, J. Appl. Phys. 31, 1978 (1960).
2. V. C. Wilson ARS Space Power Systems Conf., Santa Monica, California, September 27-30, 1960.
3. I. Langmuir, Phys. Rev. 38, 1656 (1931).
4. J. D. Cobine, Gaseous Conductors. McGraw-Hill Book Co., Inc. New York (1941).

of the mobility. Our results, however, show that although the calculated cross sections are of the right order of magnitude, difficulties most likely associated with back diffusion of electrons to the emitter prevent the precise determination of scattering cross sections. Nonetheless the data should be of considerable value in connection with converter design since the combined effects of electron transport and back diffusion in a transverse magnetic field in cesium vapor are not at present calculable from first principles.

An empirical result useful for converter design is obtained as follows:

$$\frac{I_0}{I} = 1 + \frac{4.8 \times 10^{-3} d^{1.7} B^2}{p^{1/2}}$$

where I_0 is the current in the absence of the magnetic field, I with magnetic field, d is emitter-collector spacing in inches, B is magnetic field in gauss and p is Cs pressure in mm Hg.

II. Experimental Technique and Results

Cell current measurements were made with cells of two different structures as shown in Figure 1. Both cells utilized a 0.005 inch by 0.080 inch by 1 inch tungsten ribbon filament heated directly with halfwave rectified A.C. power. The anode in one case consisted of plane parallel copper plates with cathode-anode spacings of 0.020 inches. The anode in the other case was a 0.500 inch diameter stainless steel cylinder which thus had an average cathode-anode spacing of 0.225 inches, about an order of magnitude larger than the first cell. The tubes were mounted in an oven inside a solenoid magnet the field of which could be continually varied up to about 350 gauss.

The circuit shown in Figure 2 was used for the measurements. Cell currents were determined by the voltage drop across a known resistance during the time that the filament voltage was zero, using a calibrated oscilloscope. To reduce the scatter of the data associated with changes in

filament emission a switch was used that simultaneously closed the magnet current circuit and replaced the cell load resistance by an alternative resistance box. Thus the load resistance when the magnetic field was present could be increased to compensate for the reduced cell current. In this way the cell voltage and internal fields remained constant. A Clare Hg-wetted relay synchronously opened the anode lead during the filament heating pulse. A battery was added to the circuit to supply positive potentials to the anode. The required cesium vapor pressure was established by immersing a side tube containing the cesium ampule in a Sn-Pb eutectic bath which could be controlled to within about 1°C . The rest of the envelope was heated to a higher temperature to prevent Cs condensation. The communicating apertures between the diode and the tube envelope were sufficient that estimates of the thermal transpiration effect lead to the conclusion that appreciable pressure differences do not exist between the cathode-anode region and the cesium reservoir over most of the region of interest.

The results of the measurements were found to depend upon filament temperature and cell potential as well as expected dependence upon cesium pressure and magnetic field strength. With the larger spacing cell the results with lower filament temperatures and higher filament temperatures were not far different while intermediate temperatures gave a greater reduction in cell current with magnetic field. Since at the higher temperature used one would expect sufficient ions to be formed by contact ionization at the cathode to neutralize the electron space charge and since the space charge is not as severe a problem at the lowest cathode temperatures where electron emission is smaller, the higher current reductions for intermediate temperatures appear to be associated with additional space charge effects associated with the reduced electron mobility in a magnetic field. In Figure 3 are plotted some of the results for the larger spacing cell. We have plotted data only for the higher emitter temperature (2000°K) where the effects of space charge should be negligible. It should be remembered, however, that the magnetic field greatly decreases the electron mobility

without a comparable decrease in the cesium ion mobility. The ratio of the current in the absence of the magnetic field to that with the magnetic field has been plotted vs. the square of the magnetic field strength for three cesium reservoir temperatures and two cell potentials. Note that the current reductions are somewhat less for higher anode potentials. Included is the curve for the cesium reservoir at room temperature--where electron-cesium atom scattering is negligible. Because of the contact potential difference, the curve obtained with a battery potential of 1.56 volts probably corresponds to approximately a zero field condition between the electrodes.

Figure 4 shows the results for the closer spacing cell. All of the I_0/I vs. B^2 curves in Figure 4 are linear, except the one corresponding to $T_{Cs} = 250^\circ\text{C}$ with a filament temperature of 609°K and +8.8 volts cell potential. Most of the results with this cell were independent of cell potential as shown in Figure 5 until potentials sufficient to cause inelastic scattering and perhaps volume ionization are reached. It is evident that there is considerable variation in the slopes. The decrease in slope with increase in cesium pressure is less than might be expected as discussed in the next section.

In the low magnetic field region where qualitative comparison is possible the results are in reasonable agreement with those of Houston².

III. Interpretation

The calculations of Schock¹ for electron transport perpendicular to the magnetic field in a vacuum grossly overestimate the effect of the magnetic field when cesium vapor is present. One expects the electron transport in this case to be dominated by the relations for the mobility and diffusion in the magnetic field.⁵

$$\mu = \frac{\mu_0}{(1+\omega^2\tau^2)} \quad , \quad D = \frac{D_0}{(1+\omega^2\tau^2)} \quad (1)$$

where μ_0 and D_0 are the values in the absence of the magnetic field, $\omega = \frac{e}{m} B$ and τ is the period between collisions. Equations (1) are

5. W. P. Allis, Handbuch der Physik XXI, 383, Springer-Verlag, Berlin (1956).

strictly valid only if the collision frequency is independent of electron velocity but are also a good approximation in other cases for sufficiently high magnetic fields.

In cases where there is no space charge and only elastic collisions Langmuir³ found that

$$I = \frac{4}{3} I_{\text{sat}} \frac{\lambda}{x} \frac{V_1/V_0}{\ln(1 + V_1/V_0)}$$

where I_{sat} is the saturation current, λ is the electron mfp, x is plate separation, V_1 is cell potential and V_0 is the initial electron energy. Since both the diffusion constant and mobility are proportional to the mean free path one would expect in this case that

$$\frac{I_0}{I} = \frac{\mu_0}{\mu} = 1 + \omega^2 \tau^2 \quad (2)$$

where I_0 , μ_0 are the values without and I , μ in the presence of a transverse magnetic field. The question of space charge limited currents in the presence of a scattering medium has been considered by Cobine⁴ and in greater detail by Shockley and Prim⁷. Where initial velocities can be neglected they obtain

$$I = \frac{9K \epsilon_0 \mu V^2}{8 x^3} \quad (3)$$

for the plane parallel case with electrode spacing x , a result analogous to the Langmuir-Child's Law for the vacuum diode. If Eq. (3) were to

7. W. Shockley and R. C. Prim, Phys. Rev. 90, 753, (1953).

apply then Eq. (2) would also be valid. Eq. (3) does assume that the electron mobility is independent of energy, as has recently been pointed out by Forman⁸ who derives another expression valid for rare gases under certain conditions.

Our measurements shown in Figures 2 and 3 are approximately consistent with a relation of the form $\frac{I_o}{I} = 1 + K B^2$ as expected from Eq. (2). But there is some scatter in the data and some departure from linearity. Furthermore, the slope K of the curve $\frac{I_o}{I}$ vs B^2 , which should be proportional to τ^2 and hence to $\frac{1}{\text{pressure}^2}$, is found not to vary in the proper way with pressure. There is also a dependence on electrode spacing. The most likely source of this discrepancy would appear to be the back diffusion of electrons from the plasma to the electrodes which might reasonably be expected to depend upon pressure, magnetic field and spacing. While, in principle, measurements of this sort might be used with an assumed mobility dependence to determine the back diffusion contribution, it is felt that the results are not sufficiently precise to merit this.

For converter operation the results, of course, are directly applicable. The results in Figures 3 and 4 should give reasonable estimates within perhaps a factor of 2 of the magnitude of the effect. For other spacings and pressures, estimates can be made by use of the empirical result

$$\frac{I_o}{I} = 1 + \frac{4.8 \times 10^{-3} d^{1.7} B^2}{p^{1/2}}$$

where d is the emitter-collector spacing in inches, B is in gauss and p is the pressure in mm Hg. The reduction in cell current should be diminished somewhat at higher ion concentrations because of the larger scattering cross section of Cs^+ compared to neutral Cs.

8. R. Forman, Phys. Rev. 123, 1537 (1961).

A summary of the available data on electron scattering by Cs atoms is shown in Figure 6. The solid curve shows Brode's data. The circles show the results as originally given by Boeckner and Mohler, but in a later paper they indicated that their electron density measurements were in error at the higher pressures and the squares show these results corrected by Phelps⁹ using the results given by Mohler's paper. Steinberg's data was also used to calculate collision frequencies and his values at the two lower Cs pressures are shown here although his electron densities presumably also may be in error. It should be noted that the data of Brode need not necessarily agree with that of Mohler since Mohler's results are for a mobility measurement while Brode's measurements would be sensitive to very small angle scattering. One might expect Brode's results to yield a larger collision frequency than Mohler's contrary to Figure 6.

We wish to thank A. V. Phelps for several discussions.

9. A. V. Phelps, Private communication.



Fig. 1 - Photograph of the cells used for measurements

DWG 623A135

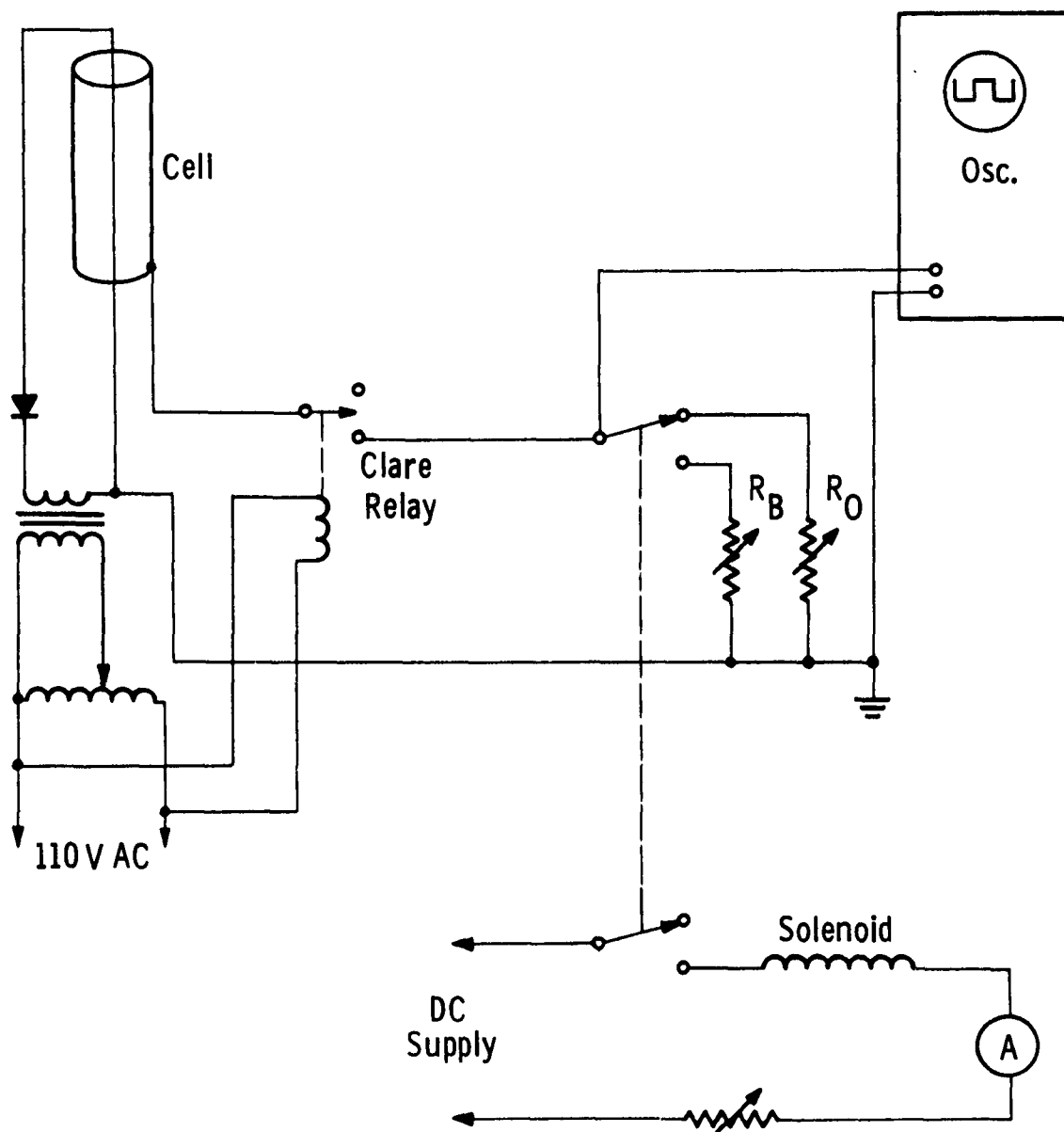


Fig. 2—Circuit for measuring dependence of cell current upon magnetic field strength

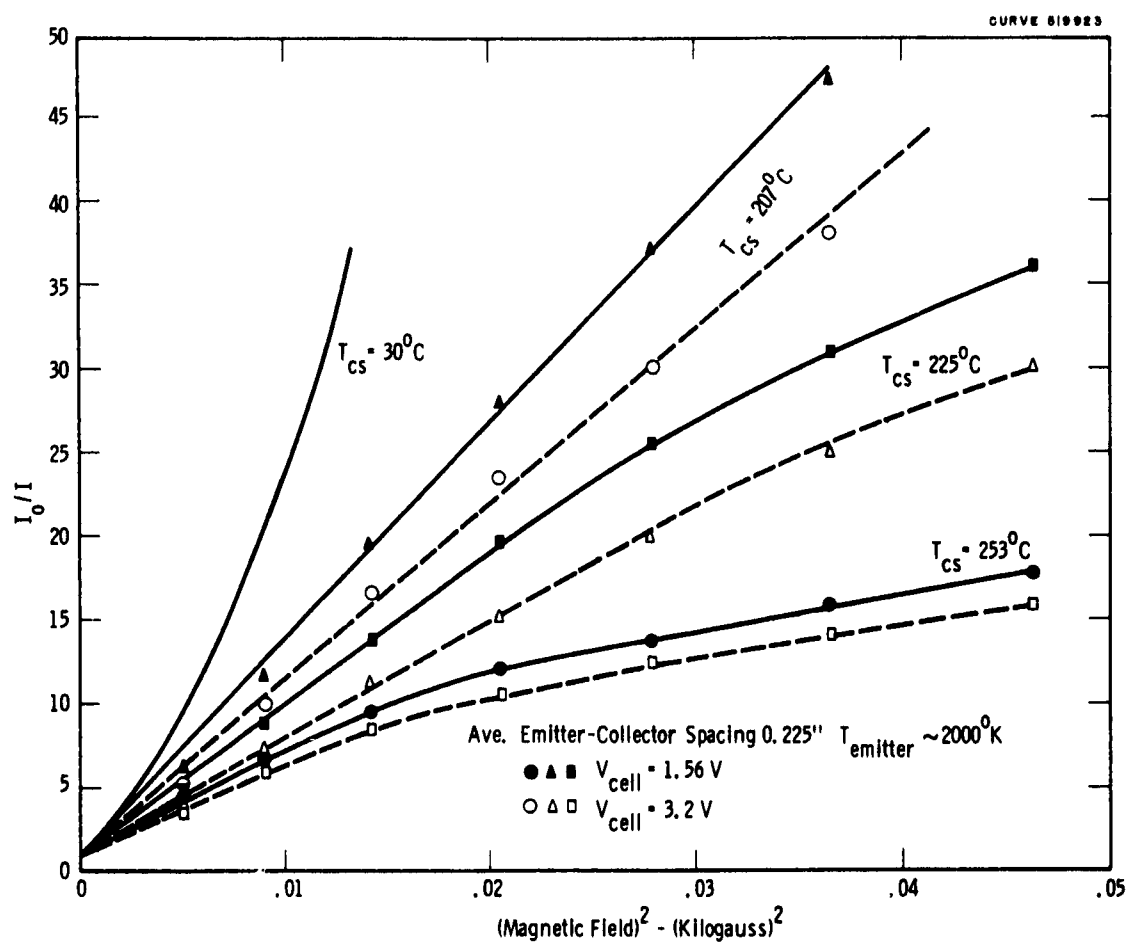


Fig. 3— I_0/I vs. $(\text{Magnetic Field})^2$

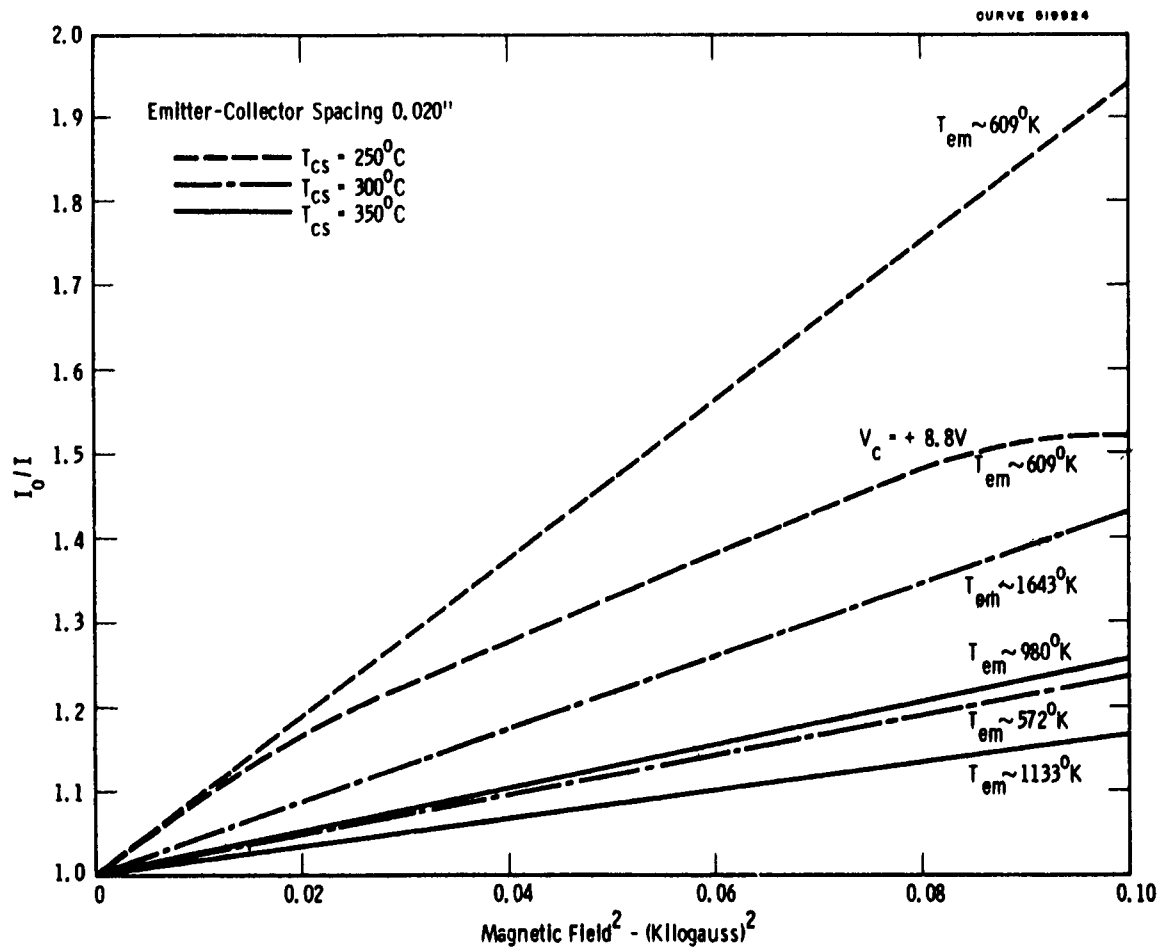


Fig. 4— I_0/I vs. (Magnetic Field)²

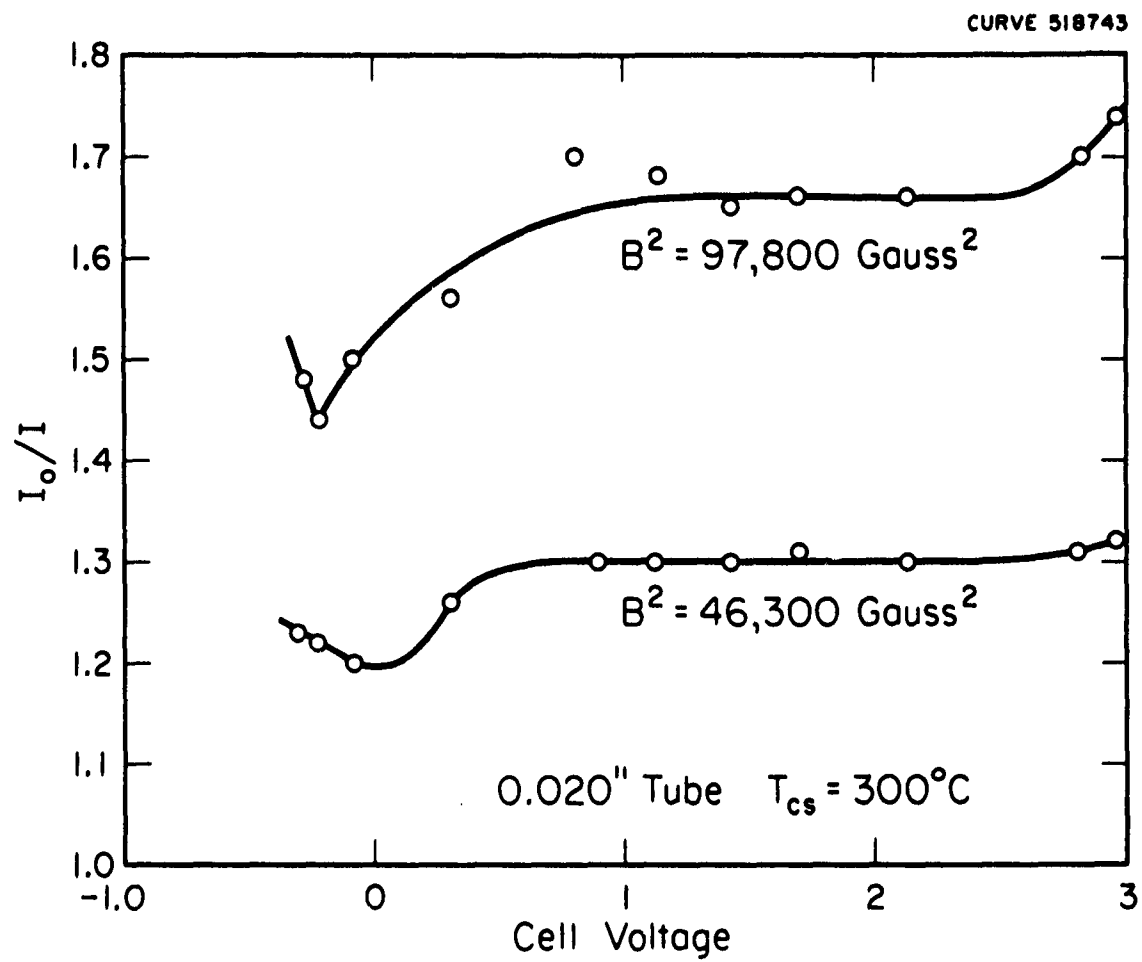


Fig. 5 - Dependence of I_o/I on cell potential V .

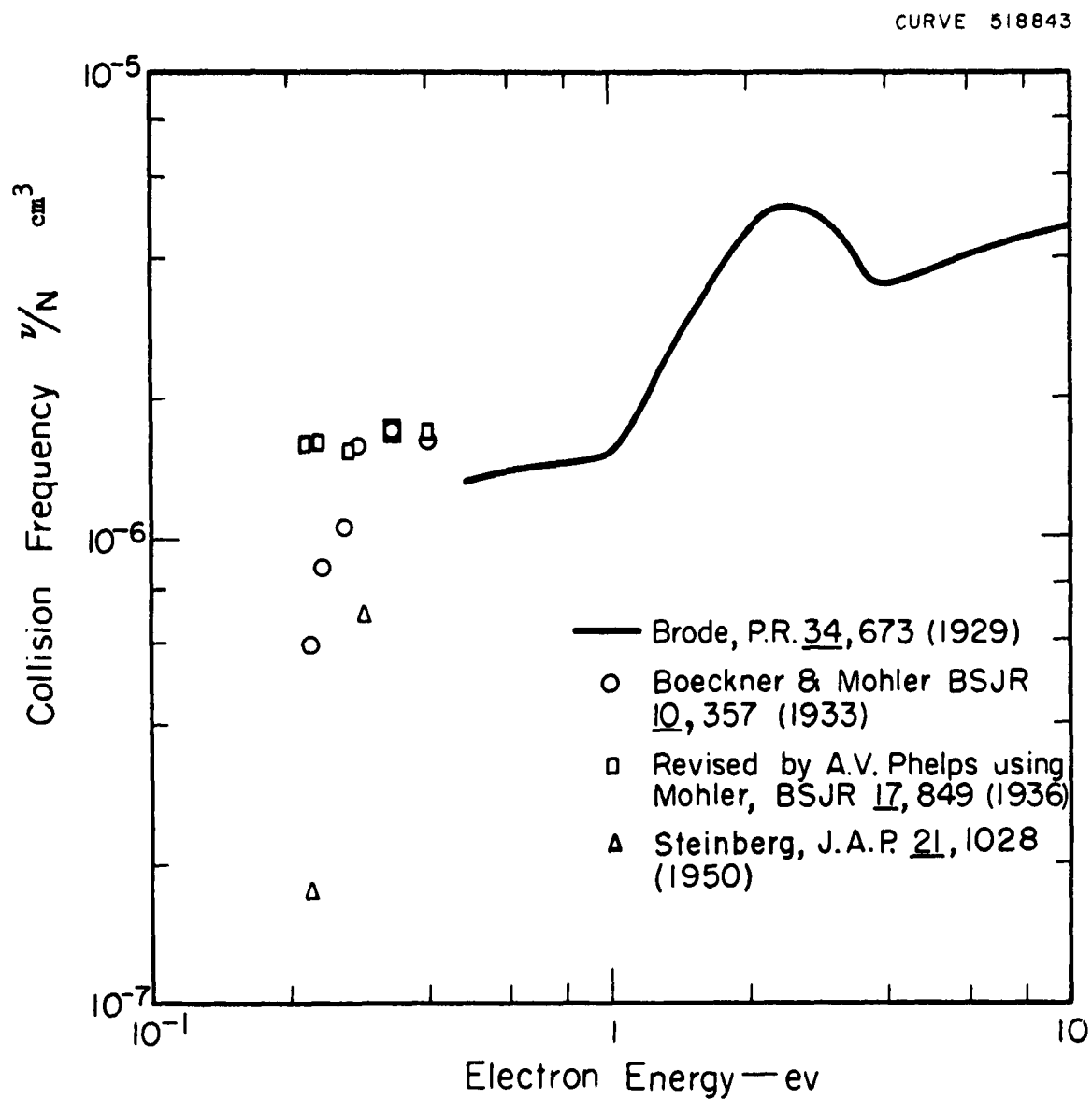


Fig. 6 - Available data on electron scattering in cesium vapor. Collision frequency Cs density per cm^3 is plotted vs. electron energy.

Section II

FABRICATION OF ELECTRON BEAM HEATED BUTTON-CATHODE CELL

by

R. J. Zollweg, M. Gottlieb, C. R. Taylor

FABRICATION OF ELECTRON BEAM HEATED BUTTON-CATHODE CELL

R. J. Zollweg - M. Gottlieb - C. R. Taylor

Fabrication has recently been brought to completion on a cell in which the cathodes are indirectly heated by electron beam bombardment. The assembled cell is shown in the photograph in Figure 1. It is an all metal system which is demountable at two shear gasket seals into three sections. A photograph of the disassembled cell components is shown in Figure 2. The two pieces on the right are joined together in the final braze and form the collector assembly. The section on the left is the electron gun assembly. It will be continuously pumped by an auxiliary vacuum system. The electron gun filament is mounted on two of the high voltage lead throughs, and the other two may be used for a focusing cone for the beam, if necessary. The collector is the bottom surface of the central cylinder of the right hand structure. It is made of stainless steel, but plates of other anode materials may be fastened over it. The collector cylinder is hollow, and a heater may be inserted inside to regulate the temperature of the anode. The position of the anode can be adjusted by means of the flexible bellows, which is driven by the three micrometer screws. The cathode and anode are insulated from each other by the alumina seal above the bellows, and by the ceramic posts attached to the three micrometer screws. The cathode-anode area is viewed through a sapphire window just beneath the bellows. The sapphire disc is brazed to a kovar cylinder with BT

solder using titanium hydride as flux. The cathode temperature and electrode spacing are measured through this window. The cathodes to be used in this cell are in the form of buttons, $1/2$ " in diameter and $1/8$ " thick. These buttons are brazed onto a 0.010" thick tantalum foil. A photograph of the entire cathode assembly is shown in Figure 3. The cathode in the photograph is tungsten, and the braze was accomplished by melting a niobium foil, whose melting temperature is lower than that of either tungsten or tantalum, between the button and the tantalum. The niobium alloys with both metals, and forms a good thermally conducting bond between them. Other brazing techniques may have to be used with other cathode materials. The sealing gasket is the outer, flat edge of the tantalum support foil, which is sufficiently ductile to form a shear seal. Each such seal can then be made only once with one support foil. The cell will be connected to a vacuum system through a Granville-Phillips brakeable valve for processing.

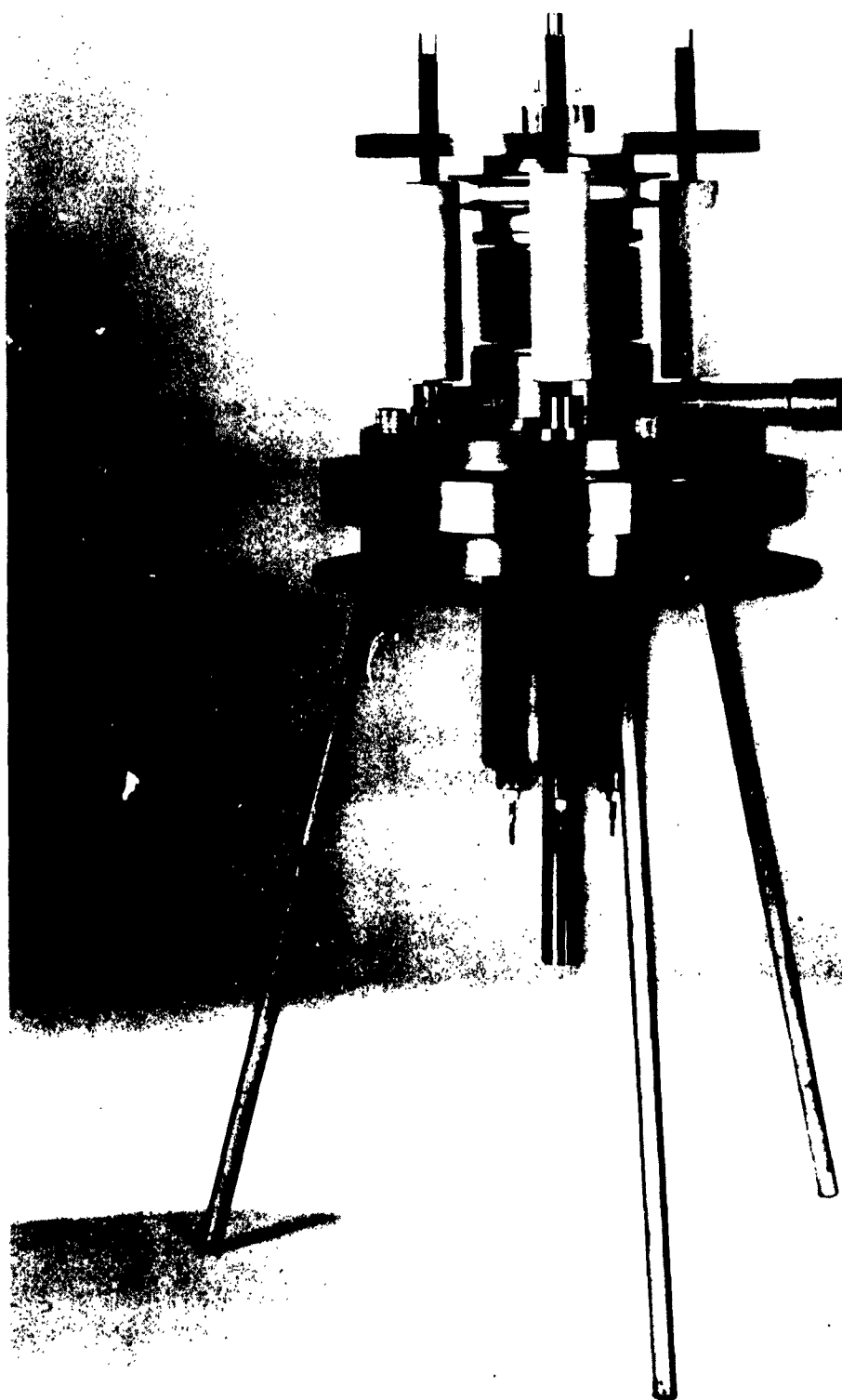


Figure 1: Assembled Electron Beam Heating Cell



Figure 2: Electron Beam Heating Cell Components

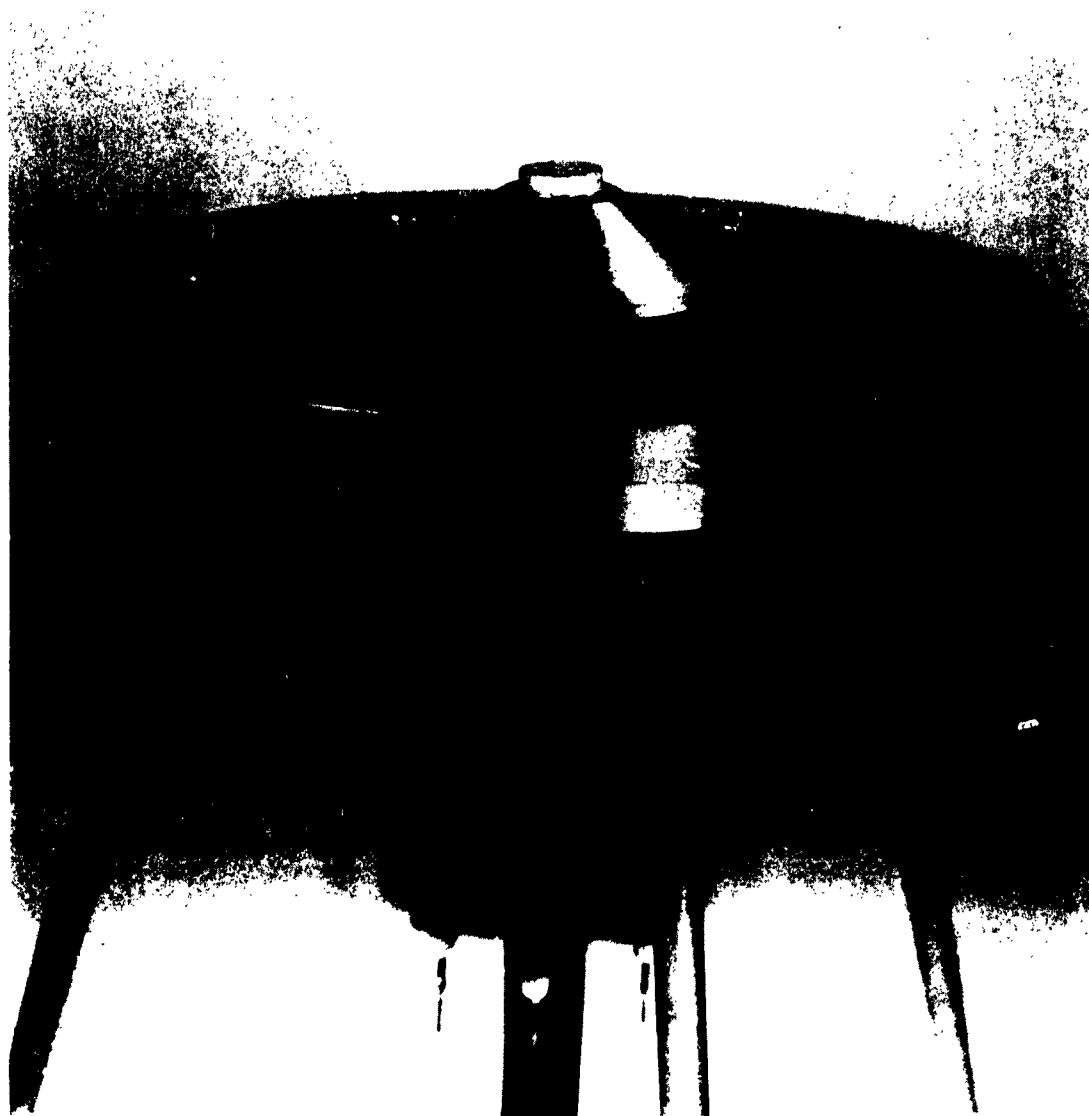


Figure 3: Button Cathode Assembly

Section III

THE LIFETIME AND EFFICIENCY OF A THERMIONIC ENERGY CONVERTER

by

L. S. Richardson, A. E. Fein, M. Gottlieb, G. A. Kemeny, R. J. Zollweg

THE LIFETIME AND EFFICIENCY OF A THERMIONIC ENERGY CONVERTER

L. S. Richardson, A. E. Fein, M. Gottlieb, G. A. Kemeny and R. J. Zollweg

I. Introduction

The design, construction, and operation of all devices are dictated by their required lifetimes. This requirement varies from minutes for a rocket motor to years for a commercial power plant. The mechanisms of failure must be considered in order to predict this lifetime. In a thermionic energy converter, the basic cause of failure is the evaporative transfer of cathode materials. Other causes such as corrosion, mechanical failure, or radiation damage can in most cases be prevented by ingenious design. Evaporative loss, however, is an inherent limitation because of the high operating temperatures required. To predict the lifetime of a thermionic energy converter, only the allowable loss and the rate of evaporative transfer must be known. The allowable loss is determined by the exact mechanism of failure. Whisker formation, changes in the thermal emissivities, and changes in the work functions are examples of such mechanisms, any of which may be caused by evaporation and/or deposition. The rate of evaporative transfer is dependent upon the geometrical configuration, the operating temperatures, the materials of construction, and the internal pressure of the device.

An energy converter must possess a useful energy output as well as a useful lifetime. In order to compare the operation of different

energy converters, some criterion of comparison must be chosen. Some possible criteria are the efficiency, the output power, or the power to weight ratio. Each of these is important in certain applications; for example, a stationary land-based power station is usually an efficient low cost device while a space power plant is usually a light device. In this paper, the efficiency has been taken as the criterion. This choice was made for several reasons: 1) The efficiency is always of interest to the designer regardless of the application of the device. 2) Calculation of the power-to-weight ratio requires a detailed knowledge of the heat source and sink, and is thus dependent upon considerations beyond the scope of this paper. This point will be discussed further in a later section. 3) The output power and other possible criteria are more specifically related to particular applications than is the efficiency.

A number of authors have calculated efficiencies of thermionic energy converters using a number of different approximations.⁽¹⁾ While the efficiency is a function of a large number of variables, in principle most of these variables are determined by a relatively small number of parameters. If the materials of construction and their properties are known, then the efficiency is a function only of the cathode-to-anode spacing, the cathode and anode temperatures, the means of space charge neutralization, and the lead and load resistances. In most converters presently under investigation, cesium vapor is used for space charge neutralization, and frequently also for modification of the cathode and anode work functions, as recently patented by G. R. Feaster.⁽²⁾ In this case, the efficiency is also a function of the cesium pressure. In all but the most recent calculations

of efficiency referred to above, the interrelationships of work functions, emissivities, temperatures, etc., have been largely ignored. Furthermore, few of the calculations have considered variations in load resistance or the presence of back current. None of the calculations have attempted to optimize the values of anode and cesium temperature while simultaneously optimizing lead and load resistance. A recent report (3) summarized a method for this simultaneous optimization.

Both lifetime and efficiency can be shown to be functions of the same design parameters: operating temperatures, internal pressure, materials of construction, and geometrical configurations. For a converter built of a given material and operating in the most efficient manner possible, lifetime can be shown to decrease with increasing efficiency. The balancing of the desires for high efficiency and long lifetime requires the knowledge of how these quantities change as the design parameters are changed. In this paper, a proposed method for calculating these quantities is discussed. The relationship of efficiency and lifetime derivable from these calculations is also presented.

The methods by which lifetime and efficiency can be calculated are described in Sections II and III respectively. The relationship between these two properties is discussed in Section IV.

II. Lifetime

A simple approach is to estimate lifetime by dividing the allowable surface recession by the rate of evaporation into vacuum. Since no measurements of the allowable surface recession have appeared in the literature, a

value of 2.5 microns was used as a conservative estimate. This value, equivalent to about 10^4 layers of atoms, is small compared to the spacing of most converters presently under consideration. In a later section the exact value used will be shown to be unimportant. Figure 1 shows the results of this calculation for molybdenum, columbium, tantalum, and tungsten (4).

Several important effects occur, particularly in the cesium diode, that are neglected in this calculation. The presence of a partial cesium coverage may increase or decrease the rate of loss. The presence of contaminant gases (such as water vapor) in the device may also change the rate of loss. Experimental measurements under very carefully controlled conditions are necessary to determine the magnitudes of these effects. Another effect of considerable importance is the reduction of evaporative transfer caused by back-scattering from the cesium atmosphere present in the anode to cathode gap. The magnitude of this effect can be estimated by a relatively simple method.

A first approximation is to assume that all atoms that strike the cold surface (anode) stick and that the partial coverage of cesium has no effect on the evaporation of atoms from the cathode.

For relatively large spacings, the rate of loss is limited by the rate of diffusion through the cathode-to-anode gap. If the diffusion constant D does not change within the gap, then the flux R of metal transported is

$$R = D \frac{\Delta p}{d} \quad (1)$$

where $\Delta \rho$ is the difference in density of evaporated atoms at the cathode and anode, and d is the width of the cathode-to-anode gap. The evaporative flux R_v at any temperature T is given by

$$R_v = \rho V/4 \quad (2)$$

where ρ is the density and V is the arithmetic average velocity of the evaporating species.⁽⁵⁾ Since the pressure and temperature of evaporated atoms adjacent to the electrodes are nearly equal to those characteristic of the electrodes, $\Delta \rho$ is equal to the difference of densities characteristic of cathode and anode. Since the cathode temperature is considerably higher than the anode temperature, the density at the cathode ρ_c is much greater than that at the anode ρ_a . Thus $\Delta \rho$ is equal to ρ_c and the transport flux is

$$R = \frac{4D}{V} \frac{R_{vc}}{d} \quad (3)$$

where R_{vc} is the normal evaporative flux at the cathode temperature.

The quantity D/V has the dimensions of length and is proportional to the mean free path, λ . Hard sphere calculations (6) show that D/V equals $\lambda/3$.

Thus,

$$R = (4/3)(\lambda/d) R_{vc} \quad (4)$$

The evaporative transport problem is analogous to the neutron scattering problem in a non-absorbing medium, where R_{vc} is analogous to the incoming neutron intensity and R to the intensity transmitted. C. W. Maynard has solved this neutron scattering problem numerically for small spacings (7). Examination of his results between $1/4$ and 4 mean free paths shows that the equation

$$R = R_{vc} / (1 + 3d/4\lambda) \quad (5)$$

fits the results very accurately. For large spacing this expression approaches that of equation 4.

A more general approach is to consider the space as a succession of reflecting and transmitting slabs. The transmission through each of these slabs must have the same functional relationship to thickness as the transmission through the assembly. If the multiple reflections are summed up, assuming isotropic behavior, the functional relationship is

$$f(\sum_1 x_1) = \left(1 + \sum_1 \left(\frac{1-f(x_1)}{f(x_1)} \right) \right)^{-1} \quad (6)$$

where x_1 is the thickness of the i th slab and $f(x_1)$ is the fraction transmitted through a thickness x_1 .

It can easily be shown that the only function which obeys this relationship is

$$f(x) = (1 + ax)^{-1} \quad (7)$$

This implies that $R = \frac{R_{vc}}{1+ad}$ is the general form of the solution to the transport equation. For a sufficiently large d , the constant term can be neglected in comparison with ad , thus reducing the equation to the diffusion case where a is $3/4\lambda$. The scattering approach of Maynard also led to the same value for the constant. Both approaches are based on all collisions being of the hard sphere variety. Thus equation 5 is the general solution for transport where the factor $3/4$ will be different if the collisions do not obey the hard sphere model.

An experimental verification of equation 5 was attempted. A diode was constructed using a molybdenum cathode and a nickel anode. A schematic diagram of this cell is shown in Figure 2. Four different anode to cathode spacings were used. The cathode was held at a fixed temperature for a measured length of time, after which the nickel anodes were analyzed for total molybdenum content. The spectrographic analysis had a sensitivity of about 2 micrograms of molybdenum. The reproducibility of analysis was estimated to be about 15% of the analyzed value. Table I summarizes the results of the first test of this cell. The ratio of the fluxes R_{vc}/R is clearly the same as the ratio of the amounts, G_v/G .

If these data are plotted as a function of spacing (Figure 3) equation 5 can be used to calculate values of the mean free path. The mean free path deduced is about 8.6 microns at a cesium pressure of 1 mm of Hg.

No other measurement of mean free path under these non-isothermal conditions was found in the literature. Theoretical estimates assuming isothermal conditions were 0.9 to 20 times the experimental value, depending on the assumptions made.

Since the mean free path is inversely proportional to the pressure and is not a sensitive function of the temperatures, the following relationship was assumed to hold true for the transport flux

$$R = (1 + 0.087 \text{ pd})^{-1} R_{vc} \quad (8)$$

for the pressure p in mm of Hg and the spacing d in microns. The value of 0.087 is based upon only one series of experiments and should be accepted only with considerable reservation.

From equation 8, it is possible to determine lifetime as a function of cathode temperature, spacing, and cesium bath temperature. The relative lifetime, defined as the ratio of the lifetime in a gas filled diode to the lifetime in vacuum, is equal to R_{vc}/R . In Figure 4 the relative lifetime is plotted as a function of spacing and cesium bath temperature which determines the pressure. Better determinations of the mean free path as a function of pressure may change the values shown in this figure, but the general validity of the figure should not be affected. The lifetime will obviously increase with increasing cesium pressure and spacing.

Table I - Experimental Determination of Molybdenum Transport

<u>Spacing d (microns)</u>	<u>Amount Transported G(μg)</u>
155	19
226	12
450	6.2
450	2.6

Temperature = 2100°K

Time = 49,200 seconds Area of Cell = 0.2 cm²

Evaporation in Vacuum, $G_v = 250 \mu\text{g}$ (Reference 4)

Cesium Temperature, 552°K

Cesium Pressure, 1.0 mm of Hg

III. Efficiency

The basic equation used for the calculation of the efficiency, η , of a thermionic diode is

$$\eta = \frac{J V_o}{W + H_c - H_a + K \Delta T - Q_J + X} \quad (9)$$

where J is the net current density, V_o is the output voltage (internal voltage minus the potential drops in leads and plasma), W is the net thermal radiation to the anode, $H_c - H_a$ is the net energy carried by the electrons from the cathode to the anode, $K \Delta T$ is the heat lost by conduction through leads and plasma, Q_J is that part of the Joule heating in leads and plasma that returns to the cathode, and X is the support losses. Minor terms, such as thermoelectric effects, have been neglected. Space charge is assumed to be neutralized, either intrinsically by cesium ionized by the cathode or by some other means.

This expression can be optimized with respect to both lead resistance and load resistance. If this is done, the values of efficiency are functions of the materials of construction and only 4 parameters - the cathode temperature, the anode temperature, the anode-to-cathode spacing, and the cesium bath temperature. A complete description of the optimization procedure is presented elsewhere.⁽³⁾ In this calculation, several effects ignored by most other authors are considered and shown to be significant. In particular, the effect of back current, thermal conduction through the plasma, and electrical resistivity of the plasma have been calculated. The effects of varying the load resistance upon the behavior of both the forward and back currents have also been included.

The diode analyzed for this paper consists of two plane parallel tungsten electrodes separated by a gap filled with cesium vapor. The pressure of the cesium vapor is determined by the temperature of the cesium reservoirs. The temperatures of the cathode and anode were considered fixed by means of temperature reservoirs and are taken as independent parameters of the device. The thermal emissivities of the cathode and anode were assumed to be unaffected by cesium coverage and were taken to be functions of the temperature of the respective surfaces as given in the literature.⁽⁸⁾ The work functions of the cathode and anode were determined by the work of Taylor and Langmuir as functions of the appropriate surface temperature and the plasma pressure.⁽⁹⁾ For this computation, it was necessary to fit the data of Taylor and Langmuir empirically and extrapolate to the values required. In Figure 5 are shown curves of work function versus surface temperature for several cesium bath temperatures as calculated from this empirical formula. These curves agreed very well with the work of Taylor and Langmuir within the range of their measurements. The values of plasma thermal conductivity and plasma resistance as functions of cesium bath temperature were taken from the experiments of Gottlieb and Zollweg.⁽¹⁰⁾

These calculations were carried out on a high speed digital computer for more than 5000 different combinations of spacing, and cathode, anode, and cesium bath temperatures. At the values of lead and load resistance which yielded the maximum efficiency for each of the given combination of parameters, some forty different properties, such as power delivered to load, external voltage, net current, etc., were tabulated in addition to the efficiency.

Some sample curves of efficiency are given in Figs. 6-9. These were drawn by holding two of the four parameters constant and plotting curves

of constant efficiency as a function of the remaining two. These curves represent the efficiency of a diode which has been optimized with respect to both lead and load resistances. In Figure 6, the cathode temperature and spacing have been fixed and the efficiency has a maximum occurring at a unique combination of cesium and anode temperatures. This maximum is a general occurrence for all of the possible combinations of spacing and cathode temperature, although its precise location will depend upon the particular values of spacing and cathode temperature considered. It should be mentioned that these maxima may only be local and that higher efficiencies may be obtainable at lower anode temperatures. However, anode temperatures less than 600°K were not considered to be reasonable from a design standpoint. A complete set of such curves have been presented elsewhere.⁽³⁾ Figures 7 and 8 are drawn similarly to Figure 6 except the temperature fixed was that of the cesium bath or anode, respectively. Curves of the latter two types do not display a maximum of efficiency since higher efficiencies can always be obtained by going to a sufficiently higher cathode temperature.

In Figure 9, the anode and cesium temperatures have been held constant and curves of constant efficiency have been drawn as a function of the spacing and cathode temperature. For a fixed value of cathode temperature, it can be shown that an optimum value of spacing exists. However, these spacings are extremely small (less than 2.5 microns) and not realizable. Therefore, for spacings larger than this, it can be seen that efficiency decreases with increasing spacing.

A summary of the maxima obtainable from plots of the type of Figure 6 is shown in Figures 10 and 11. In these figures are shown three

sets of curves as functions of cathode temperature - maximum attainable efficiency and the anode and cesium bath temperatures necessary to attain that efficiency. Each set consists of five curves corresponding to five different spacings. There are several important features of these curves which should be noted. There is, for a fixed spacing, a wide range of cathode temperatures in which the ultimate efficiency is relatively independent of cathode temperature. Thus, a small improvement in the temperature capability of most existing materials does not produce a large improvement in efficiency of operation. Further, the anode temperature required for maximum efficiency is seen to be within the range 900°K to 1100°K regardless of the cathode temperature or spacing.

It should be emphasized at this point that the numerical results presented in the figures and in the above discussion refer to a device with tungsten anode and cathode. For other materials, the numerical values might change considerably, but it is believed that the qualitative nature of the results should be the same.

It must also be recalled that these calculations are based on the assumption that space charge has been eliminated. Since there is a minimum cesium temperature at which this is true, certain areas of the curves presented (particularly at the lower cesium temperatures) are inaccurate. Fortunately, from the limited data available in the literature, the optimum operating points do not appear to be in this excluded area.

IV. Relationship of Efficiency and Lifetime

With the aid of the calculations and experiments in Parts II and III, it is possible to determine efficiency and lifetime as functions of

only four parameters -- cathode, anode, and cesium bath temperatures and the cathode-anode spacing. If this determination be made, then for a fixed spacing, a maximum efficiency can be found for a given minimum evaporative lifetime. The measurement of mean free path summarized in a previous section were made using a molybdenum cathode. The relative lifetimes deduced from this value should not be seriously different for tungsten, since both atomic diameter and chemical behavior are very similar. A curve of maximum efficiency as a function of the evaporative lifetime for tungsten is shown in Figure 12 for a 125 micron spacing diode. Similar curves can be drawn for other spacings. This efficiency has been simultaneously maximized with respect to anode, cathode, and cesium temperatures for a fixed lifetime. In principle, this procedure could be continued to determine an optimum value of spacing. However, impracticably small values of spacing result.

The extremely large values of lifetime for tungsten shown in Fig. 12 are clearly of no practical significance. However, for materials of higher vapor pressure than tungsten, an analogous curve would be useful. In particular, if the electron emission properties of molybdenum in the presence of cesium were the same as those of tungsten, then the lifetime scale would be shifted as indicated in Fig. 12. It is clear that under these conditions, a required lifetime of 1 year or greater will result in an efficiency less than 20% for molybdenum. It must be recalled that this statement is based on the allowable surface recession being 2.5 microns. However, the efficiency in the region of interest for molybdenum is not a sensitive function of lifetime. Allowing 10 times the recession used here does not markedly increase the possible efficiency.

If accurate emission data were available, calculations of the type discussed here could be carried out for other materials. Similarly, lifetime calculations could be carried out if measurements of mean free path for other materials were available. While experimental investigations of these data are presently being made by various laboratories, little information is available in the literature.

V. Power to Weight Ratio

As mentioned in Section I, it may often be more desirable to design a system with a maximum value of the ratio of output power to system weight in lieu of maximum efficiency. This is an extremely difficult problem to solve in general since the weight of the diode itself is negligible, and the weight of the system is the dominant factor. Thus, the construction of the system must be known in great detail. For example, in the case of a reactor-powered thermionic converter, a reactor core, shield, assembly, reflector, and radiator would have to be designed for each choice of spacing and cathode, anode, and cesium temperatures in order to determine the weight of the system.

It is possible, however, to say a few things in a semi-quantitative way about the problem. Consider the radiator, which is responsible for a large part of the weight of a space power system. Let P_o be the power output, P_i the input power, η the efficiency of conversion, and T_a the anode temperature. Then by definition of η

$$P_o = \eta P_i \quad (10)$$

The amount of power, P_w , which the radiator must dump as waste heats is given by

$$P_w = P_i - P_o = (1-\eta)P_i \quad (11)$$

If the waste heat is radiated

$$P_w = C_1 A T_a^4 \quad (12)$$

where A is the surface area of the radiator and C_1 is some numerical constant. Further, if the weight W_r of the radiator is proportional to its area,

$$W_r = C_2 A \quad (13)$$

When combined, the above equations yield for the ratio of output power to radiator weight

$$P_o/W_r = (C_1/C_2)(\frac{\eta}{1-\eta}) T_a^4 \quad (14)$$

The quantity $\eta(1-\eta)^{-1}$ is a monotonically increasing function of η so that for fixed anode temperature, maximizing the efficiency will maximize P_o/W_r as well. However, in many cases, the anode temperatures cannot be considered fixed. A procedure similar to that used in the preceding section can be followed using the maximum power-to-weight ratio, instead of

efficiency as the criterion. The results are very similar to those of Section III in that higher cathode temperatures result in higher power-to-weight ratios. Figure 13 shows the results of optimizing P_o/W_r for a 5 mil spacing tungsten diode.

A comparison of the results using the two different criteria, efficiency (Fig. 10) and power-to-weight ratio (Fig. 13), shows that a significant decrease in efficiency is the price that must be paid for the maximum power-to-weight ratio. This is particularly true in the region between 1600 and 2200°K cathode temperatures where the optimum efficiency (Fig. 10) does not vary rapidly with temperature.

In Figure 13 the relative values of the power-to-weight ratio and the optimum anode temperatures are also plotted. The peak in anode temperatures near a cathode temperature of 2500°K is almost certainly a local maximum, since the power-to-weight ratio can obviously be increased by going to infinite anode temperatures, using a "slightly larger" value of cathode temperature.

VI. Conclusions

When for a fixed spacing and cathode temperature all other parameters are optimized using efficiency as the criterion, the resulting optimum efficiency is a relatively insensitive function of the cathode temperature in the temperature range 1600 to 2200°K. Clearly, a small improvement in temperature capability will not result in a significant improvement in efficiency. Only a large increase in operating temperature provides a marked improvement. In order to operate a thermionic converter of the type discussed here at 25% efficiency, a cathode temperature above 2200°K is necessary. Only tungsten is capable of a reasonable lifetime at this temperature.

A thermionic converter using tungsten electrodes operating with a cathode temperature of 1600 to 2200°K would have an efficiency between 15 and 20% and an indefinite lifetime. If the emission characteristics of molybdenum are similar to those of tungsten a molybdenum diode could be constructed with a lifetime greater than one year at an efficiency less than 20%.

The introduction of cesium into a thermionic energy converter has two opposing effects upon the efficiency. Thermal and electrical losses occur in the cesium, while the reduction of cathode and anode work functions allows more efficient operation. As the pressure of cesium is increased from zero, the efficiency is increased reaching a maximum. Above this critical value of cesium pressure, the efficiency decreases because of the increasing electrical and thermal losses in the plasma. The attainment of maximum efficiency depends critically upon establishing the optimum cesium pressure. The use of a cathode material possessing a larger affinity for cesium would make possible lower cesium pressure to obtain a given work function. The plasma losses would then be lower. The net result would be a higher efficiency of operation. In short, the use of a cathode material of higher affinity for cesium will result in increased efficiency. It can be shown that the converse is also true. Thus, consideration of the cesium affinity is of considerable importance in the selection of a cathode material.

From examination of the operating characteristics of thermionic converters (such as Figure 6) it is seen that efficiency is a relatively insensitive function of anode and cathode temperature and of spacing. The cesium pressure, on the other hand, is quite a critical parameter and should

be controlled very closely. The lead and load resistances are also critical parameters.⁽³⁾ Operation away from these critical values can decrease the efficiency by a sizeable fraction. These relationships should be carefully considered in the design of thermionic converters.

The evaporative lifetime of a thermionic converter can be increased by increasing the spacing and the cesium pressure. While the data presented here are only preliminary, the lifetime of a cesium filled diode will probably be at least 10 times that estimated by the use of evaporation rates into vacuum.

The data necessary for calculations of the type described are extremely scarce and relatively unreliable. The obtaining of more extensive and more accurate information would allow the design of thermionic converters to be made in a relatively routine fashion. For tungsten such a design has been made and the device is presently being built.

The calculations of efficiency have been checked against the results of the few experimental devices available in the literature. Where sufficient information is given to allow comparison, the agreement has been quite reasonable. While the calculations are not to be considered as the exact theoretical results, the values are probably quite close to reality. While the model of plasma is not entirely realistic and the effect of space charge has been largely ignored, the errors introduced are small in the regions of interest. Devices of 35% efficiency are clearly impractical, while a 20% efficient device can probably be built with present techniques and materials.

Acknowledgements

Some of the work described herein has been performed under Air Force Contract AF33(616)-8292.

References

1. N. S. Rasor, J. Appl. Phys., 31, p. 163 (1960);
J. M. Houston, J. Appl. Phys. 30, p. 481 (1959);
J. H. Ingold, J. Appl. Phys. 32, p. 769 (1961);
A. Schock, J. Appl. Phys. 32, p. 1564 (1961)
G. N. Hatsopolous and J. Kaye, Proc. I.R.E. 46, p. 1574 (1958).
2. U. S. Patent No. 2,980,819 issued to G. R. Feaster, April 18, 1961.
3. L. S. Richardson and A. E. Fein, Interim Scientific Report No. 2,
on AF33(616)-8292.
4. J. W. Edwards, H. L. Johnston, and P. E. Blackburn, J. Am. Chem. Soc.
74, p. 1539 (1952).
R. Speiser, P. E. Blackburn, and H. L. Johnston, J. Electrochem. Soc.
106, p. 52 (1959).
J. W. Edwards, H. L. Johnston, and P. E. Blackburn, J. Am. Chem. Soc. 73,
p. 172 (1951).
O. Kubaschewski and E. L. Evans, "Metallurgical Thermochemistry", Pergamon
Press, 1958, p. 335.
5. S. Dushman, "Vacuum Technique", Wiley, 1949, p. 17.
6. Ibid, p. 74
7. C. W. Maynard, Nuclear Sci. and Eng. 6, p. 174 (1959).
8. W. E. Forsythe and E. M. Watson, J. Opt. Soc. of Amer., 24, p. 114 (1934).
9. J. B. Taylor and I. Langmuir, Phys. Rev. 44, p. 423 (1933).
10. Unpublished Research, M. Gottlieb and R. Zollweg.

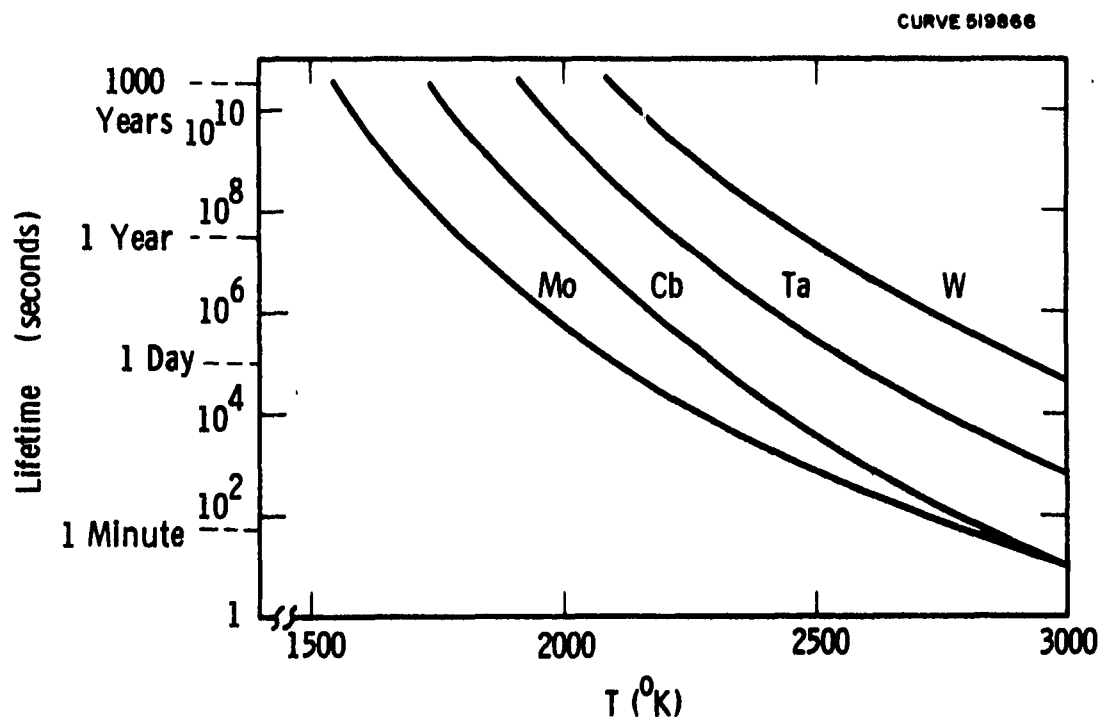


Fig. 1—Time to lose 2.5 microns by evaporation from molybdenum, columbium, tantalum, and tungsten as a function of temperature.

DWG 623A068

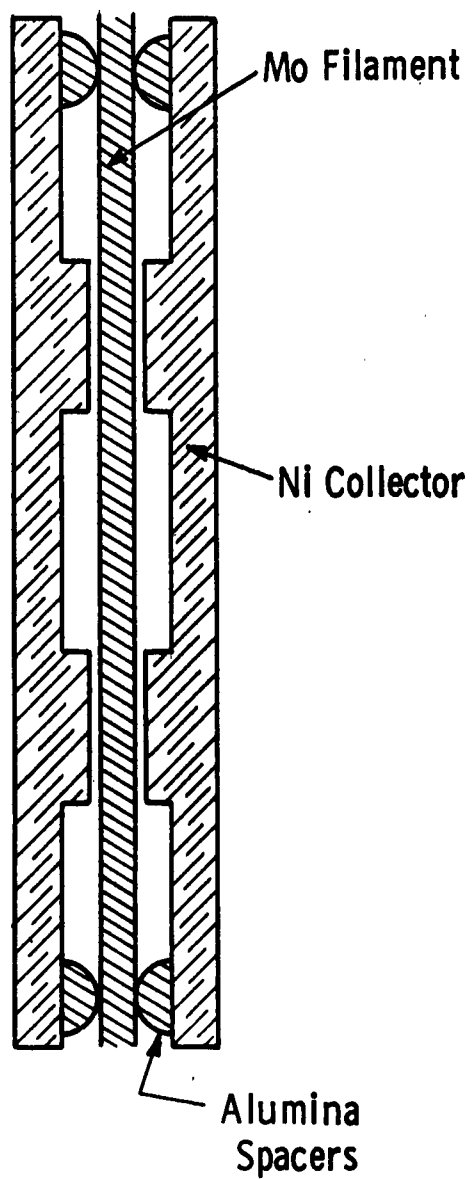


Fig. 2—Schematic diagram of cell for determination of evaporative transport.

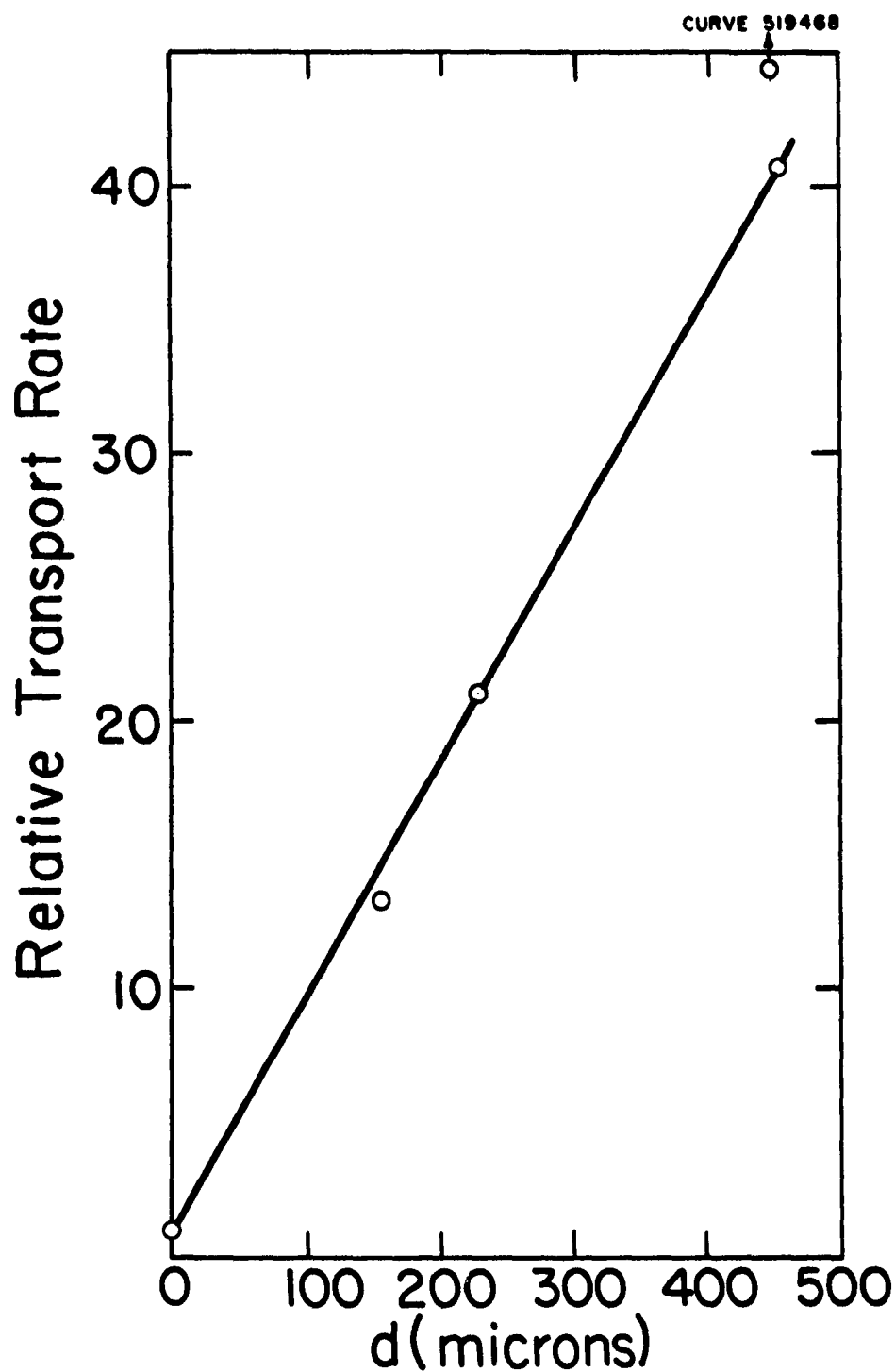


Fig.3 -The relative transport rate as a function of spacing.

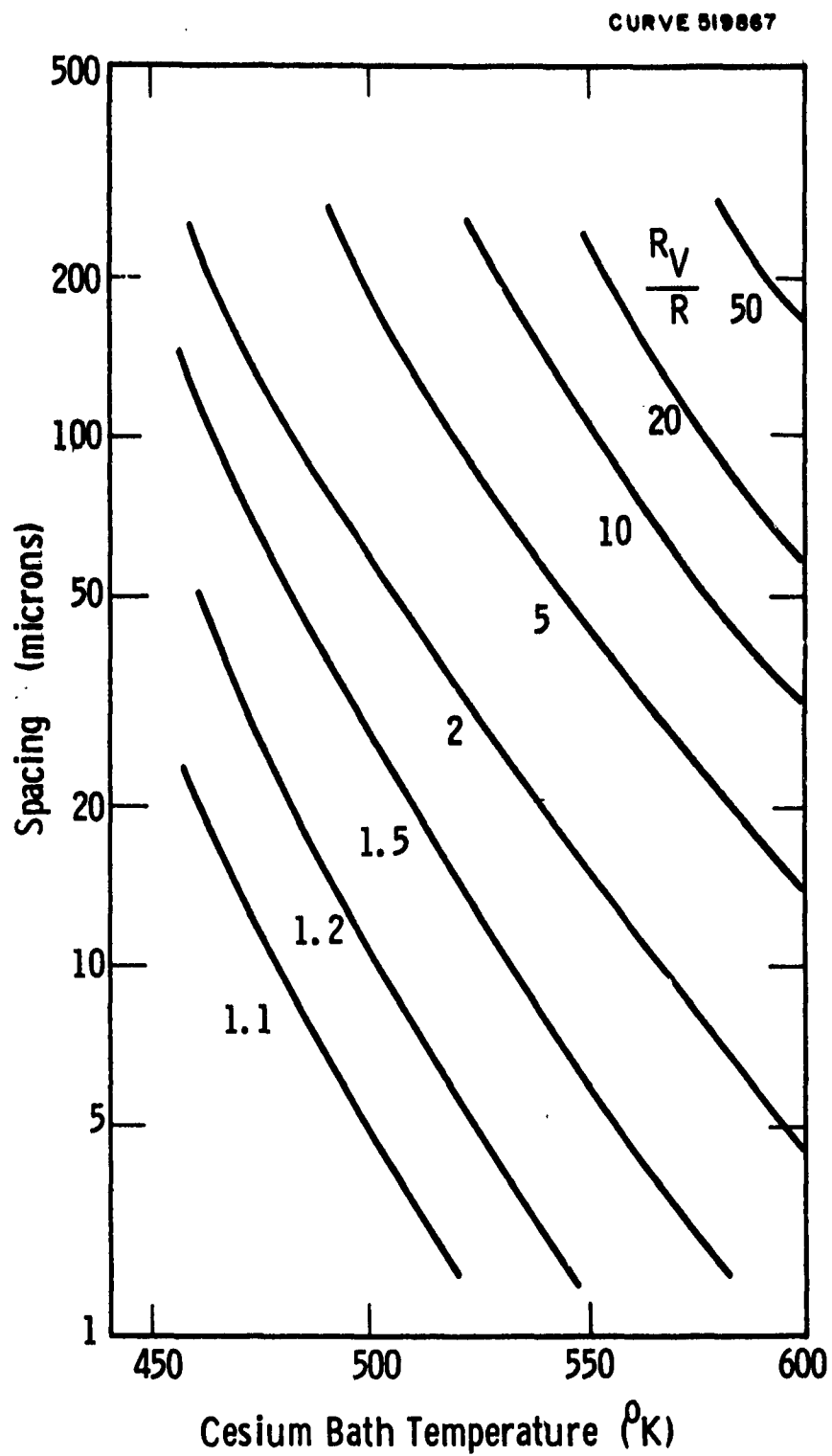


Fig. 4—Relative lifetime of a cathode as a function of cesium bath temperature and spacing.

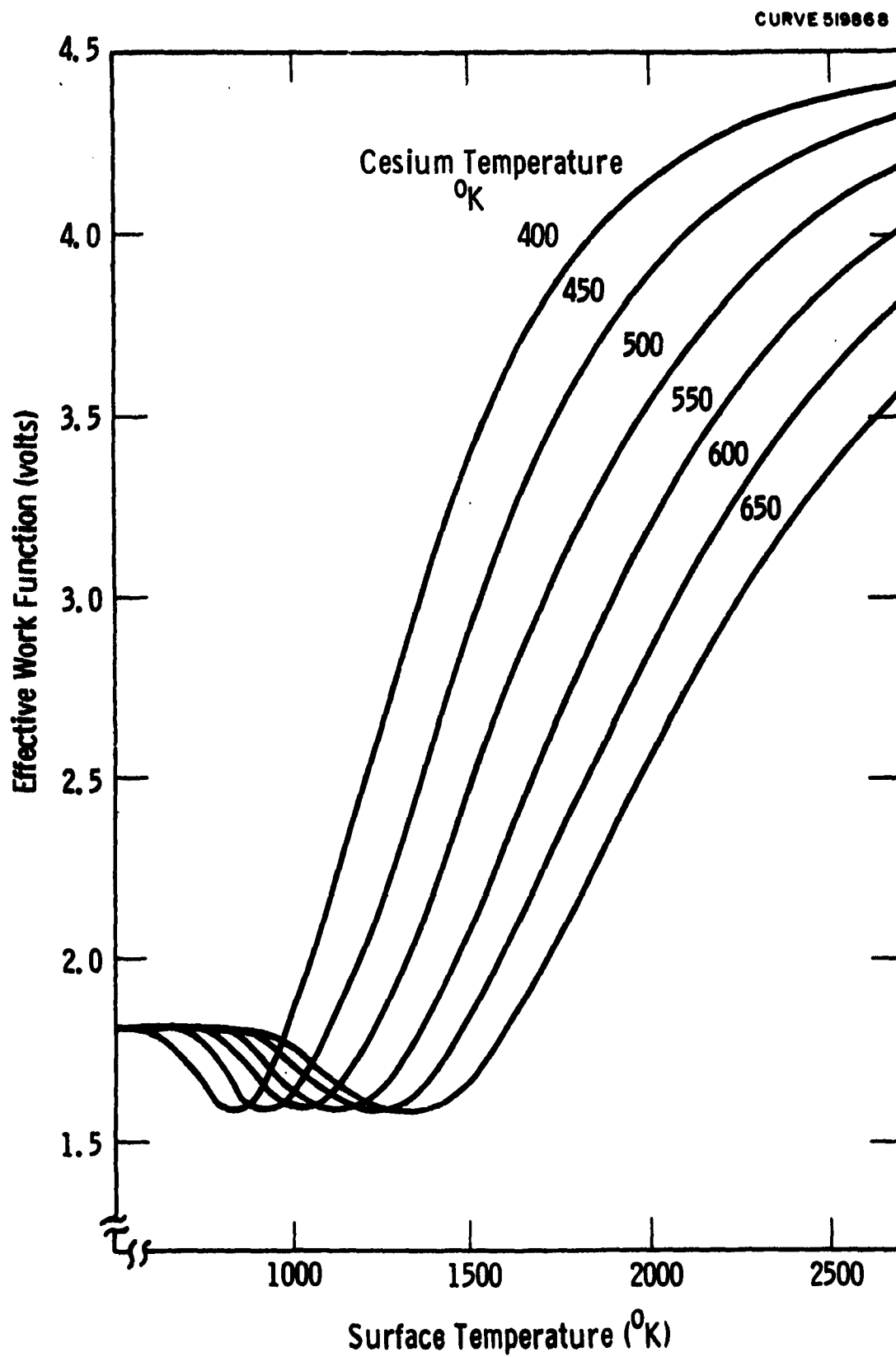


Fig. 5—Work function as a function of cesium bath temperature and surface temperature.

CURVE 519549

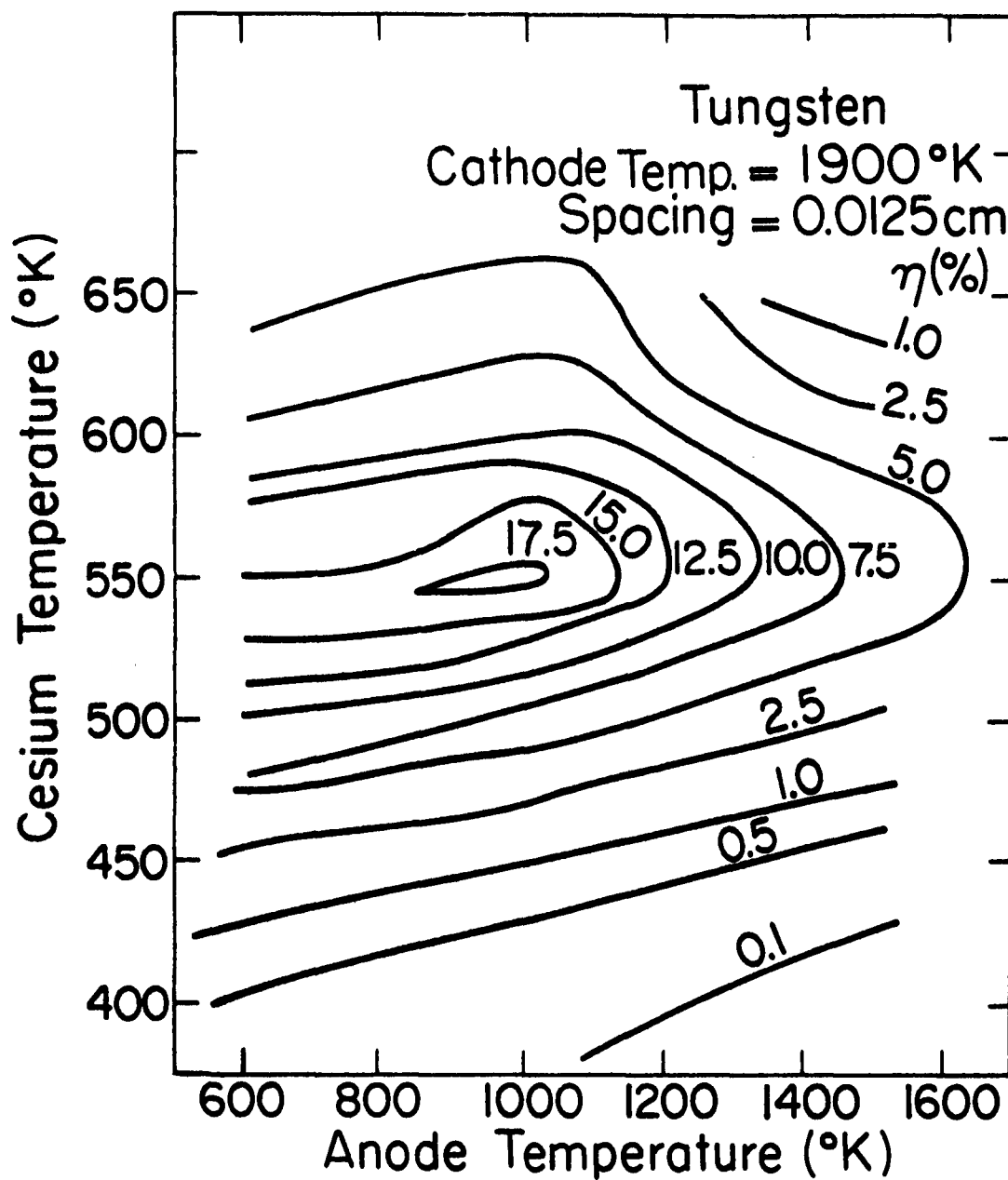


Fig.6-Efficiency as a function of anode and cesium bath temperatures.

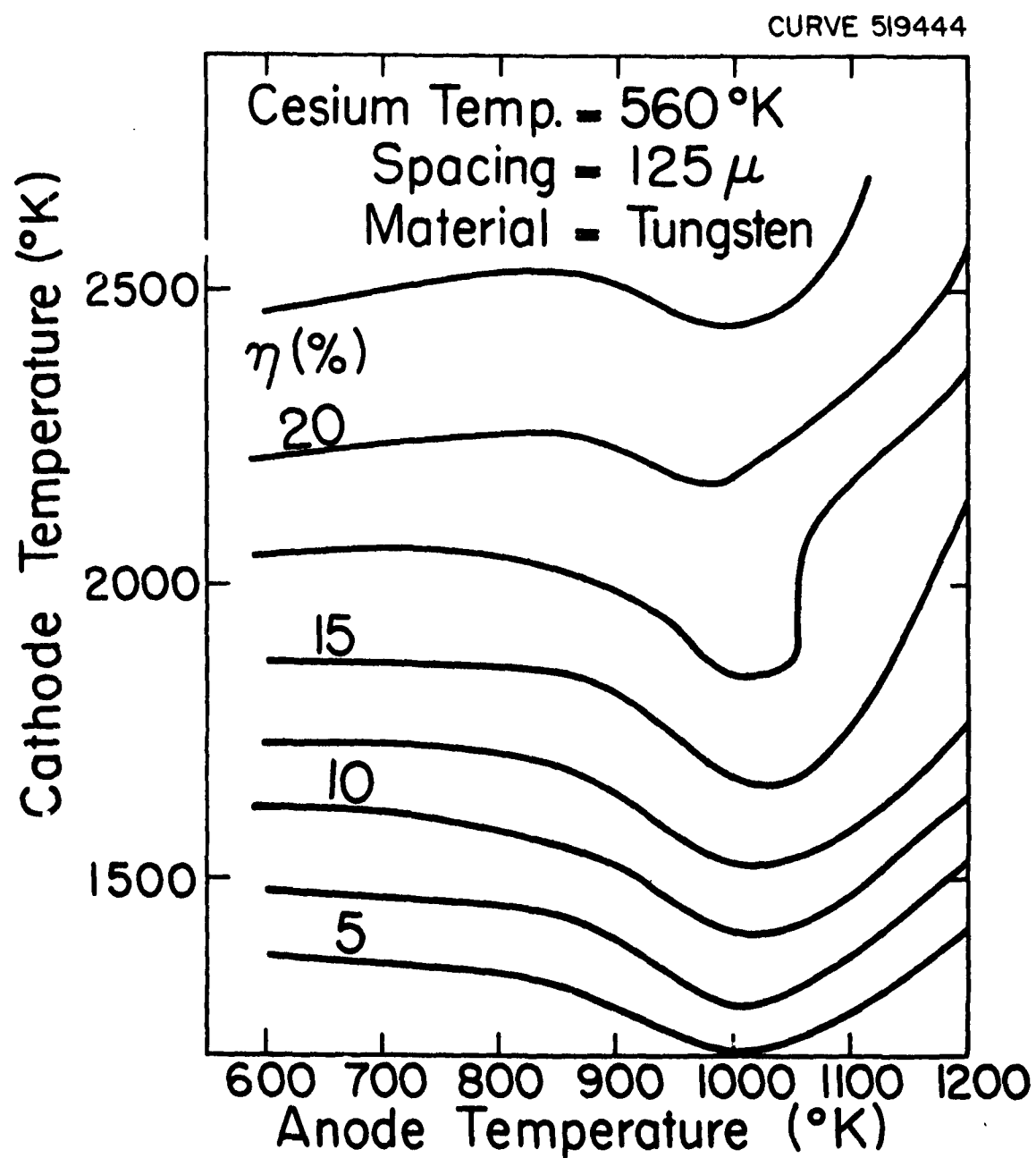


Fig.7-Efficiency as a function of cathode and anode temperatures.

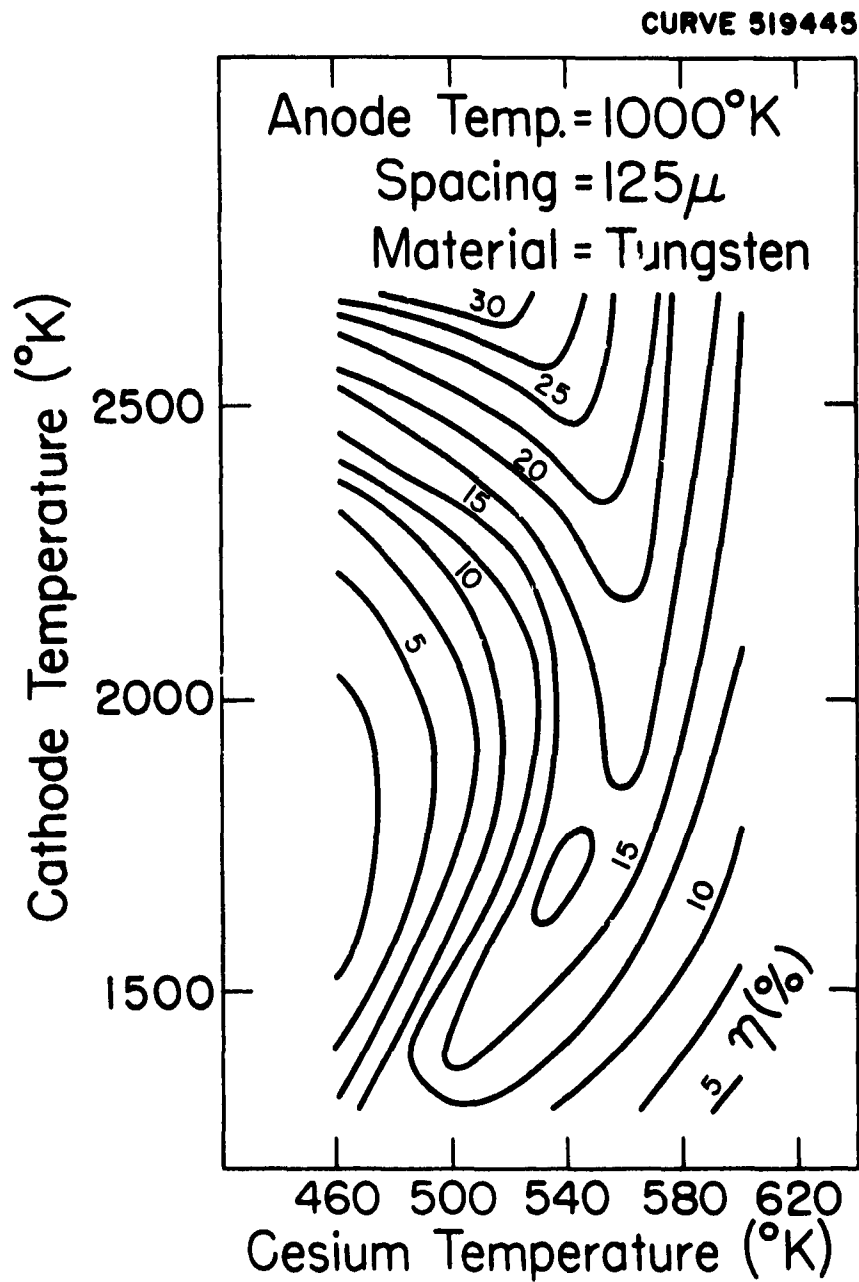


Fig.8 - Efficiency as a function of cathode and cesium temperatures

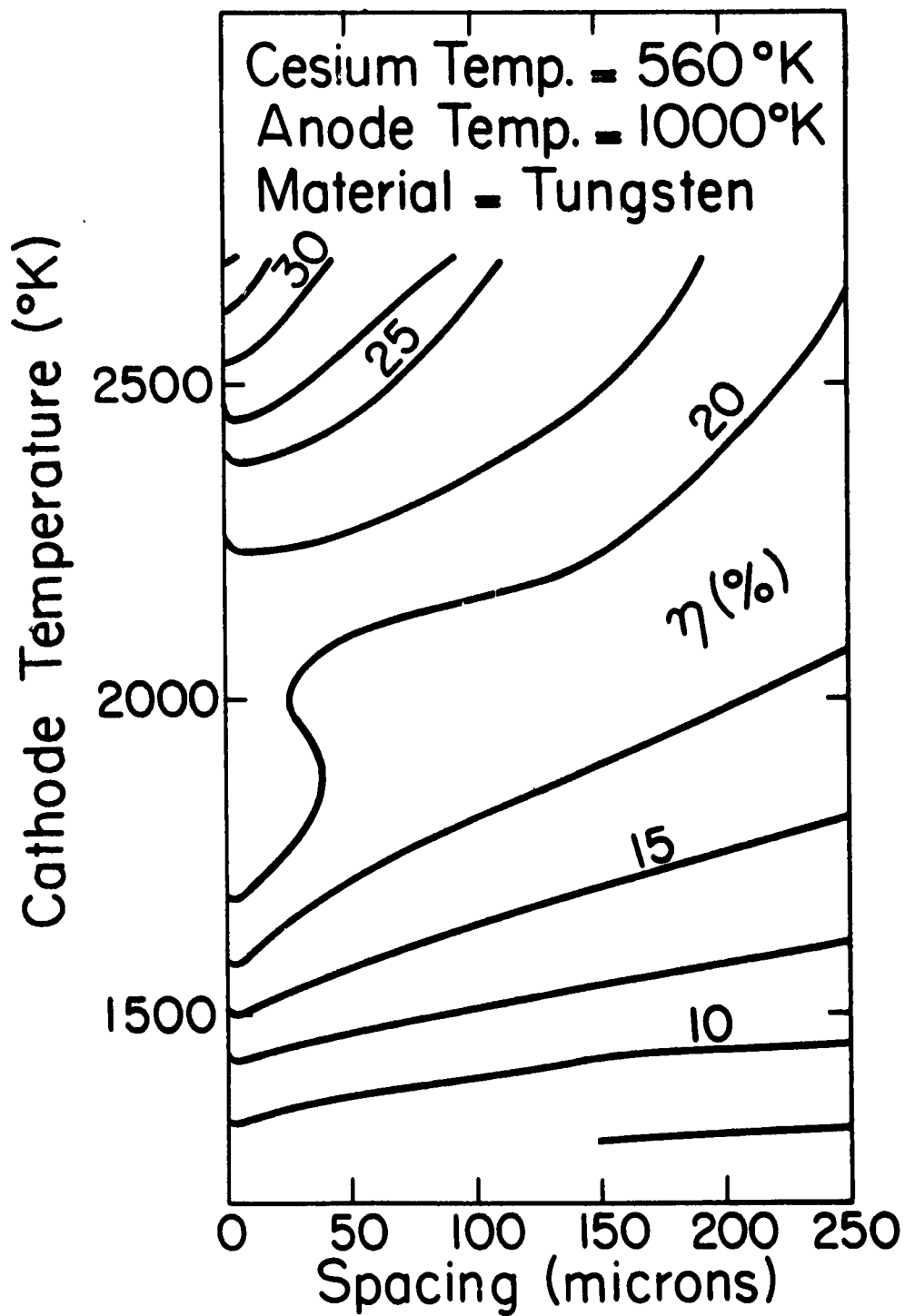


Fig.9-Efficiency as a function of spacing and cathode temperature.

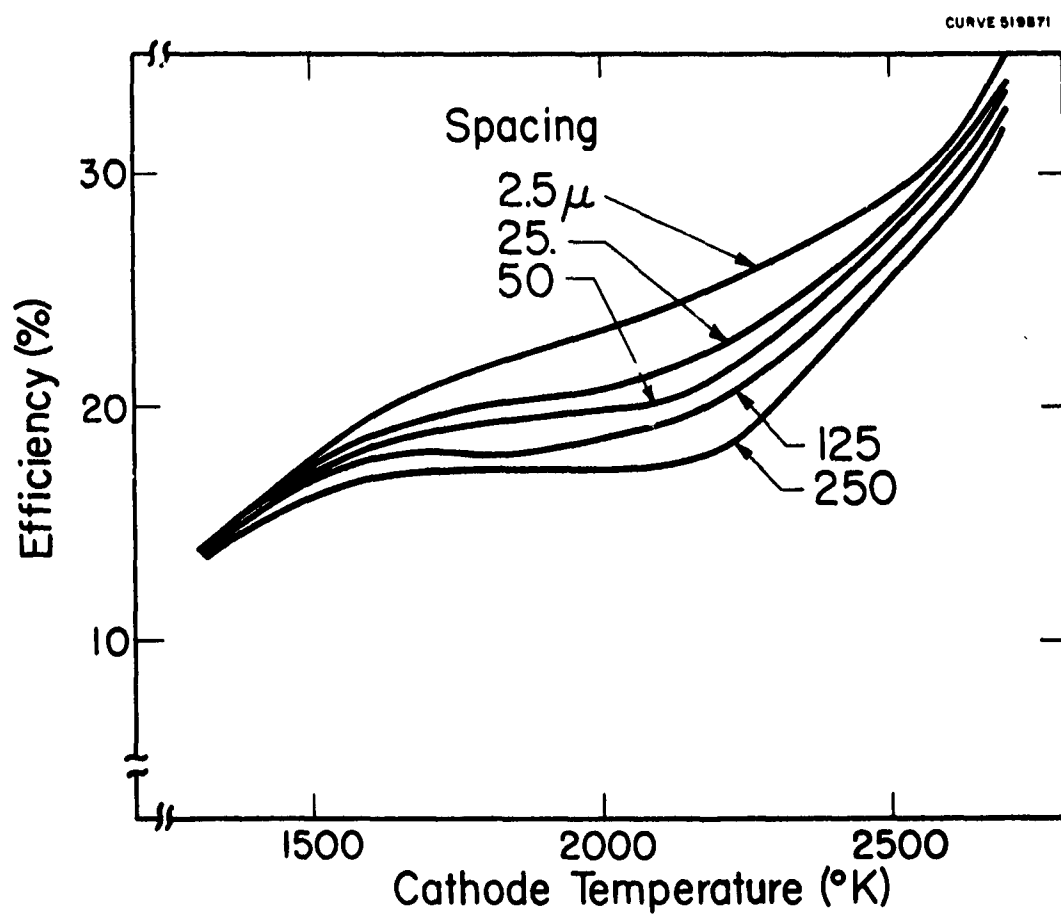


Fig.10-Optimum efficiency as a function of cathode temperature.

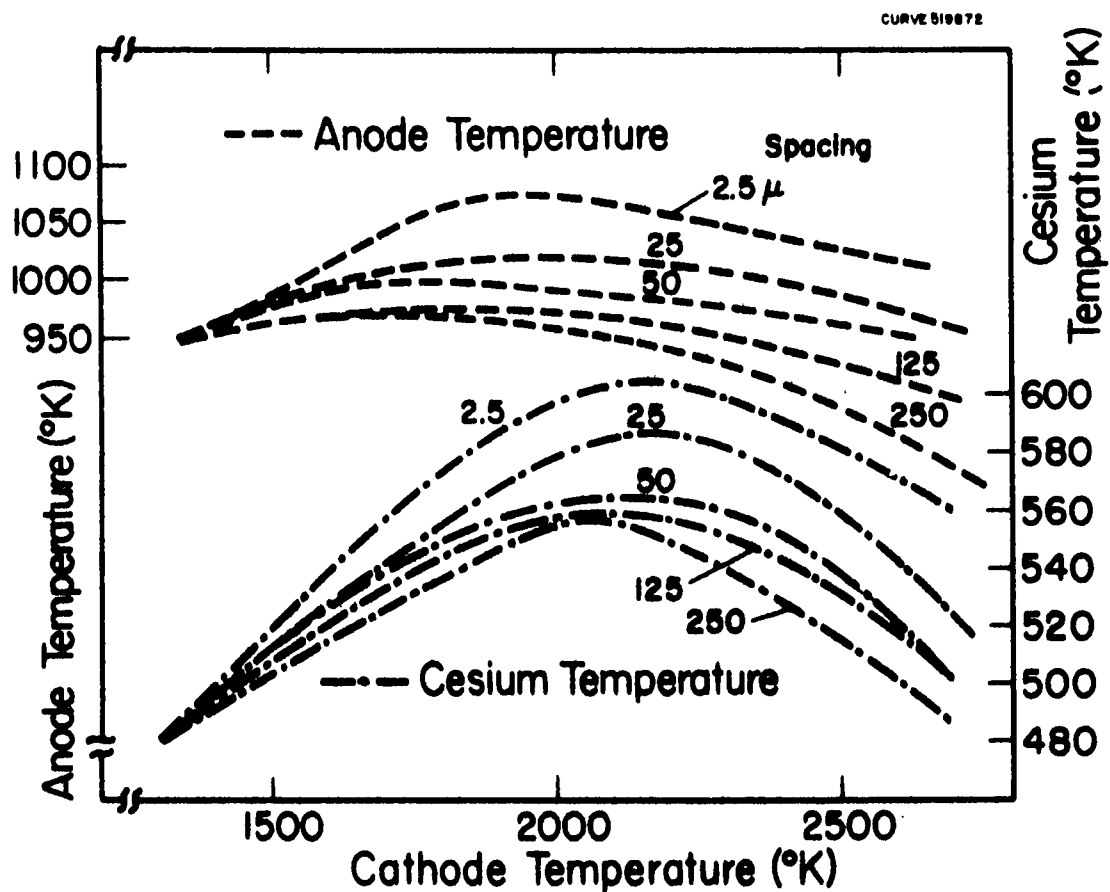


Fig. II - Optimum anode and cesium temperatures as a function of cathode temperature.

CURVE 519870

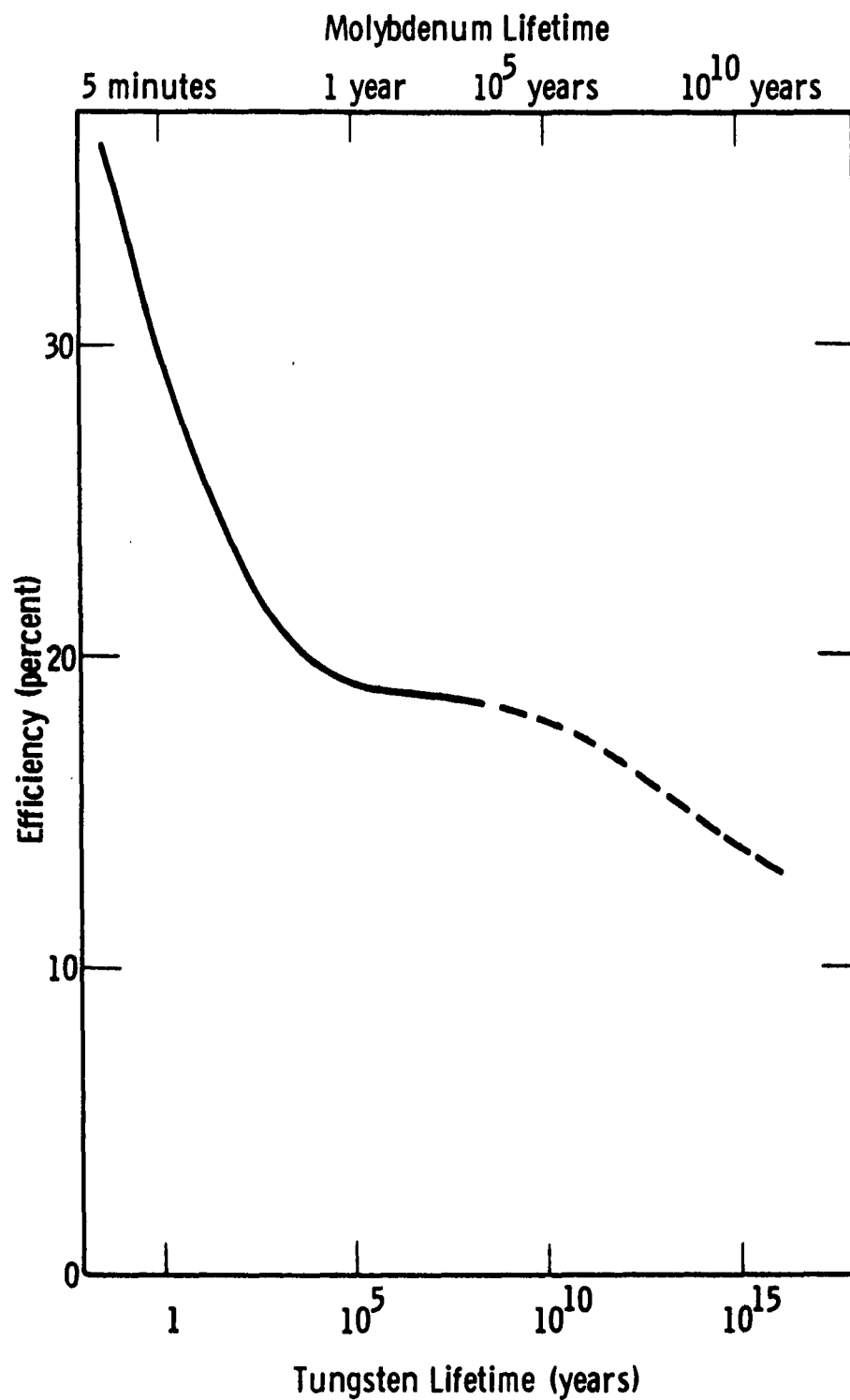


Fig. 12—The relationship between evaporative lifetime and efficiency for tungsten and molybdenum

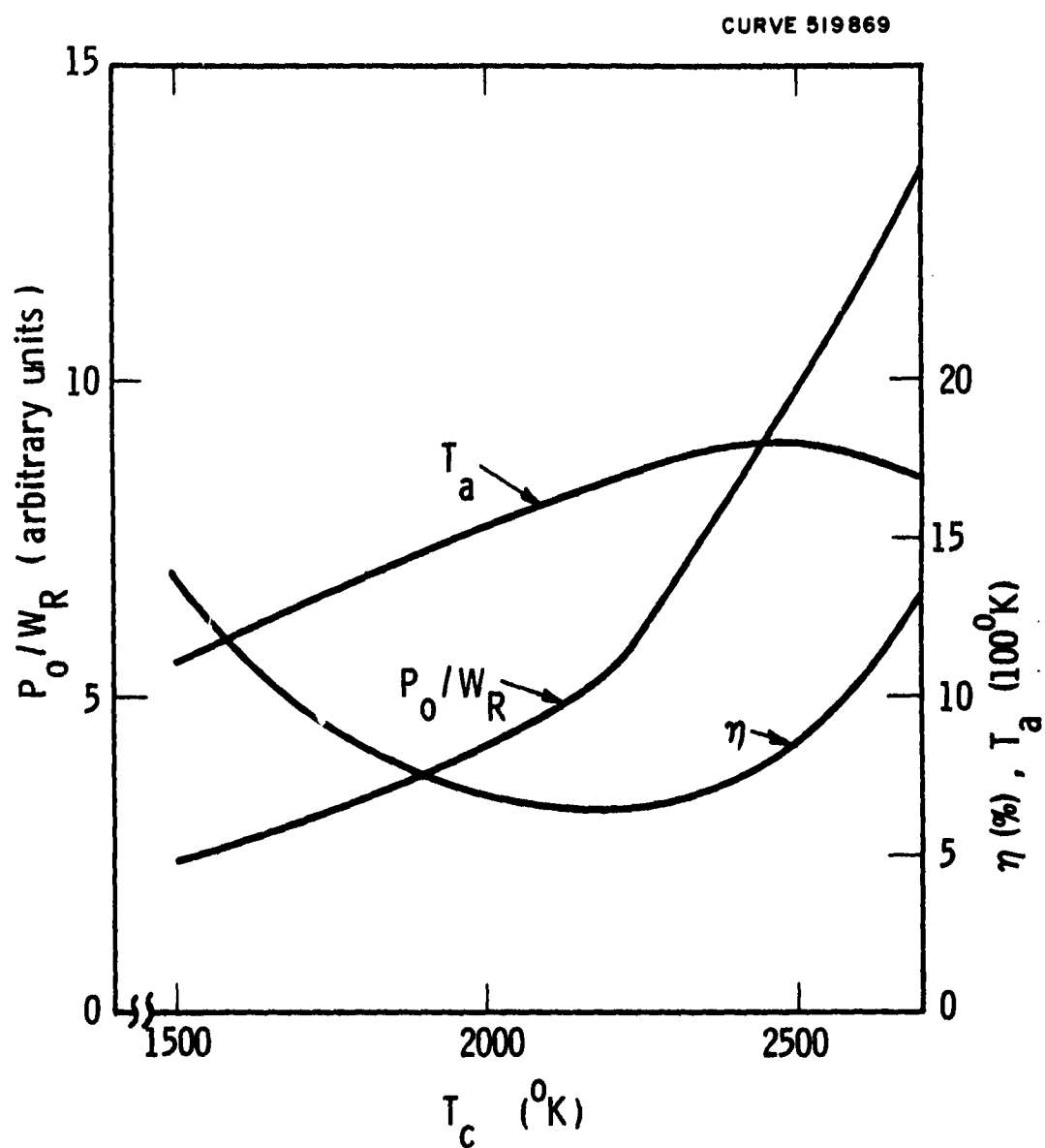


Fig. 13—Power to weight ratio, optimum anode temperature, and efficiency at minimum weight as a function of cathode temperature.

Section IV

THE CALCULATION OF THE EFFICIENCY OF ENERGY CONVERSION BY THERMIONIC EMISSION

by

A. E. Fein and L. S. Richardson

THE CALCULATION OF THE EFFICIENCY OF ENERGY CONVERSION BY
THERMIONIC EMISSION

A. E. Fein and L. S. Richardson

Introduction

As early as 1953, the possibility of using thermionic emission as a means of converting thermal energy directly into electrical energy was discussed.⁽¹⁾ Since that time, a number of papers have appeared in the literature describing the operation of devices utilizing this means of energy conversion.⁽²⁾ These papers have used the efficiency of the device as a criterion of comparison with other energy converters. While many of the authors have described the effects of varying some of the many parameters governing the operation of a thermionic converter, none have considered all of the effects simultaneously. Certain important effects, such as back current and varying load resistance, have not been analyzed carefully, if at all. In this paper, an attempt is made to maximize efficiency by simultaneously optimizing cesium pressure (including the effects on work function), anode temperature, load resistance and lead resistance. The effects of varying cathode temperature and anode-to-cathode spacing are also included. It is the purpose of this paper to construct a model predicting the behavior of a thermionic converter for the use of designers or experimenters. Results of numerical computation of efficiency will also be presented.

While many properties are of importance in the operation of a thermionic converter, once the materials for construction of cathode and anode have been chosen, only a few independent parameters remain. The geometrical configuration, the electrode temperatures, the means of space charge neutralization, and the resistances of the lead and load are the only variables which can be adjusted. The most common means of space charge neutralization (recently patented by G. R. Feaster⁽³⁾) is the use of a cesium atmosphere in the interelectrode gap. Most of the experimental cells and almost all of the converter designs use geometry which is equivalent to plane parallel electrodes. Since the lead and load resistances can be simultaneously optimized to yield maximum efficiency, the four independent variables in a conventionally designed thermionic converter are the cathode and anode temperatures, the cesium pressure, and the inter-electrode spacing. A later section will show that the anode temperature and cesium pressure can also be simultaneously optimized. Thus, once the basic design of a converter has been made, the choice of materials, spacing, and cathode temperature will fix all other parameters, if maximum efficiency is sought.

II. Description of the Operation of a Thermionic Diode

In this section, a mathematical model describing the behavior of a thermionic diode will be set up and used to evaluate the efficiency of such a device. For the sake of mathematical convenience, the operation

will be expressed in terms of variables which are not all independent. (For example, thermal emissivity is a function of surface temperature.) This will not affect the derivations described below. Before numerical calculations can be performed, however, the actual interrelationships among the physical parameters must be taken into account. A description of the manner in which this will be done will be deferred until the analysis of the operation of the thermionic diode has been presented.

A. Description of Model Used

Stripped of the numerous parts necessary in its construction, the thermionic diode can be basically represented by the schematic of Fig. 1. A cathode surface in contact with a heat reservoir at an absolute temperature T_c thermally emits electrons across a gap to an anode in contact with a heat reservoir at a temperature T_a . The electrons are returned from the anode to the cathode through an external load.

In practice, certain effects take place which tend to prevent the flow of a reasonable current. The most serious of these is the formation of a space charge in the space between the cathode and anode. This space charge forms a potential barrier for the electron leaving the cathode and can reduce the number of electrons reaching the anode (and therefore the current through the load) by many orders of magnitude. Two different methods are presently in use to overcome the problem of space charge. The simplest of the two, in theory, is the method of close-

spacing. It is known⁽⁴⁾ that the reduction of current flow by space charge is very sensitive to the distance between the cathode and anode. For separations of 0.0002 in. or less, the detrimental effects of space charge can be made almost negligible.⁽⁵⁾ The second common method of reducing or eliminating space charge is by the use of a positively ionized vapor (usually cesium) in the gap between the anode and cathode. The electrostatic potential set up by the ions will then counteract the retarding potential of the electronic space charge and permit an increased flow of electron current.

The introduction of the plasma results in a loss of energy available to the load by conducting heat from the cathode to the anode and by scattering electrons in the region between the cathode and the anode. In addition, the plasma may modify the values of the chemical potential of both the anode and cathode.

In this paper, it will be assumed that the space charge in the region between the anode and cathode has been eliminated by using a plasma. It will be assumed that the sole effect of the plasma on the behavior of the diode is to introduce a "plasma electrical resistance," R_p , and a "plasma thermal conductance," K_p . The former will contribute to an internal voltage drop inside the diode, and the latter to a thermal conduction of energy across the cathode-anode gap. Also, only the case of plane parallel plates one square centimeter in area* will be considered.

* In this regard, it must be remembered that the value of resistance must correspond to electrodes of unit area, and that net current densities calculated will be numerically equal to currents.

Let ϕ_c and ϕ_a be the work functions of the cathode and anode respectively. (When similar quantities are defined for both the cathode and anode, a subscript "c" will refer to the former and "a" to the latter.) The potential seen by an electron in going from the cathode to the anode will then be represented by one of three possible cases depicted by Fig. 2. The mode of operation will be classed as uphill if $V > \phi_c - \phi_a$ (Fig. 2a), downhill if $V < \phi_c - \phi_a$ (Fig. 2b), and flat if $V = \phi_c - \phi_a$ (Fig. 2c)

The saturation emission current densities will be denoted by J_{cs} and J_{as} . By Richardson's equation

$$J_{cs} = AT_c^2 \exp(-\phi_c/KT_c) \quad (1)$$

$$J_{as} = AT_a^2 \exp(-\phi_a/KT_a) \quad (2)$$

where A is Richardson's constant, equal to $120 \text{ amp cm}^{-2} \text{ deg K}^{-2}$; and, if k is Boltzmann's constant, and e the electronic charge, $K = k/e = 8.616 \times 10^{-5} \text{ volts deg K}^{-1}$. In the flat mode the net current density, J, from the cathode to the anode is simply the net saturation current density, J_s

$$J = J_{cs} - J_{as} = J_s \quad (3)$$

In general, this is not true, and the net current must be written

$$J = J_c - J_a \quad (4)$$

where in the uphill mode

$$J_c = J_{cs} \exp \left[-(V - \phi_c + \phi_a)/KT_c \right] \quad (5)$$

$$J_a = J_{as}$$

and in the downhill mode

$$\begin{aligned} J_c &= J_{cs} \\ J_a &= J_{as} \left[\exp - (\phi_c - V - \phi_a)/KT_a \right] \end{aligned} \quad (6)$$

The heat input to the cathode and power output to the load must be known in order to calculate the efficiency of operation of a thermionic generator. The power output is simply the load voltage times the current, where the load voltage is equal to the emf, V , generated by the diode minus the voltage drops due to plasma resistance (R_p) and lead resistance (R_L).

$$P_{out} = J(V - J(R_L + R_p)) \quad (7)$$

By the first law of thermodynamics the total heat input to the cathode is equal to the total energy leaving the cathode. The latter can be expressed as the sum of several terms:

- 1) Heat radiated from cathode to anode, W .
- 2) Support and end losses, X .
- 3) Heat absorbed by electrons leaving the cathode and reaching the anode, H_c .
- 4) Heat conducted from cathode to anode by lead wires and plasma, H_k .
- 5) Heat returned to the cathode by electrons arriving from the anode, H_a .
- 6) Heat returned to cathode from the Joule heating of lead wires and plasma, H_J .

The first four effects carry heat away from the cathode while the last two bring heat to the cathode.* The total heat input, H_{in} , to the cathode can be evaluated.

* Minor losses due to thermoelectric effects and the energy required to ionize the plasma will be ignored.

$$H_{in} = W + H_c + H_k - H_a - H_J + X \quad (8)$$

The individual terms are readily calculable. The thermal radiation term W is given by the Stefan-Boltzmann law**

** It is here assumed that both the anode and the cathode are gray bodies.

$$W = \sigma F (T_c^4 - T_a^4) \quad (9)$$

where, if ϵ_c and ϵ_a are the total emissivities of a parallel cathode and anode, the view function F is⁽⁶⁾

$$F = (\epsilon_c^{-1} + \epsilon_a^{-1} - 1)^{-1} \quad (10)$$

and σ is the Stefan-Boltzmann constant (5.67×10^{-12} watts cm^{-2} deg K^{-4}).

The heat carried by thermal conduction away from the cathode is

$$H_\kappa = (K_p + K_L) (T_c - T_a) \quad (11)$$

where K_p and K_L are the thermal conductances of the plasma and the leads respectively. It will be assumed that the Joule heat returned to the cathode is simply one-half the total Joule heat produced in the leads and in the plasma.* Thus

* This result is obtained rigorously in reference 2d.

$$H_J = (1/2) (R_L + R_p) J^2 \quad (12)$$

In order to compute H_c and H_a , the mode of operation must be considered. From Fig. 2, it is seen that in the downhill mode an electron leaving the

cathode must have absorbed an amount of heat at least equal to ϕ_c . Similarly, an electron arriving at the cathode from the anode must also have absorbed at least that amount of heat. For the uphill mode, this minimum amount of absorbed heat is $V + \phi_a$. Define

$$\phi = \text{Max} (\phi_c, \phi_a + V) \quad (13)$$

The value of ϕ is thus the minimum heat absorbed by an electron traversing the diode in any mode. In addition to this minimum heat ϕ , there is some kinetic energy which the electron may possess. If the electrons immediately outside the cathode or anode have a Maxwellian distribution characteristic of the temperature of the surface which they have left, it can be shown that, on the average, this additional kinetic energy will be $2KT$ where T is the temperature of the emitting surface. Thus

$$H_c = J_c (\phi + 2KT_c) \quad (14)$$

and

$$H_a = J_a (\phi + 2KT_a) \quad (15)$$

The efficiency, defined as the ratio of output power to heat in, is then given by

$$\eta = \frac{J [V - J (R_L + R_p)]}{W + J_c(\phi + 2KT_c) + (K_L + K_p)(T_c - T_a) - J_2(\phi + 2KT_2) - J^2(R_L + R_p)/2 + X} \quad (16)$$

In practice, the load resistance, R_{load} , is a quantity which can be varied at will. However, mathematically the internal voltage

$$V = J(R_L + R_p + R_{load}) \quad (17)$$

is much more convenient to use. Therefore, in lieu of R_p , R_L and R_{load} being considered as three independent variables, R_p , R_L and V will be used, the transformation being non-singular. It must be kept in mind, therefore, in the following analysis that, if, for example, a variation of R_L at constant V is considered, a variation in R_p and/or R_{load} is necessary. The value of the variable V is not completely optional. There are limits on V , and values outside of these limits are not physically obtainable. It is only the load resistance which can be physically varied from zero to infinity, short and open circuit respectively. Each case yields an equation which may be solved for the internal voltage. The minimum value for V , V_{sc} , is obtained from the short circuit equation

$$0 = V - J (R_L + R_p) \text{ at } V = V_{sc} \quad (18)$$

Equation (18) is transcendental and cannot be solved analytically. The open circuit voltage V_{oc} is determined by the condition

$$J = 0 \text{ at } V = V_{oc} \quad (19)$$

An analytic solution to (19) for V_{oc} can be obtained from (4), (5) and (6)

$$V_{oc} = \phi_c - \phi_a + KT \ln (J_{cs}/J_{as}) \quad (20)$$

where

$$T = T_c \text{ if } J_{cs} > J_{as}, \text{ and } T = T_a \text{ if } J_{as} > J_{cs}.$$

B. Optimization of Lead Resistance

The efficiency (16) can be optimized with respect to the lead resistance at fixed V as follows:

If A_c , L , ρ , and κ are respectively the cross-sectional area, length, electrical resistivity, and thermal conductivity of the leads

$$R_L = \rho L / A_c \quad (21)$$

$$K_L = \kappa A_c / L \quad (22)$$

By the Wiedemann-Franz law ρ and κ of a metallic conductor at a temperature T_0 are related by the equation

$$\rho = \lambda T_0 / \kappa, \lambda = 2.44 \times 10^{-8} \text{ watt-ohm-deg K}^{-2} \quad (23)$$

If T_0 is assumed to be the average of T_c and T_a

$$K_L = (\lambda/2 R_L) (T_1 + T_2) \quad (24)$$

Thus K_L can be replaced in (16) by its value in terms of R_L from (24) and obtain an expression which can be reduced to

$$\eta = \beta \eta_0 \quad (25)$$

where η_0 is the efficiency of an identical diode with ideal leads (i.e., $R_L = 0$, $K_L = 0$)

$$\eta_0 = \frac{J[V - JR_p]}{W + J_c(\phi + 2KT_c) - J_a(\phi + 2KT_a) + K_p(T_c - T_a) - J^2 R_p / 2 + X} \quad (26)$$

and

$$\beta = (1-\gamma) \left\{ 1 - \frac{\eta_0}{2} \left(\gamma - \frac{1}{G\gamma} \right) \right\}^{-1} \quad (27)$$

$$G = (V - JR_p)^2 [(T_c^2 - T_a^2)]^{-1} \quad (28)$$

$$\gamma = \frac{JR_L}{V - JR_p} \quad (29)$$

From (17) therefore

$$\gamma = \frac{R_L}{R_L + R_{load}} \quad (30)$$

Thus physically the parameter γ is the fraction of the external emf of the diode which appears across the leads; or equivalently, it is the ratio of the lead resistance to the total external resistance. Its range therefore is from 0 to 1.

The efficiency can then, in principle, be maximized with respect to the lead resistance R_L . Using the representation of (25) and noting that R_L enters only through the dimensionless parameter γ , it is found that the efficiency optimized with respect to R_L is (quantities evaluated at that value of R_L giving maximum efficiency will be denoted with an overhead bar)

$$\bar{\eta} = \eta_0 \bar{\beta} \quad (31)$$

where

$$\bar{\beta} = \frac{\sqrt{1+B} - 1}{\sqrt{1+B} + 1 - \eta_0} \quad (32)$$

$$\bar{R}_L = [(V - JR_p)/J][(\sqrt{1+B} - 1)/B] \quad (33)$$

$$\bar{\gamma} = JR_p / (V - JR_p) \quad (34)$$

$$B = G(2 - \eta_0)\eta_0 \quad (35)$$

As the value of B ranges from zero to infinity, the value of $\tilde{\gamma}$ will range from $1/2$ to zero. Thus under no conditions will more than half the external emf appear across the leads when they are optimized.

Obviously, $\tilde{\beta} < 1$. The quantity $\tilde{\beta}$ is the fraction to which the efficiency of the ideal diode with ideal leads (zero electrical resistance and zero thermal conductivity) has been reduced when the physical leads have been optimized. Considered as a function of η alone (V , T_c , T_a fixed), $\tilde{\beta}$ can be shown to be monotonically decreasing. Thus the tendency of the leads to decrease the efficiency is greater for an ideal diode with a large efficiency. This can be explained qualitatively from the fact that the higher efficiency diodes have in general the larger electric currents and that the larger the current, the larger the voltage drop in the leads. However, $\tilde{\eta}$ is still a monotonically increasing function of η_0 .

If non-optimum leads are used, a decrease in efficiency will result. This effect will be considered for the most pessimistic case by adjusting the parameters so that B is as small as possible. This can be done by making G as small as possible. For the values $T_a = 0^\circ\text{K}$, $T_c = 3000^\circ\text{K}$, and $V - JR_p = 1$ volt, G is equal to 4.55. Fig. 3 shows the results of calculations of β as a function of η_0 and γ . Also shown in that figure is the locus of the maximum of the curves, $\tilde{\beta}$. Several features of these curves are of interest. At a critical value of γ equal to $G^{-1/2}$

(0.47 in this case), the curves for different values of η_0 intersect. For γ greater than this critical value, β is a monotonically decreasing function of η_0 , but very weakly dependent upon η_0 . For γ less than this critical value, β is a strong monotonically increasing function of η_1 .

Curves of $\bar{\gamma}$, $\bar{\eta}$, and $\bar{\beta}$ as functions of η_0 are presented in Fig. 4 for the values of T_c , T_a and V used above.

It is clear from Figs. 3 and 4 that there is a serious loss in efficiency due to the leads. Even when this loss is minimized by optimizing the value of the lead resistance, it is seen that for the case considered, the ideal efficiency, η_0 , is decreased by amounts ranging from 18% (at $\eta_0 = 0.1$) to 42% (at $\eta_0 = 1.0$). For less pessimistic cases, the loss is less severe, but still appreciable. It should be emphasized that the curves of Fig. 4 are for optimized leads. For non-optimized leads, the loss of efficiency is much greater as can be seen from Fig. 3.

It is seen from Fig. 4 that, for almost the entire range $\bar{\eta}$ is, to a good approximation, a linear function of η_0 . This fact is borne out by expanding equation (31) in a series about $\eta_0 = 1$.

$$\bar{\eta} = \left(\frac{\sqrt{1+G} - 1}{\sqrt{1+G}} \right) \left[1 - \frac{G(1 - \eta_0)}{G + 1} - \left(\frac{3 - \sqrt{1+G}}{2G} \right) \left(\frac{G(1 - \eta_0)}{G + 1} \right)^2 + \dots \right] \quad (36)$$

For the case considered, ($G = 4.55$),

$$\bar{\eta} = .574 \left[1 - 0.82 (1 - \eta_0) - 0.047 (1 - \eta_0)^2 + \dots \right] \quad (37)$$

The high degree of linearity of $\bar{\eta}$ as a function of η_0 observed for this case does in fact occur in general. This is seen by examining the coefficients of the linear and second order terms in (36). For the case treated, the ratio of the coefficient of the second order term to that of the first order term is 0.057. For values of $G > 4.55$, the ratio decreases until at $G = 8$, it becomes zero. For larger values of G , the ratio becomes negative and obtains a maximum magnitude of 0.042 at $G = 35$. Thus the special case which has been considered actually exhibits the largest deviation from linearity. Therefore, to a good approximation (less than 5% error) $\bar{\eta}$ (for $\eta_0 > 0.1$) can be computed from only the first two terms of (36). Similarly, for small η_0 , equation (31) can be expanded in a series of powers of η_0 . Thus $\bar{\eta}$ can be written

$$\bar{\eta} = \begin{cases} (\sqrt{1+G} - 1)(1+G)^{-3/2} \left[1 + G\eta_0 + \dots \right] & \eta_0 > 0.1 \\ \eta_0 \left[1 - 2\sqrt{\eta_0/2G} + 2(\eta_0/2G) \dots \right] & \eta_0 < 0.1 \end{cases} \quad (38)$$

For the lower series of (38), it is again noted that for the case of minimum G treated, the fit is the poorest, and that for larger values of G the approximation improves.

C. Optimization of Load Resistance (Internal Voltage)

The assumption has often been made in the literature that the flat mode of operation yields the maximum attainable efficiency for a given diode. This assumption is not necessarily valid, as a simple numerical example will show. If $R_p = 0$, $\phi_c = 2.5$ volts, $\phi_a = 1.5$ volts, $T_c = 2200^\circ\text{K}$, $T_a = 0^\circ\text{K}$, and ϵ_c and $\epsilon_a = .25$, then $\eta_0 = 34.5\%$ when operating in the flat mode. Using the same parameters, but operating in the uphill mode, so that $V = 1.5$ volts, η_0 is equal to 41.5%. At the same time, a reduction of power density from 1090 watts/cm² to 117 watts/cm² and a reduction of current density from 1090 amps/cm² to 77.8 amps/cm² takes place. Thus not only has the efficiency increased upon increasing the output voltage, but both the current density and the power density have been considerably reduced. The reduction of the power density is of significant value because a comparable power must be dissipated at the anode, and the dissipation of large quantities of power can pose a serious engineering problem. Similarly, the handling of large current densities is difficult; thus the reduction of the output current density is also of engineering importance.

In this example, the decrease of the current and power densities was accompanied by a significant increase in efficiency. Cases can be constructed in which the change in efficiency is not significant, but in which operation in the uphill mode decreases the current and power densities by appreciable amounts.

The reason for this increase in efficiency can be seen qualitatively by considering the simple case of ideal leads, no plasma or support losses, and no back current. Then (16) can be written

$$\eta = \frac{V}{\phi + 2KT_c + W/J_c} \quad (39)$$

As long as the thermal radiation, W , is small compared to J_c , the efficiency will increase with increasing V . ($\phi = V + \phi_a$ in the uphill mode). Eventually, J_c becomes so small that W/J_c is no longer negligible. At this point, the efficiency begins to decrease with increasing V . When a maximum efficiency occurs in the uphill mode, it can be shown that this efficiency is independent of the cathode work function, ϕ_c .

Numerical calculations of (16) show that this effect exists as well for that more accurate case. Further, it is possible for the optimum efficiency to occur in the downhill mode. The fact that this can occur can easily be explained by considering the case of a diode whose parameters are such that $J_{cs} < J_{as}$. Thus the only possible mode of operation is the downhill mode and the maximum efficiency must occur in that mode.

The efficiency of (16) can be simultaneously maximized with respect to V and R_L by setting equal to zero the partial derivatives of η with respect to these variables. This procedure results in the equation for V

$$\begin{aligned}
 J + \frac{dJ}{dV} [V - 2J (\bar{R}_L + R_p)] - \bar{\eta} \frac{dJ_c}{dV} (\phi + 2KT_c) \\
 - \frac{dJ_a}{dV} (\phi + 2KT_a) + J \frac{d\phi}{dV} (\bar{R}_L + R_p) = 0
 \end{aligned}
 \tag{40}$$

where $\bar{\eta}$ and \bar{R}_L are given as functions of V by (31) ff. Equation (40) is actually two equations -- one for the downhill and one for the uphill mode of operation. It can be shown that each of these two equations always has one and only one solution for V between V_{sc} and V_{oc} . If the solution to the equation for the downhill anode lies between V_{sc} and $\phi_c - \phi_a$, there is a maximum for the efficiency in that mode. Similarly, if the equation for the uphill mode has a solution between $\phi_c - \phi_a$ and V_{oc} , there is a maximum in the uphill mode. If neither of these two conditions result, the maximum efficiency results in the flat mode ($V = \phi_c - \phi_a$).*

* In principle, it is possible for a maximum to occur in each mode. However, the range of parameters for which this can happen is small. In several thousand cases calculated, this situation has never occurred.

Once the value of V resulting in the maximum efficiency is found, the value of R_L necessary for it to be obtained is given by (33). And from these two quantities all other properties at this optimum point can be found (e.g., power out, net current, etc.).

The model of the diode used for the above calculation possesses several limitations with respect to the manner in which the plasma is included. These are important enough to warrant further discussion. It has been assumed that "sufficient" plasma has been introduced so that the space charge is eliminated. Although experiments with plasma filled diodes seem to indicate this can be done, only the crudest estimates are available of the conditions under which this is possible. Further, it is known that the introduction of plasma can result in potential sheaths at the electrodes. In lieu of considering this difficult and as yet unsolved problem, the procedure described assumes that the plasma can be considered ohmic and that an effective electrical resistance can be found. Limited experimental data indicates that this assumption is not too inaccurate. Finally, the possibility of an arc being established is ignored. Although it is definitely known that an arcing mode can be set up, this possibility does not invalidate the above calculations. What it means, however, is that if the solution for the operating point found by the described procedure falls in a region of operation which will support an arc, it is not a valid solution for the maximum efficiency. The maximum efficiency in the region where no arc occurs must then be found. In either case, to determine the optimum efficiency, the operation in the arcing mode must be analyzed and the maximum efficiency obtained there compared to the maximum efficiency of normal operation already described. Again a treatment of the operation

of a diode in the presence of an arc is a difficult unsolved problem. By comparing the optimum operating points calculated by the formulas given here to the limited experimental data available on arcs, it is found that, in general, these computed optimum points should not sustain arcs.

D. Empirical Evaluation of Parameters

In order to be able to calculate the quantities discussed, it is necessary to know the values of many parameters such as work functions and emissivities. In reality, quantities such as these are not independent, but depend on the pressure of cesium and the temperatures of the electrodes. This section is devoted to describing the relation which exists among these quantities.

The relationship of effective work function to cesium pressure and surface temperature has not been well determined. The pioneering work of Langmuir⁽⁷⁾ provided the basis for the present empirical equation. While no theoretical justification of the equation can be given, the results are in close agreement with the original data and with the extrapolations of other investigators.^(2d)

The effective work function of cesium-coated tungsten was assumed to be a function of only the fractional coverage, θ . The data of Langmuir and Taylor⁽⁷⁾ are plotted in Fig. 5. The empirical equation

$$\begin{aligned}\Phi &= 4.52 - 8.59 \theta + 6.3 \theta^2, \theta \leq .86 \\ \Phi &= 1.81, \theta \geq .86\end{aligned}\tag{41}$$

was fitted to this data. The results of this equation are also plotted in Fig. 5.

The estimation of the fractional coverage as a function of cesium pressure and surface temperature was also made by the use of a set of empirical equations. Fig. 6 shows the relation between surface temperature and coverage for two particular cesium temperatures.⁽⁷⁾

This can be well fitted by the equation

$$\theta = [1 + (T/T_0)^c]^{-1}\tag{42}$$

where T_0 and c are constants, both of which are functions of the cesium pressure (or arrival rate).

If the relationship of cesium bath temperature, T_{Cs} , to cesium pressure, P , given by Nottingham⁽⁸⁾ is used,

$$P = 2.45 \times 10^{-8} e^{-8910/T_{Cs}}\tag{43}$$

where T_{Cs} is in deg K and P in mm Hg. The relationship of c and T_0 to the temperature of the cesium bath T_{Cs} are found to be

$$c = 2.73 + 720/T_{Cs}$$

$$\frac{1}{T_0} = 0.385 (10^{-4} + 1/T_{Cs}) \quad (44)$$

Figure 6 shows the results of using these empirical equations for the two temperatures shown. Figure 7 shows the relationship of work function to cesium temperature and surface temperature. This is in fair agreement with the results of Schock^(2d), especially if the cesium temperature listed by Schock rather than the pressure is used to compare values. One particular difference is of interest. The measurements of Langmuir indicate that a minimum work function is obtained when θ is equal to $2/3$. When a full monolayer is present, the work function is assumed to be that of cesium. This higher value of the work function at full coverage has a serious effect on the efficiency when low anode temperatures are used.

The thermal emissivities of tungsten is given by several references as a function of temperature. The data used here are those of Forsythe and Watson.⁽⁹⁾

Values of plasma electrical resistance and thermal conductance are not available in the literature. Gottlieb and Zollweg⁽¹⁰⁾ have recently measured the thermal conductance of cesium plasma. An empirical fit to their results is shown in Figure 8. These data were fitted well by the empirical equation.

$$\kappa_p = 1.5 \times 10^{-4} \{1 - \exp(-40 Pd)\} \quad (45)$$

where P is the cesium pressure in mm of Hg (by (43)), d the spacing in cm and κ_p the thermal conductivity of the plasma in watt-cm/deg K. The electrical resistance was estimated from J-V curves taken by Gottlieb and Zollweg. The results are quite preliminary in nature. For the calculations discussed hereafter, the plasma resistivity, ρ_p , was estimated by the equation

$$\rho_p = 2.67P \quad (46)$$

where P is the cesium pressure in mm Hg. (by (43)) and ρ_p is in ohm cm.

III. Results of Numerical Calculations

Because empirical data concerning the effect of cesium coverage on the thermionic properties of materials is well known only for tungsten, calculations were made only for a device in which both the anode and cathode were made of tungsten.

Calculations of the optimum operating point according to the method described above were carried out on a high speed digital computer for more than 5000 different combinations of spacing, and cathode, anode, and cesium bath temperatures. At the values of lead and load resistance which yielded the maximum efficiency for each of the given combination of parameters, some forty different properties, such as power delivered to

load, external voltage, net current, etc., were tabulated in addition to the efficiency (a sample of such a table is shown in Table I). As already shown, for given materials of construction, the efficiency η , optimized with respect to load and lead resistance is a function of only four variables - cathode-anode spacing, and the temperature of the cathode, anode, and cesium reservoir. Because of the number of independent variables, it is possible to plot lines of constant efficiency in a large number of ways. By keeping two of the parameters constant, efficiency contours can be plotted as a function of the other two. Figures 9, 10, and 11 show respectively sample results of keeping fixed cesium temperature and spacing, anode temperature and spacing, and cesium temperature and anode temperature. It was found, however, that the most useful type of plot was obtained by fixing the spacing and cathode temperature and drawing curves of constant efficiency as a function of anode and cesium reservoir temperatures. A set of 60 (5 spacings x 12 cathode temperatures) of such plots are shown in Figure 12. It should be noticed that in each case, the efficiency has a maximum occurring at a unique combination of cesium and anode temperatures. This maximum is a general occurrence for all of the possible combinations of spacing and cathode temperature, although its precise location will depend upon the particular values of spacing and cathode temperature considered. It should be mentioned that these maxima may only be local and that higher efficiencies may be obtainable at lower

anode temperatures. However, anode temperatures less than 600°K were not considered to be reasonable from a design standpoint. Further, the anode temperature can never be less than the temperature of the cesium reservoir, for the latter must be the lowest temperature in the diode so that it will determine the pressure of the cesium vapor. Curves of the type in Figs. 9, 10, and 11 do not display a maximum of efficiency since higher efficiencies can always be obtained by going to a sufficiently higher cathode temperature. If Fig. 11 is considered at a fixed value of cathode temperature, it can be shown that an optimum value of spacing exists. However, these spacings are extremely small (less than 2.5 microns) and not realizable. Therefore, for spacings larger than this, the efficiency decreases with increasing spacing.

A summary of the maxima obtainable from plots of the type of Fig. 12 is shown in Figs. 13 and 14. In these figures are shown three sets of curves as functions of cathode temperature - maximum attainable efficiency and the anode and cesium bath temperatures necessary to attain that efficiency. Each set consists of five curves corresponding to five different spacings. There are several important features of these curves which should be noted. There is, for a fixed spacing, a wide range of cathode temperatures in which the ultimate efficiency is relatively independent of cathode temperatures. Thus, a small improvement in the

temperature capability of most existing materials does not produce a large improvement in efficiency of operation. Further, the anode temperature required for maximum efficiency is seen to be within the range 900°K to 1100°K regardless of the cathode temperature or spacing.

It should be reemphasized at this point that the numerical results presented in the figures and in the above discussion refer to a device with tungsten anode and cathode. For other materials, the numerical values might change considerably, but it is believed that the qualitative nature of the results should be the same.

It must also be recalled that these calculations are based on the assumption that space charge has been eliminated. Since there is a minimum cesium temperature at which this is true, certain areas of the curves presented (particularly at the lower cesium temperatures) are inaccurate. Fortunately, from the limited data available in the literature, the optimum operating points do not appear to be in this excluded area.

If accurate emission data were available, calculations of the type discussed here could be carried out for other materials. While experimental investigations of these data are presently being made by various laboratories, little information is available in the literature.

IV. Conclusions and Recommendations for Further Study

The following are some conclusions we have drawn from this study and some recommendations for further work.

When for a fixed spacing and cathode temperature all other parameters are optimized using efficiency as the criterion, the resulting optimum efficiency is a relatively insensitive function of the cathode temperature in the temperature range 1600 to 2200°K. Clearly, a small improvement in temperature capability will not result in a significant improvement in efficiency. Only a large increase in operating temperature provides a marked improvement. In order to operate a thermionic converter of the type discussed here at 25% efficiency, a cathode temperature above 2200°K is necessary. A thermionic converter using tungsten electrodes operating with a cathode temperature of 1600 to 2200°K would have an efficiency between 15 and 20%.

The introduction of cesium into a thermionic energy converter has two opposing effects upon the efficiency. Thermal and electrical losses occur in the cesium, while the reduction of cathode and anode work functions allows more efficient operation. As the pressure of cesium is increased from zero, the efficiency is increased reaching a maximum. Above this critical value of cesium pressure, the efficiency decreases because of the increasing electrical and thermal losses in the plasma. The attainment of maximum efficiency depends critically upon establishing the optimum cesium pressure. The use of a cathode material possessing a larger affinity for cesium would make possible lower cesium

pressure to obtain a given work function. The plasma losses would then be lower. The net result would be a higher efficiency of operation. In short, the use of a cathode material of higher affinity for cesium will result in increased efficiency. It can be shown that the converse is also true. Thus, consideration of the cesium affinity is of considerable importance in the selection of a cathode material.

From examination of the operating characteristics of thermionic converters (such as Fig. 12), it is seen that efficiency is a relatively insensitive function of anode and cathode temperature and of spacing. The cesium pressure, on the other hand, is quite a critical parameter and should be controlled very closely. The lead and load resistances are also critical parameters. Operation away from these critical values can decrease the efficiency by a sizeable fraction. These relationships should be carefully considered in the design of thermionic converters.

The calculations of efficiency have been checked against the results of the few experimental devices available in the literature. Where sufficient information is given to allow comparison, the agreement has been quite reasonable. While the calculations are not to be considered as exact theoretical results, the values are probably quite close to reality. While the model of the plasma is not entirely realistic and the effect of space charge has been largely ignored, the errors introduced are small in the regions of interest. Devices of 35% efficiency are clearly impractical, while a 20% efficient device can probably be built with present techniques and materials.

Further calculation and experiments dealing with the lifetime expected from such devices⁽¹¹⁾, indicate that operation can be expected for the order of many years for tungsten electrodes and about a year for molybdenum electrodes.

Data relating effective work functions as a function of cesium pressure which are necessary for calculations of the type described are extremely scarce and relatively unreliable. The obtaining of more extensive and more accurate information would allow the design of thermionic converters to be made in a relatively routine fashion.

Further data describing the effect of a partial cesium coverage on the thermal emission properties of surfaces is also of great importance.

As has been already mentioned, the model of an ohmic plasma is crude; it is, however, the only workable model available. It is therefore advisable to derive theoretically and to verify experimentally a more accurate description of the effects of the partially ionized plasma on the transport of electrons. Further, it is important to obtain a better picture of how the pressure of this partially ionized plasma effects the electronic space charge and the final potential distribution in the diode.

Causes, control and uses of the arcing mode are little understood. In order to intelligently design a thermionic diode, the designer must know how to suppress the arc if it is not desired or how to initiate it if it appears that operation in that mode is desirable.

It is possible that a criterion other than efficiency should be used for a particular application. For example, in a satellite power supply, maximum power to weight ratio would be required. Such calculations can be done in a manner directly analogous to that described here if the total weight of the system can be calculated. Since the thermionic elements themselves are of negligible relative weight, this means that about every operating point of the diode a complete power system must be designed to maximize the power to weight ratio. This is at present an impossible task. However, on the basis of some simple, not unreasonable, assumptions, calculations have been carried out and published⁽¹¹⁾ for a particular system of a nuclear reactor and radiator. In that publication, it was demonstrated how the ratio of output power to radiator weight alone could be maximized.

Other criterion could be power per volume, peak power density, etc. However, regardless of the criterion used, the problems pointed out here exist and must be solved before a better model of the thermionic diode can be constructed.

Bibliography

1. D. K. Coles, Westinghouse Research Report 60-94469-2-R1, June 16, 1954.
2. (a) N. S. Rasor, J. Appl. Phys. 31, 163 (1960);
 (b) J. M. Houston, J. Appl. Phys. 30, 481 (1959);
 (c) J. H. Ingold, J. Appl. Phys. 32, 769 (1961);
 (d) A. Schock, J. Appl. Phys. 32, 1564 (1961);
 (e) G. N. Hatsopolous and J. Kaye, Proc. I.R.E. 46, 1574 (1958);
 (f) "Direct Conversion of Heat to Electricity," edited by J. Kaye and J. A. Welsh, John Wiley and Sons, Inc.; New York (1960).
3. U. S. Patent No. 2,980,819 issued to G. R. Feaster, April 18, 1961.
4. W. B. Nottingham, "Thermionic Emission," HANDBUCH DER PHYSIK 21, Springer-Verlag, Germany (1956).
5. H. F. Webster, J. Appl. Phys. 30, 488 (1959).
6. (a) M. Jakob, Heat Transfer, John Wiley and Sons, Inc.; New York (1957), Vol. II, Chap. 31.
 (b) A. E. Fein, Rev. Sci. Inst. 31, 1008 (1960).
7. J. B. Taylor and I. Langmuir, Phys. Rev. 44, 432 (1933).
8. W. B. Nottingham, Tech. Rept. 373, Research Laboratory of Electronics, The Massachusetts Institute of Technology (1960).
9. W. E. Forsythe and E. M. Watson, J. Opt. Soc. of Amer. 24, 114 (1934).
10. Unpublished Research, M. Gottlieb and R. Zollweg.
11. L. S. Richardson, A. E. Fein, M. Gottlieb, G. A. Kemeny and R. J. Zollweg, paper presented at Technical Conference of the AIME, Los Angeles, Calif., Aug. 30-Sept. 1, 1961. Proceedings to be published. Also, see Westinghouse Scientific Paper 918E901-P2 (Oct. 13, 1961).

Table 1

CATHODE MATERIAL -		ANODE MATERIAL -		DATE 2/ 3/61		PAGE 384.1	
CATHODE SPACING = 0.01250 CM PLASMA BATH TEMPERATURE = 560.0 DEG K PLASMA PRESSURE = 1.274 MM PLASMA ELECTRICAL RESISTANCE = 4.246E-02 OHMS PLASMA THERMAL CONDUCTANCE = 5.653E-03 WATT/DEG K CATHODE-TEMP.=1900.0 DEG K, EMISSIVITY= 0.248, CHEM. POTENTIAL=2.961 VOLT, SAT. CURR.=6.048E 00 AMP/SQ.CM HEAT LOST BY SUPPORTS =-0. WATTS LIFETIME = 3.57E 07 DAYS							
HEAT OF VAPORIZATION = 200.0 KCAL/MOLE							
TEMP-A	600.0	800.0	950.0	950.0	1000.0	1050.0	1100.0
TLCAD	ACC.0	ACC.0	ACC.0	ACC.0	ACC.0	ACC.0	ACC.0
CHPT-A	1.8011	1.8011	1.8011	1.7633	1.7061	1.6371	1.5975
SAIJ-A	3.20E-08	3.45E-04	1.81E-03	1.29E-02	9.61E-01	2.22E 00	6.95E 00
NETSAT	6.05E 00	6.05E 00	6.05E 00	6.03E 00	5.95E 00	5.87E 00	-9.00E-01
EMIS-A	0.0520	0.0740	0.0810	0.0890	0.0970	0.1050	0.1210
VIEAFN	0.0449	0.0604	0.0650	0.0701	0.0750	0.0839	0.0927
RACFET	3.29E 00	4.33E 00	4.61E 00	4.92E 00	5.19E 00	5.62E 00	5.93E 00
CCVLT	4.2799	2.7597	2.4883	2.2039	1.9330	1.7015	1.5055
FLTVLT	1.1599	1.1599	1.1599	1.1977	1.2549	1.3411	1.3635
ITATVLT	1.1924	1.1920	1.1914	1.2239	1.2709	1.3079	1.3293
FORCLP	4.96E 00	4.97E 00	4.99E 00	5.15E 00	5.49E 00	6.05E 00	6.05E 00
BAKCLP	3.20E-08	3.45E-04	1.81E-03	1.29E-02	9.61E-01	2.22E 00	6.95E 00
NETCLP	4.2799	4.97E 00	4.99E 00	5.15E 00	5.49E 00	6.05E 00	6.05E 00
RCLP	1.63E-02	1.58E-02	1.55E-02	1.52E-02	1.47E-02	1.45E-02	1.45E-02
PLVCRP	2.11E-01	2.11E-01	2.12E-01	2.18E-01	2.29E-01	2.34E-01	2.34E-01
LDVCRP	3.16E-02	7.85E-02	7.75E-02	7.81E-02	7.94E-02	7.97E-02	7.97E-02
EXTVLT	9.00E-01	9.03E-01	9.02E-01	9.27E-01	9.63E-01	9.90E-01	1.04E 00
CCND#	1.85E-03	2.09E-03	2.16E-03	2.25E-03	2.36E-03	2.45E-03	2.52E-03
LDTHC	2.41E 00	2.29E 00	2.27E 00	2.25E 00	2.24E 00	2.20E 00	2.20E 00
PLTHNC	7.35E 00	6.22E 00	5.94E 00	5.65E 00	5.37E 00	5.09E 00	4.81E 00
PU	2.9935	2.9911	2.9925	2.9872	2.9770	2.9610	2.9610
CC	1.65E 01	1.65E 01	1.66E 01	1.71E 01	1.81E 01	1.99E 01	1.99E 01
CA	9.91E-03	1.02E-03	5.68E-03	4.07E-02	3.02E-01	1.67E 00	4.82E 00
CCCL	1.06E 01	1.06E 01	1.06E 01	1.08E 01	1.10E 01	1.10E 01	9.16E 00
JCLLEF	5.22E-01	5.24E-01	5.28E-01	5.61E-01	6.17E-01	6.46E-01	6.32E-01
JCLLEL	2.02E-01	1.93E-01	1.93E-01	2.01E-01	2.14E-01	2.20E-01	2.20E-01
PCWIN	2.32E 01	2.86E 01	2.86E 01	2.91E 01	2.98E 01	3.01E 01	2.67E 01
PCWCLT	4.45E 00	4.48E 00	4.50E 00	4.77E 00	5.19E 00	5.46E 00	4.69E 00
EFF	15.51	15.67	15.70	16.38	17.41	18.15	17.58
MCDE	U	U	U	U	U	F	D

Explanation on pages following

Explanation of Table 1

Many of the figures presented in the table (which is a direct reproduction of the computer output) are in what is known as "E-notation." That is, a number written as $3.45\text{E}-05 = 3.45 \times 10^{-5}$ or $2.47\text{E} 01 = 2.47 \times 10^1$, etc.

There are 10 columns in the table, each corresponding to a diode with the anode temperature given on the first line. The values printed in the heading of the table pertain to all 10 of the diodes.

Defined in terms of the quantities in this report, the symbols in the left-hand column are as follows. Because of the calculations having been done for a unit area of cathode, the units of the tabulated quantities may not appear consistent; but they are:

TEMP-A = T_a = anode temperature (deg K)

TLOAD = temperature of load which in these calculations and in the paper was assumed equal to T_a .

CHPT-A = ϕ_a = anode work function (volts)

SATJ-A = J_{as} = anode saturation current density (amp/cm^2)

NETSAT = $J_{cs} - J_{as}$ = net saturation current density (amp/cm^2)

EMIS-A = ϵ_a = thermal emissivity of anode

VIEWFN = F = view function

RADHET = W = heat radiated thermally (watts/cm^2)

OCVLT = V_{oc} = open circuit voltage (volts)

FLTVLT = $\phi_c - \phi_a$ = internal voltage in flat mode (volts)

INTVLT = V = internal voltage (volts)
 FORCUR = J_c = forward current density (amps/cm²)
 BAKCUR = J_a = back current density (amps/cm²)
 NETCUR = J = net current (amps/cm²)
 RLD* = \bar{R}_L = optimum lead resistance for 1 cm² cathode (ohms)
 PLVDRP = JR_p = voltage drop in plasma (volts)
 LDVDRP = $J\bar{R}_L$ = voltage drop in optimized leads (volts)
 EXTVLT = JR_{load} = external voltage applied to optimized load (volts)
 COND* = \bar{K}_L = thermal conductivity of optimized lead (watt-cm/deg K)
 LDTHC = $\bar{K}_L (T_c - T_a)$ = heat lost by thermal conduction down optimized leads (watts/cm²)
 PLTHMC = $K_p (T_c - T_a)$ = heat lost by thermal conduction across the plasma (watts/cm²)
 MU = ϕ = (volts)
 QC = $J_c (\phi + 2KT_c)$ (watts/cm²)
 QA = $J_a (\phi + 2KT_a)$ (watts/cm²)
 COOL = $Q_c - Q_a - JV$ (watts/cm²)
 JOULEP = $1/2 J^2 R_p$ = joule heating of plasma which is returned to cathode (watts/cm²)
 JOULEL = $1/2 J^2 \bar{R}_L$ = joule heating of optimized leads which is returned to cathode (watts/cm²)

POWIN = H_{in} = heat in (watts/cm²)

POWOUT = P_{out} = power out (watts/cm²)

EFF = η = efficiency

MODE = $\left\{ \begin{array}{c} U \\ F \\ D \end{array} \right\}$ if optimum occurs in $\left\{ \begin{array}{c} \text{uphill} \\ \text{flat} \\ \text{downhill} \end{array} \right\}$ mode

D'WJ. 194A566

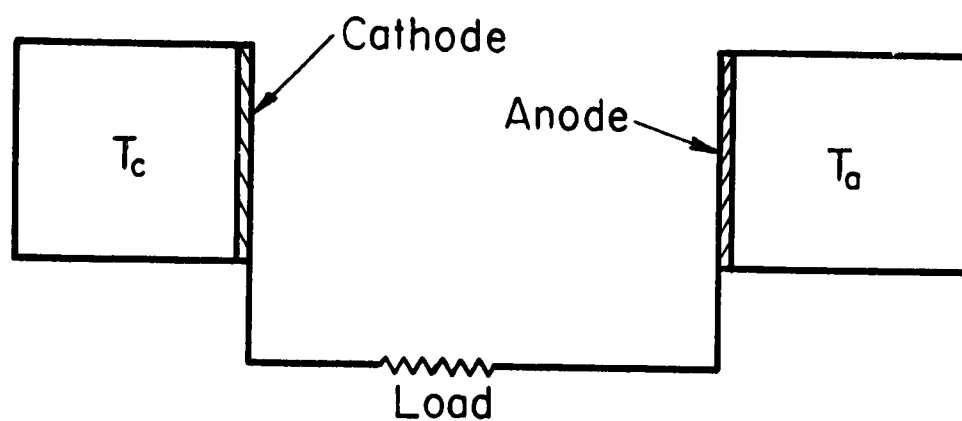


Fig. 1

Basic thermionic diode

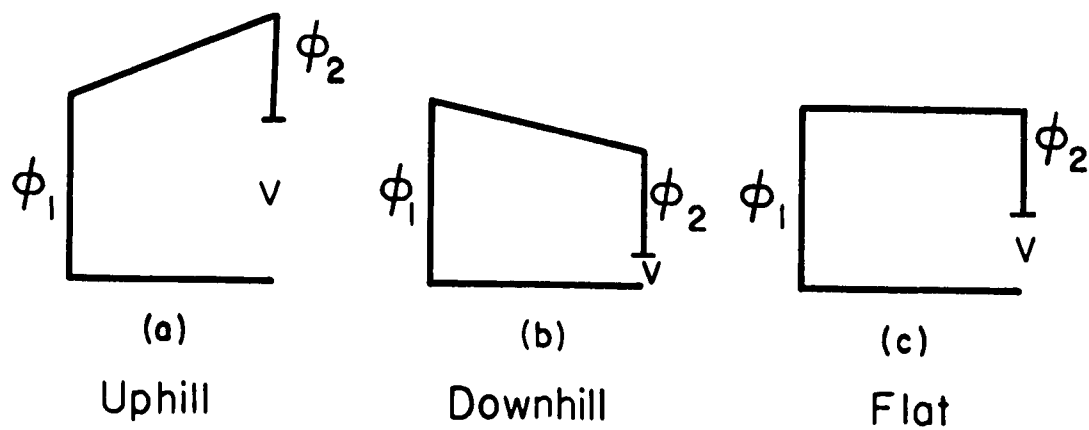


Fig. 2

Mode of operation

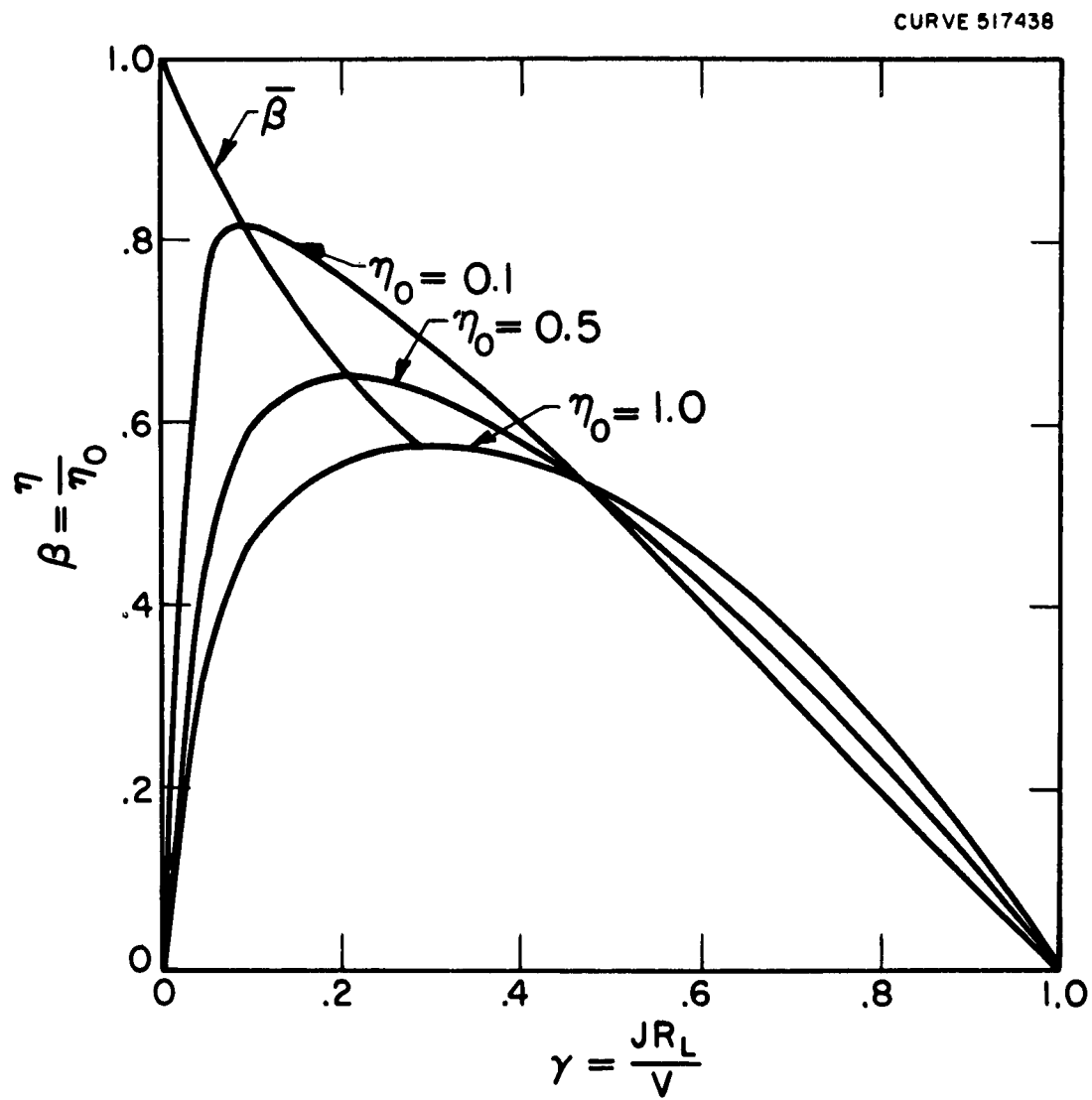


Fig. 3
 β as a function of γ and the ideal efficiency, η_0 .

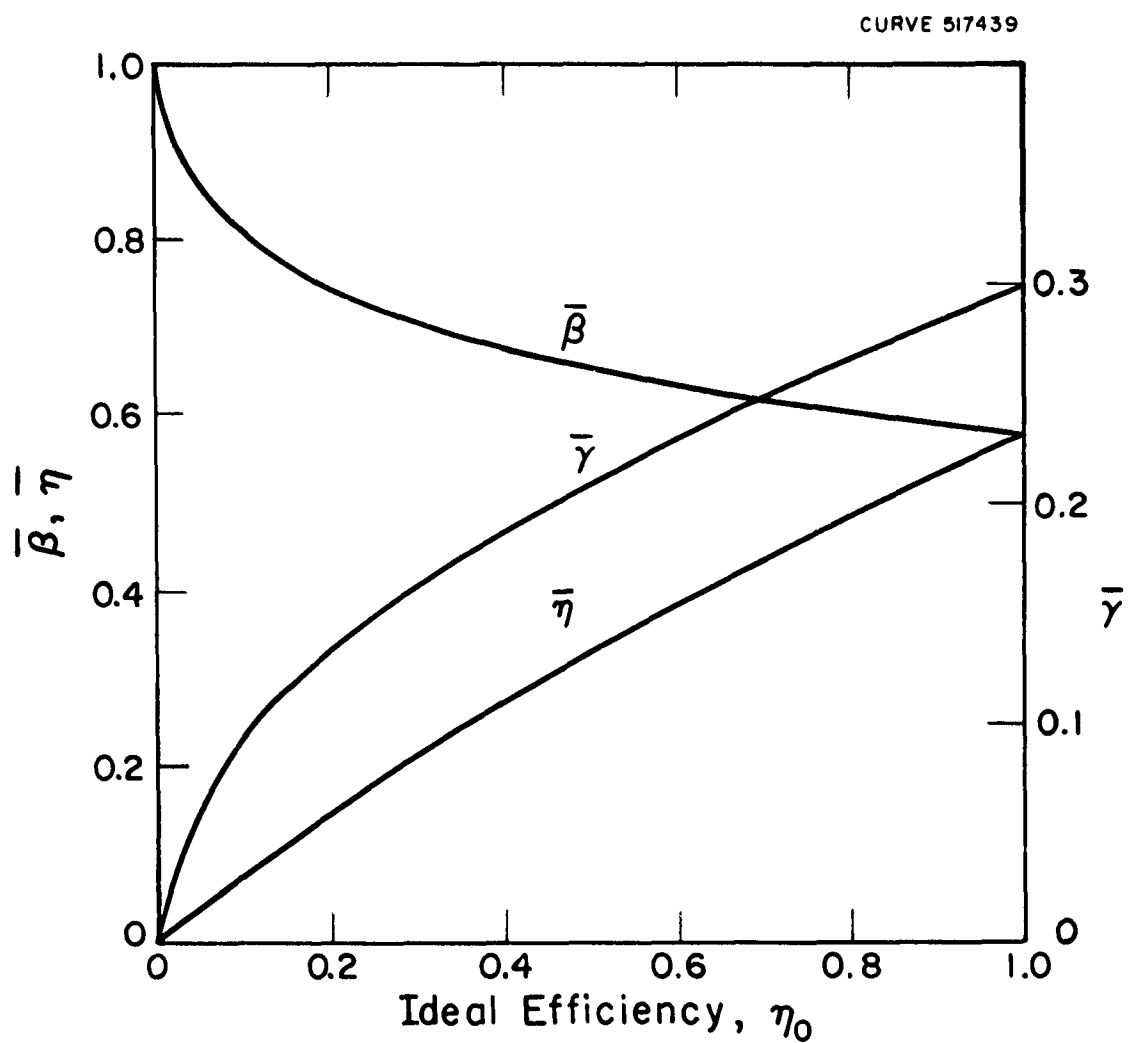


Fig. 4

Optimum values of η , γ , and β as functions of the ideal efficiency, η_0 .

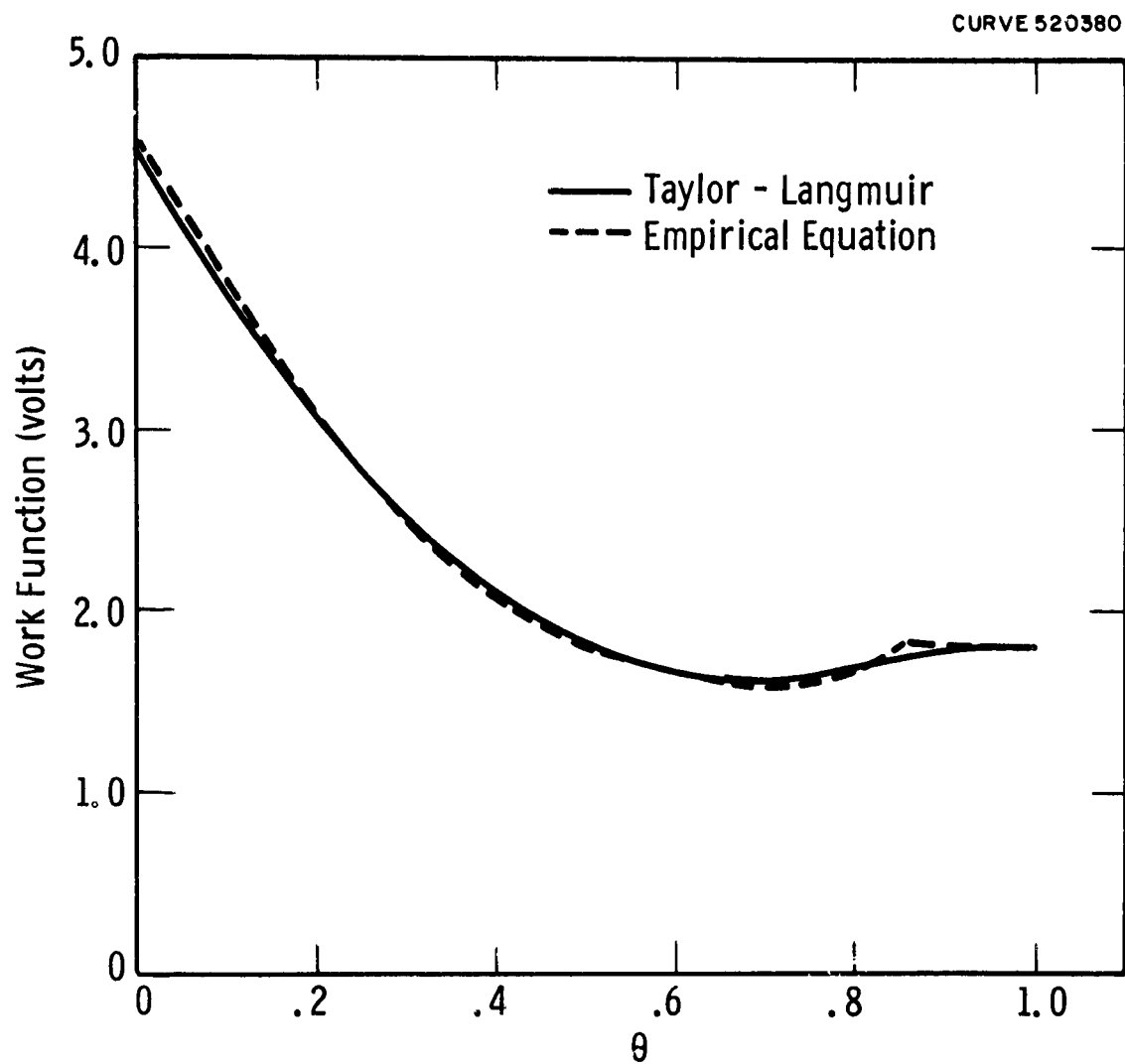


Fig. 5

Work function of tungsten as a function of fractional coverage
by cesium

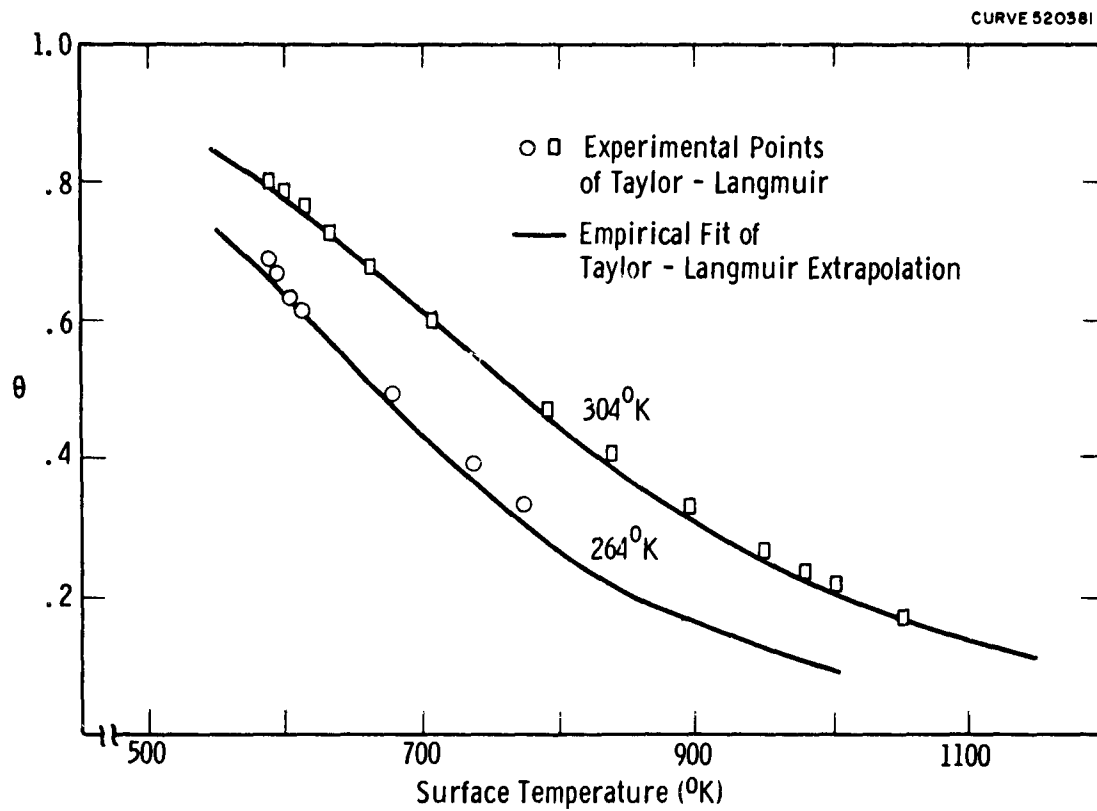


Fig. 6

Fractional coverage as a function of cesium temperature and surface temperature

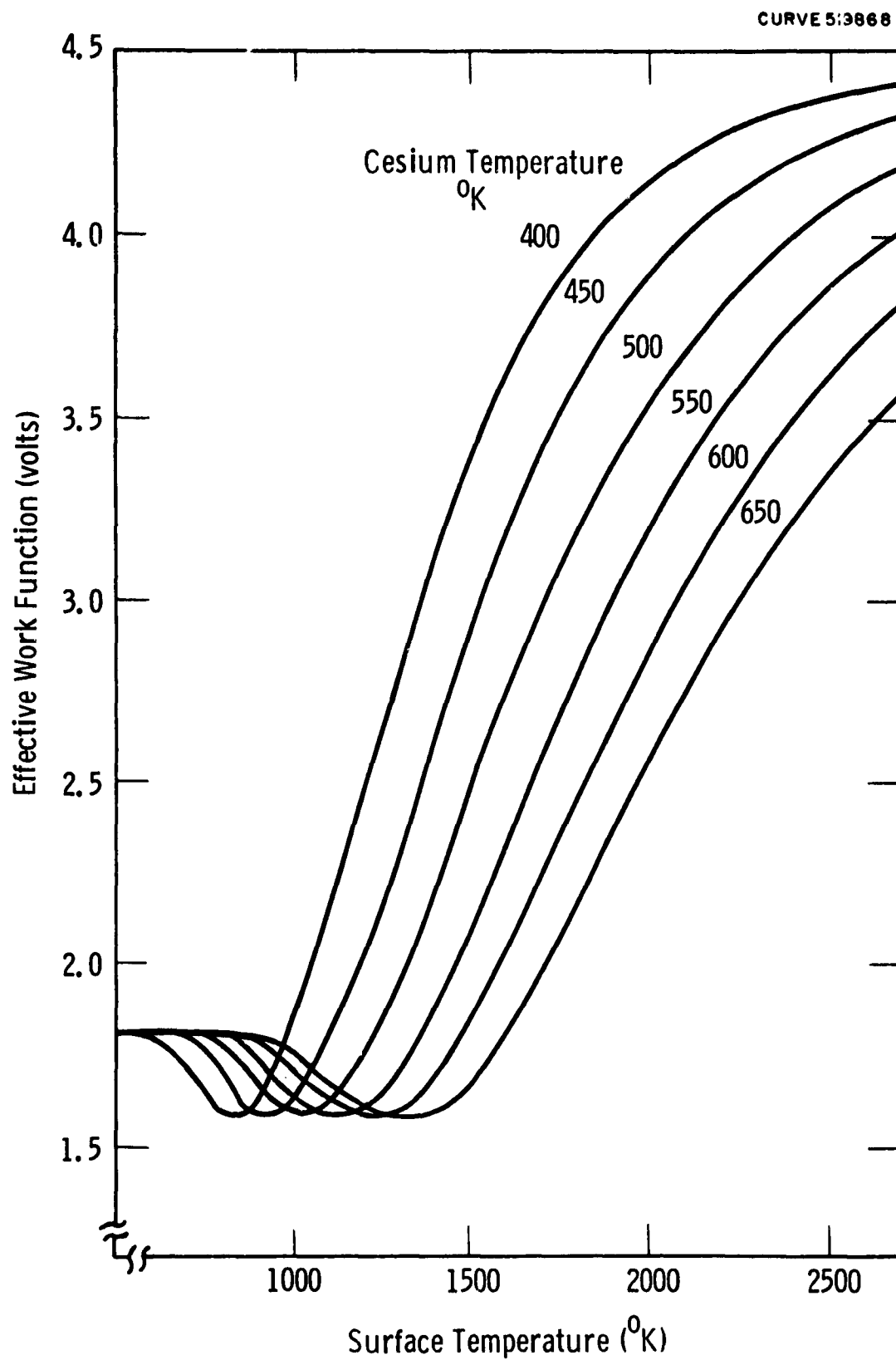


Fig. 7

Work function as a function of cesium bath temperature and surface temperature

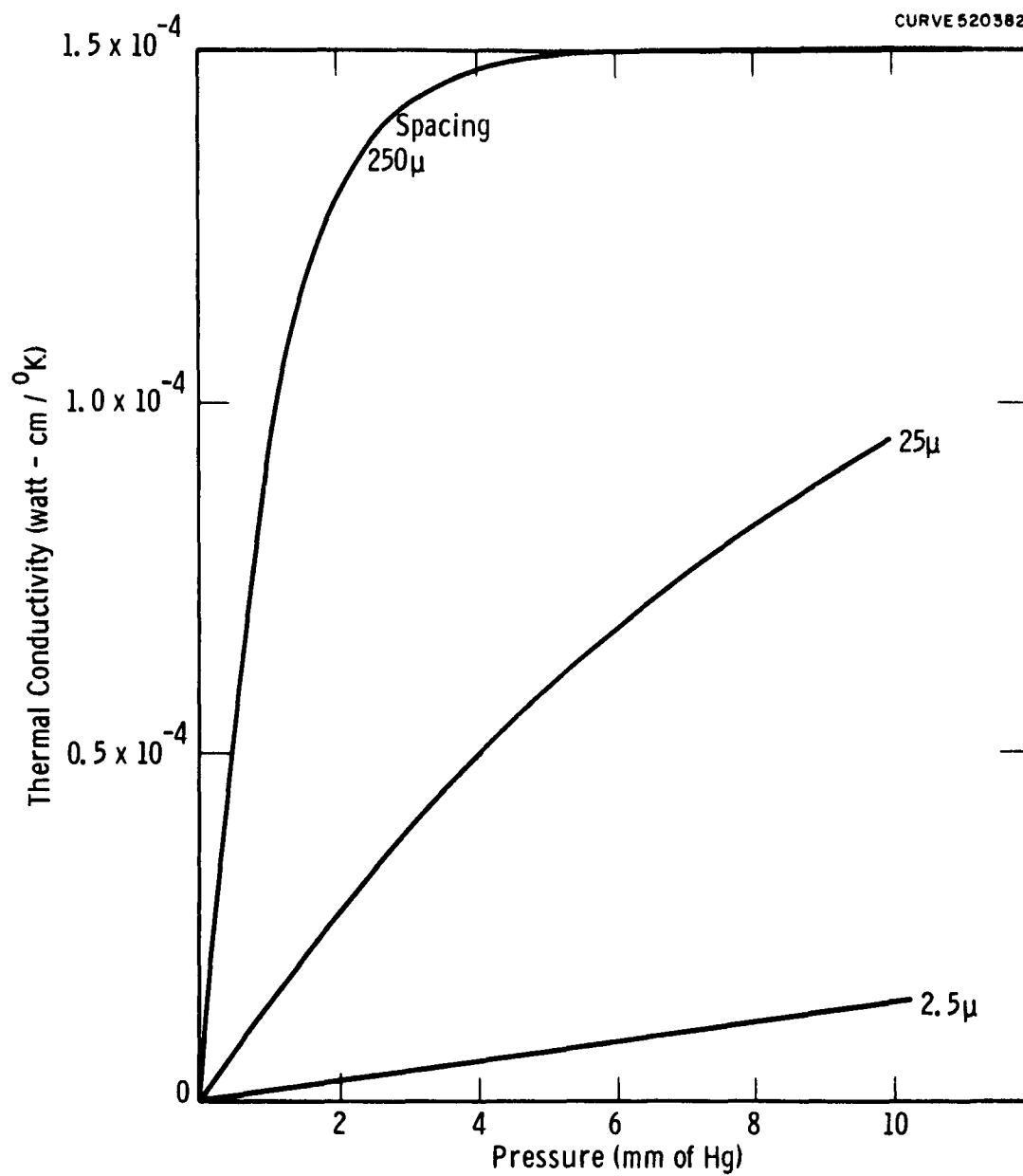


Fig. 8

Thermal conductivity of cesium plasma as a function of spacing and pressure

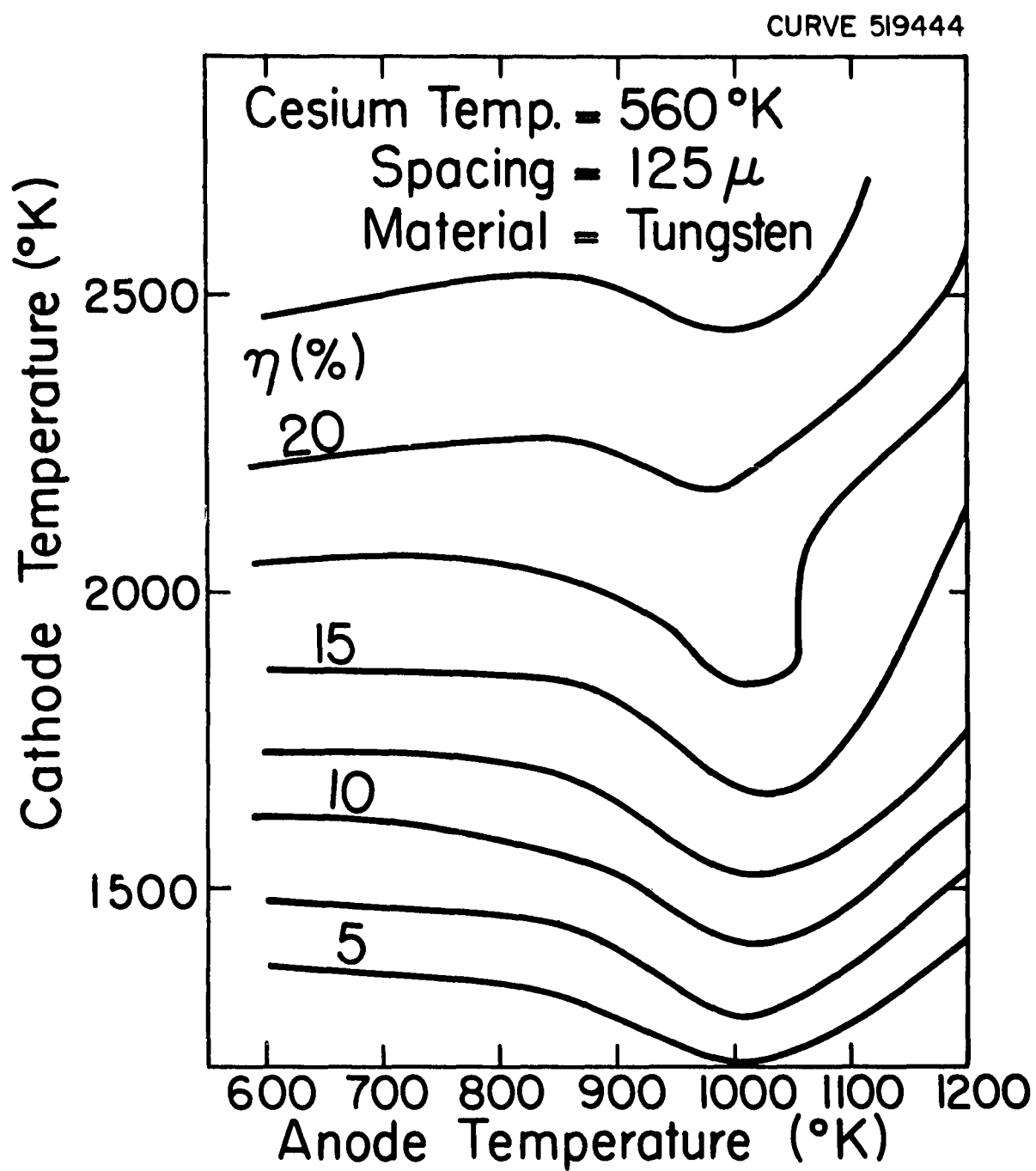


Fig. 9

Efficiency as a function of cathode and anode temperatures

CURVE 519445

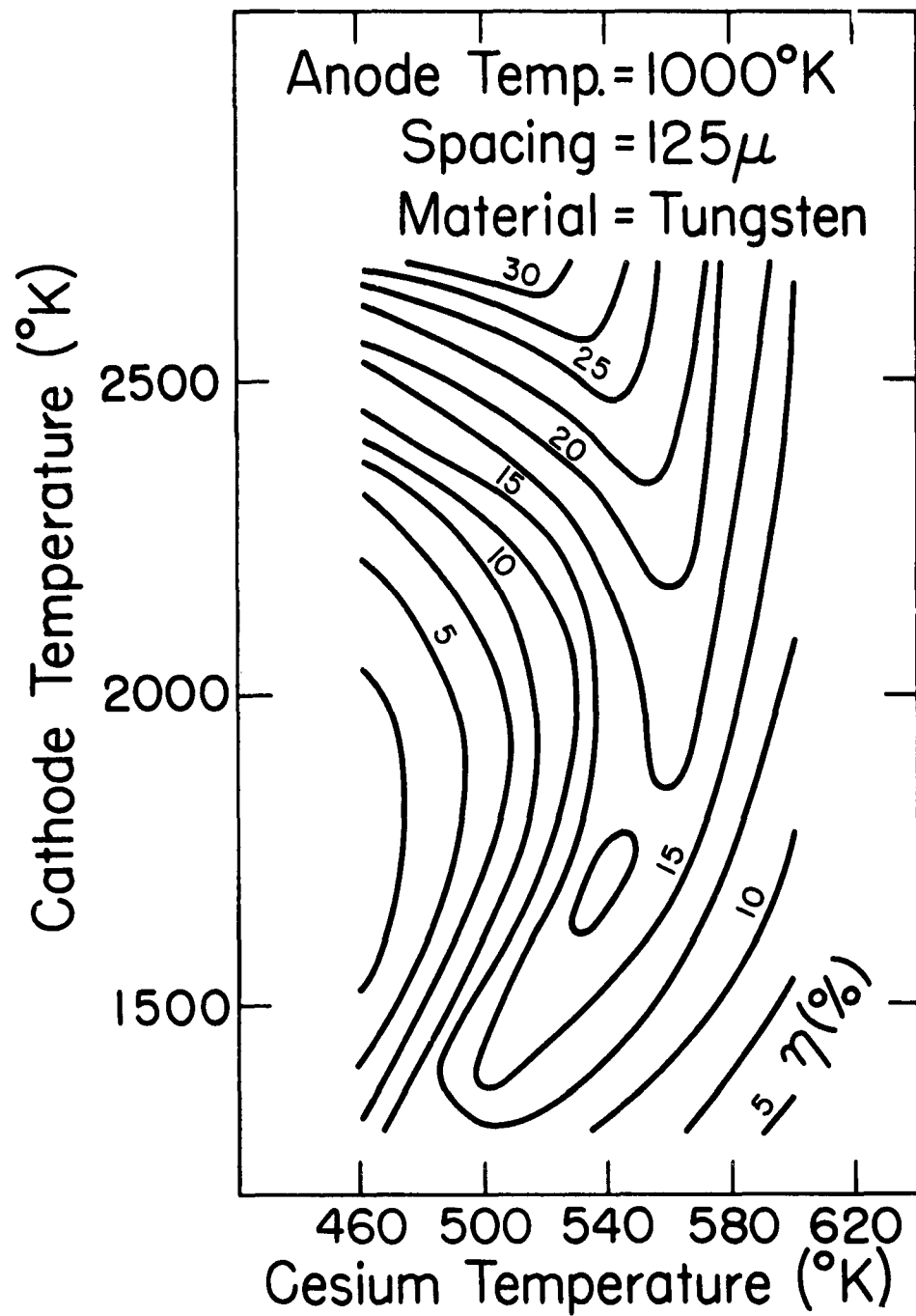


Fig. 10

Efficiency as a function of cathode and cesium temperatures

CURVE 519446

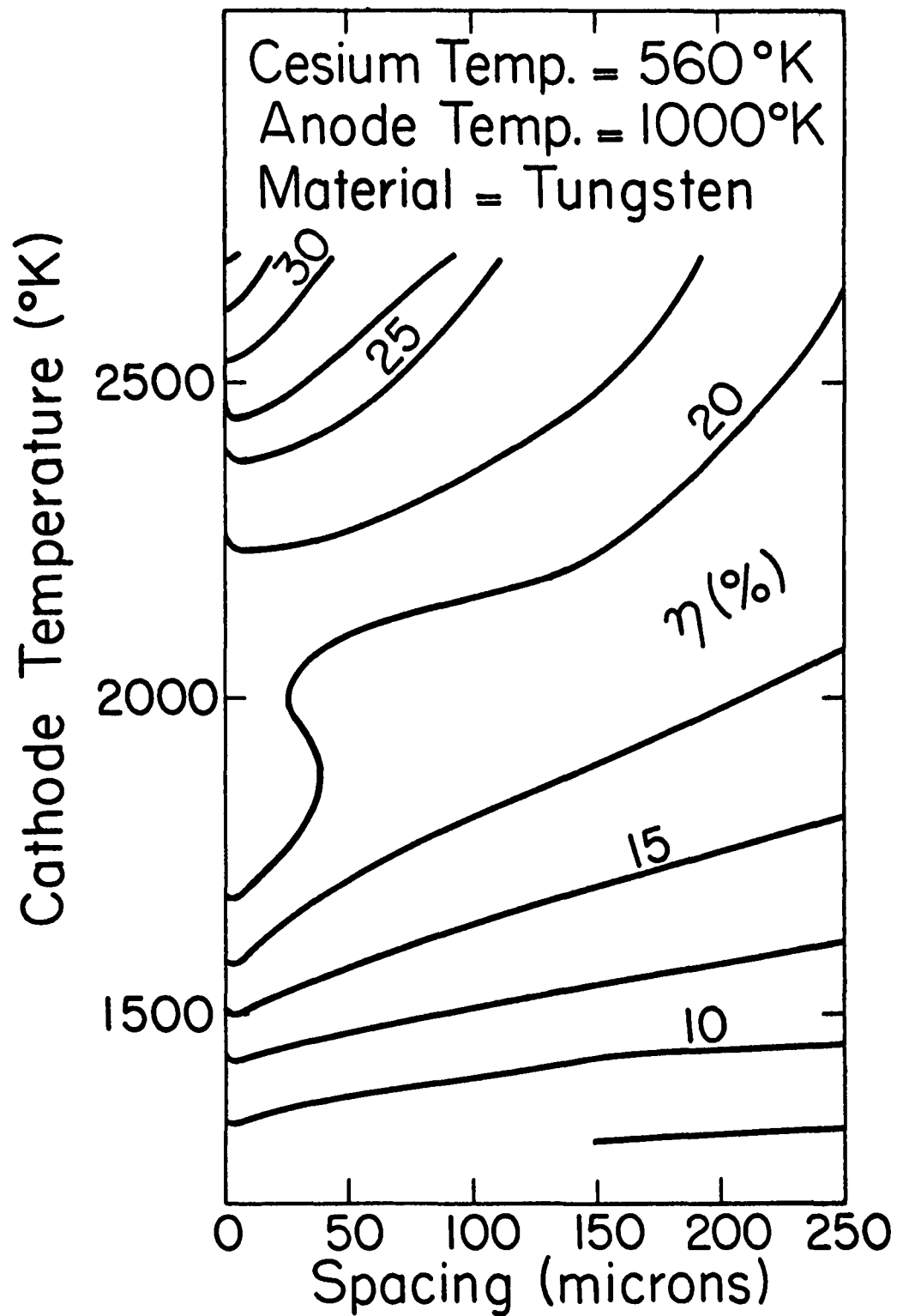


Fig. 11

Efficiency as a function of spacing and cathode temperature

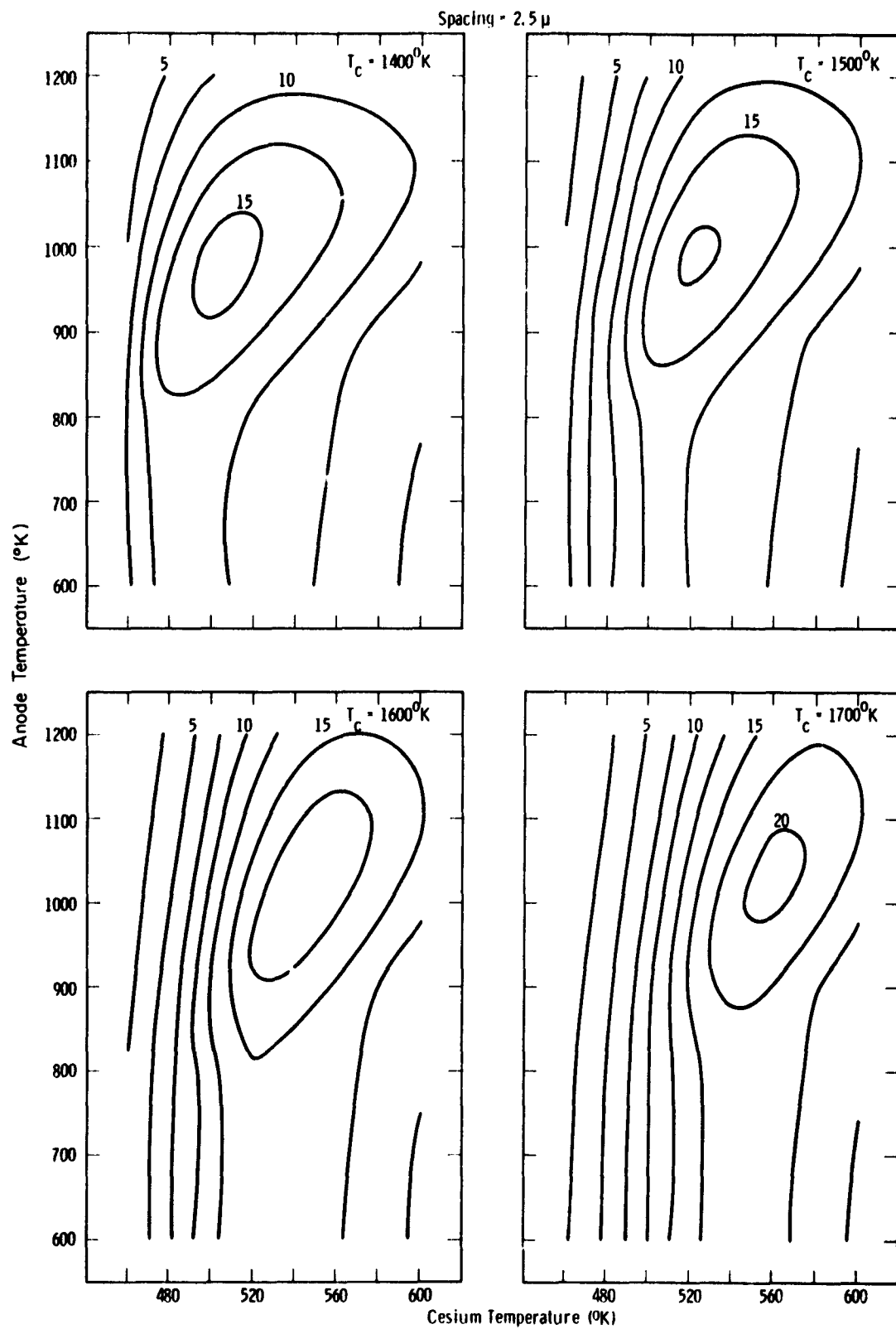


Fig. 12a

Efficiency as a Function of Spacing and Anode, Cathode, and Cesium Temperatures.

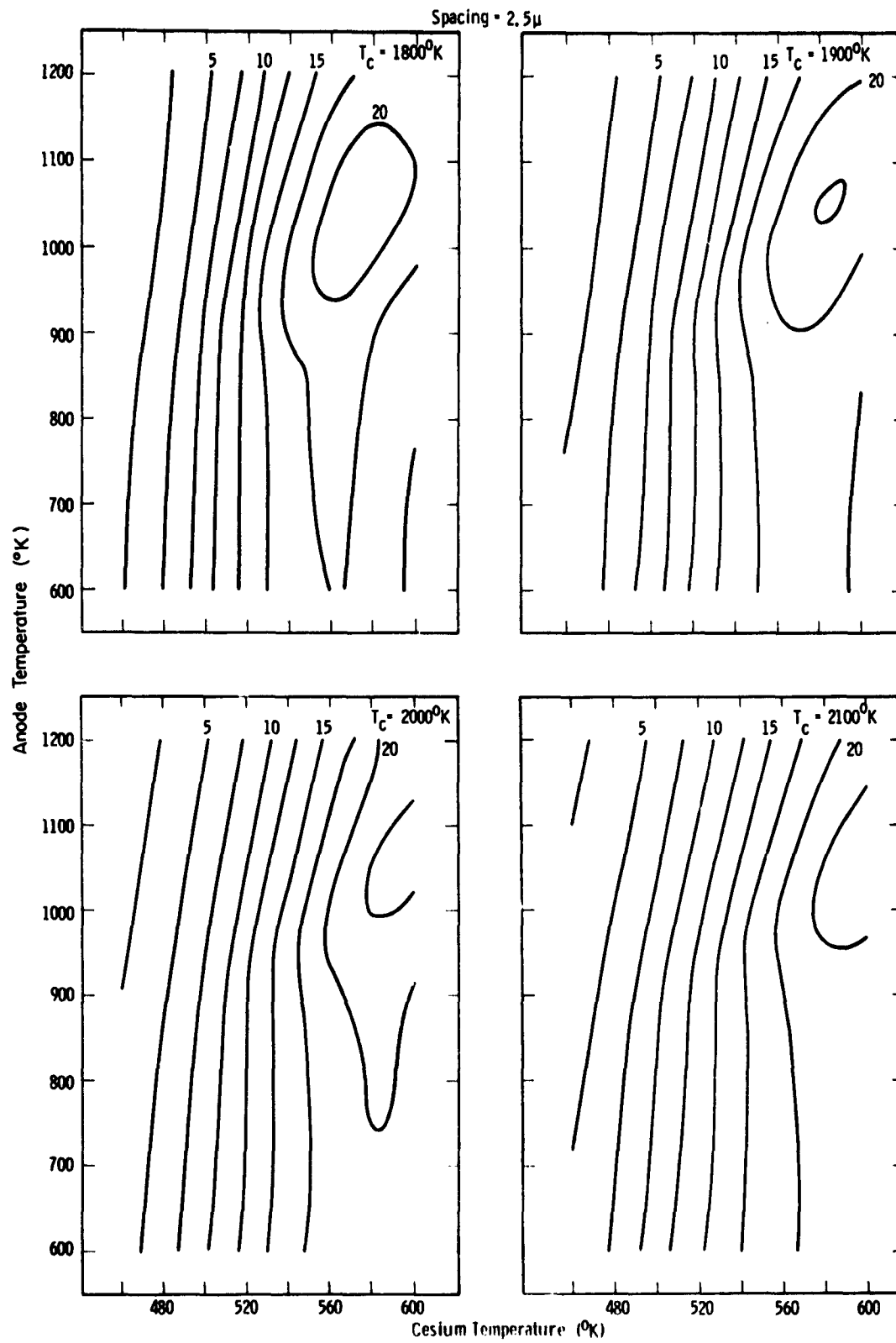


Fig. 12b

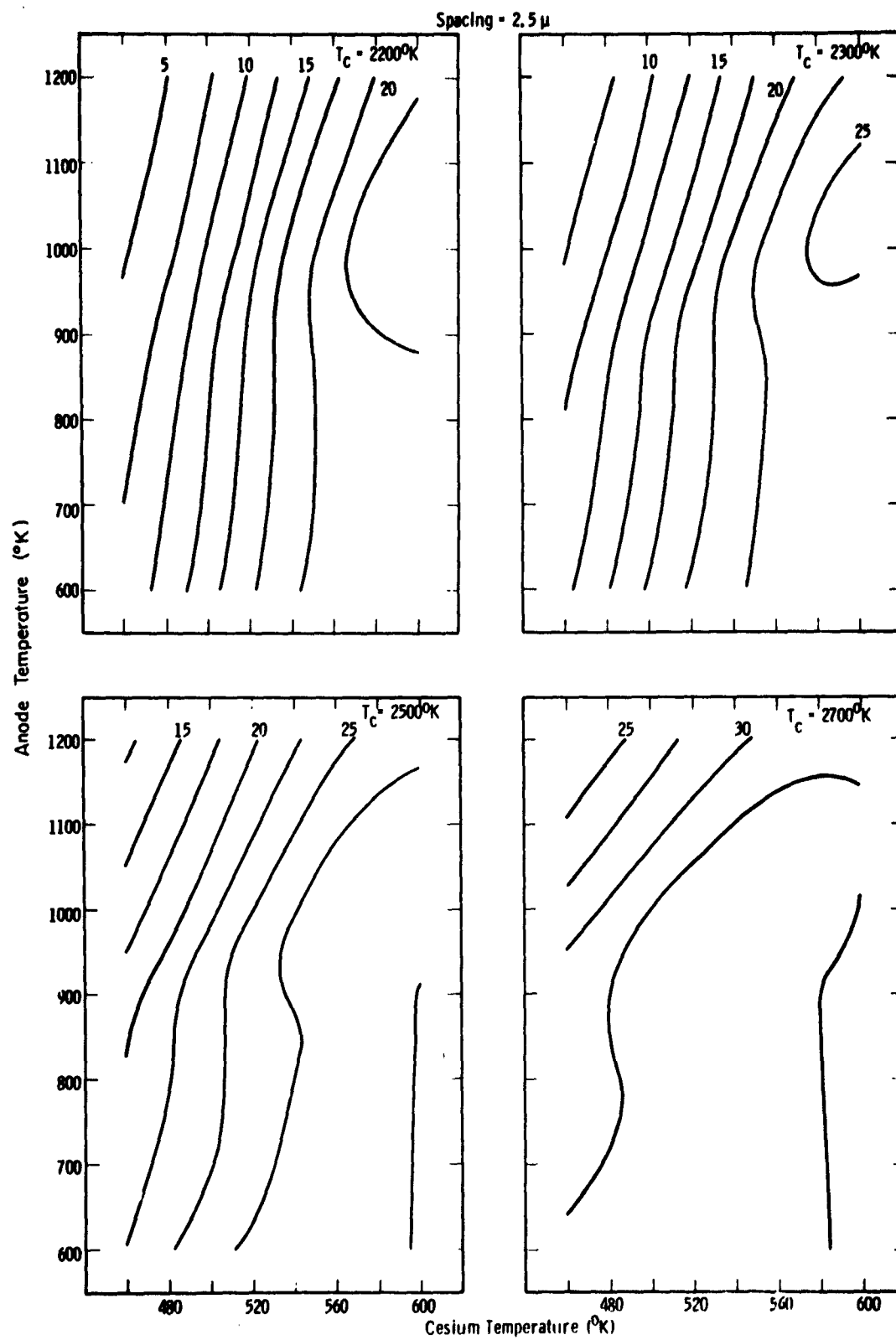


Fig. 12c

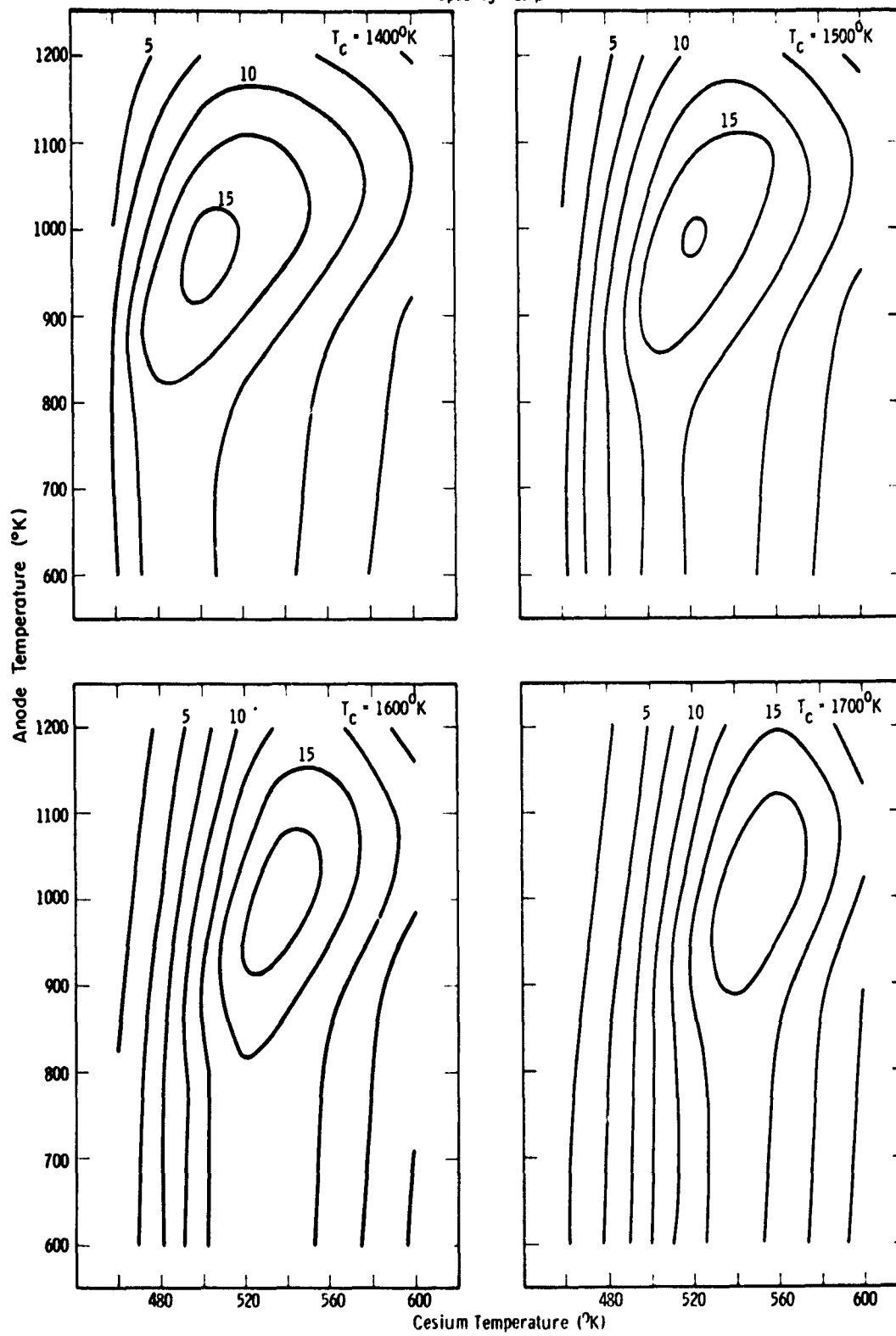
Spacing = $25\ \mu$ 

Fig. 12d

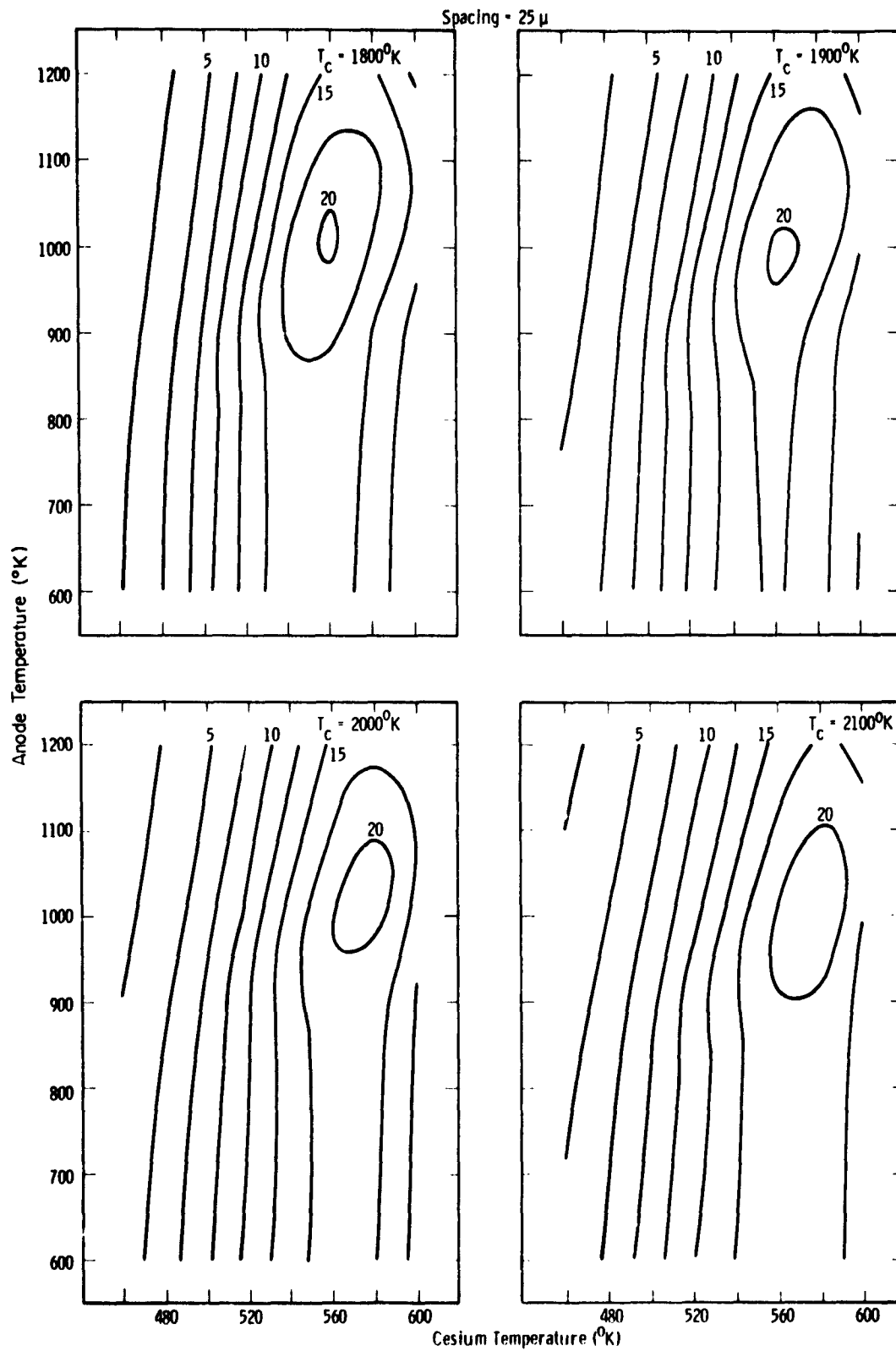


Fig. 12 e

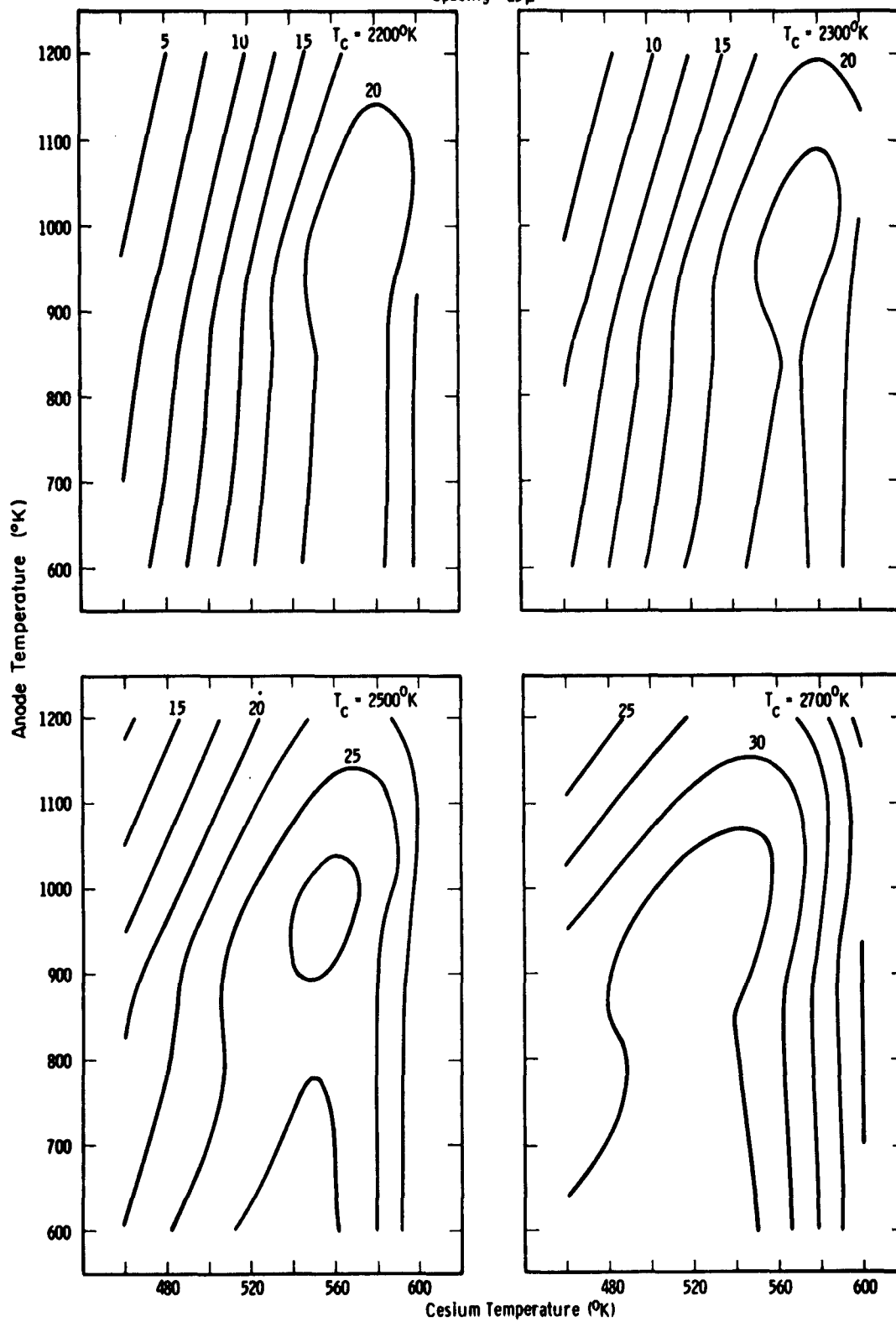
Spacing = 25 μ 

Fig. 12f

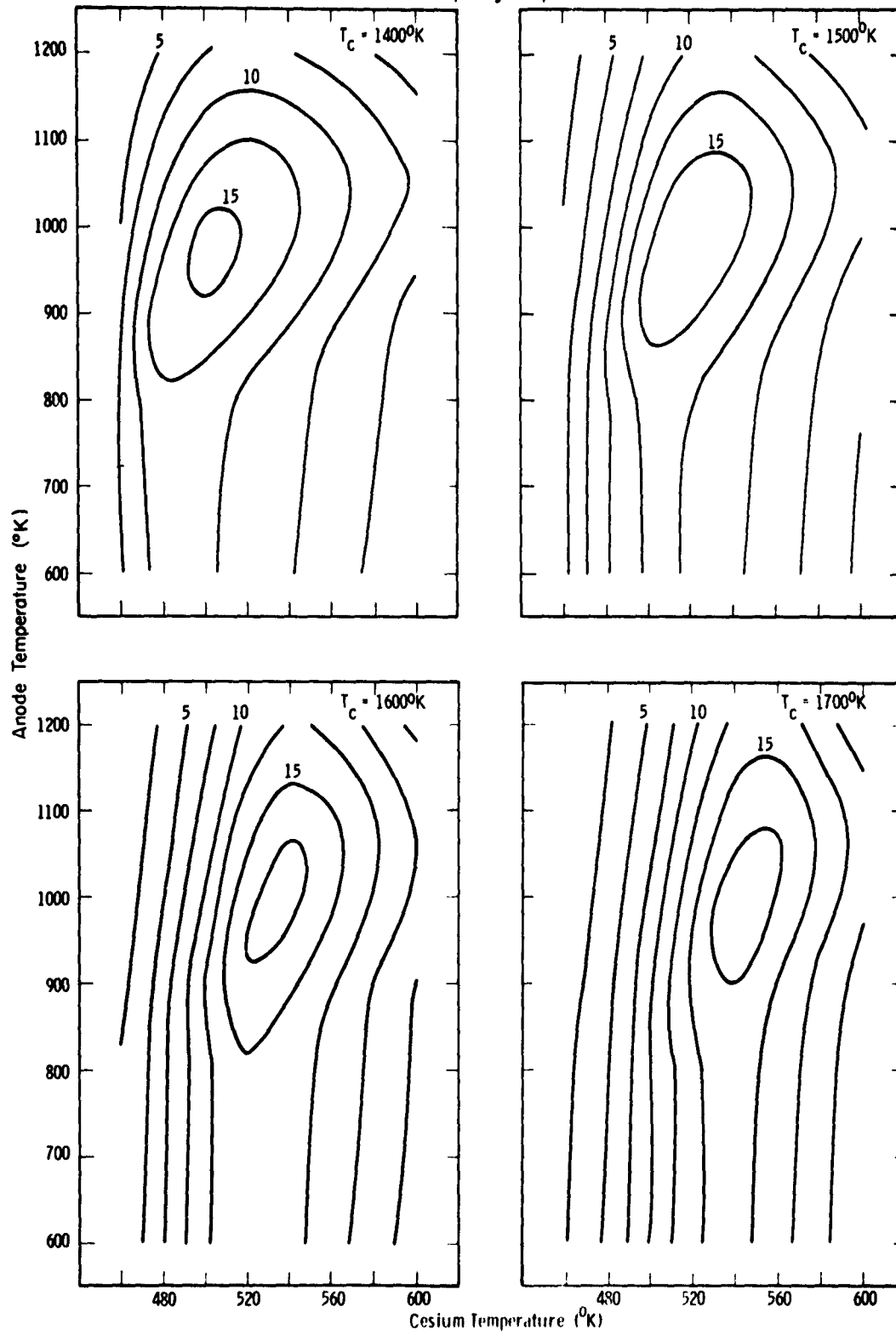
Spacing = 50 μ 

Fig. 12g

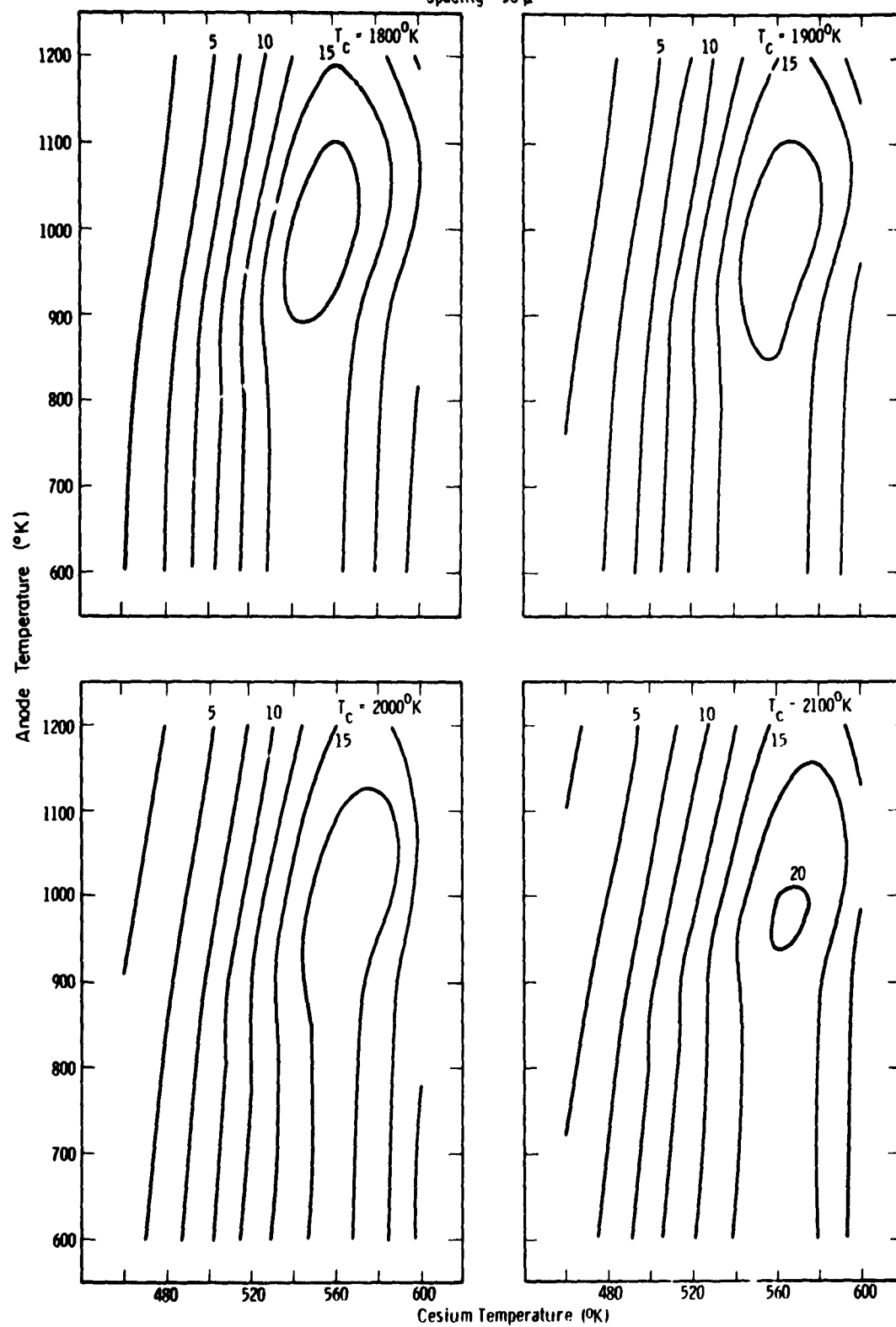
Spacing = 50 μ 

Fig. 12h

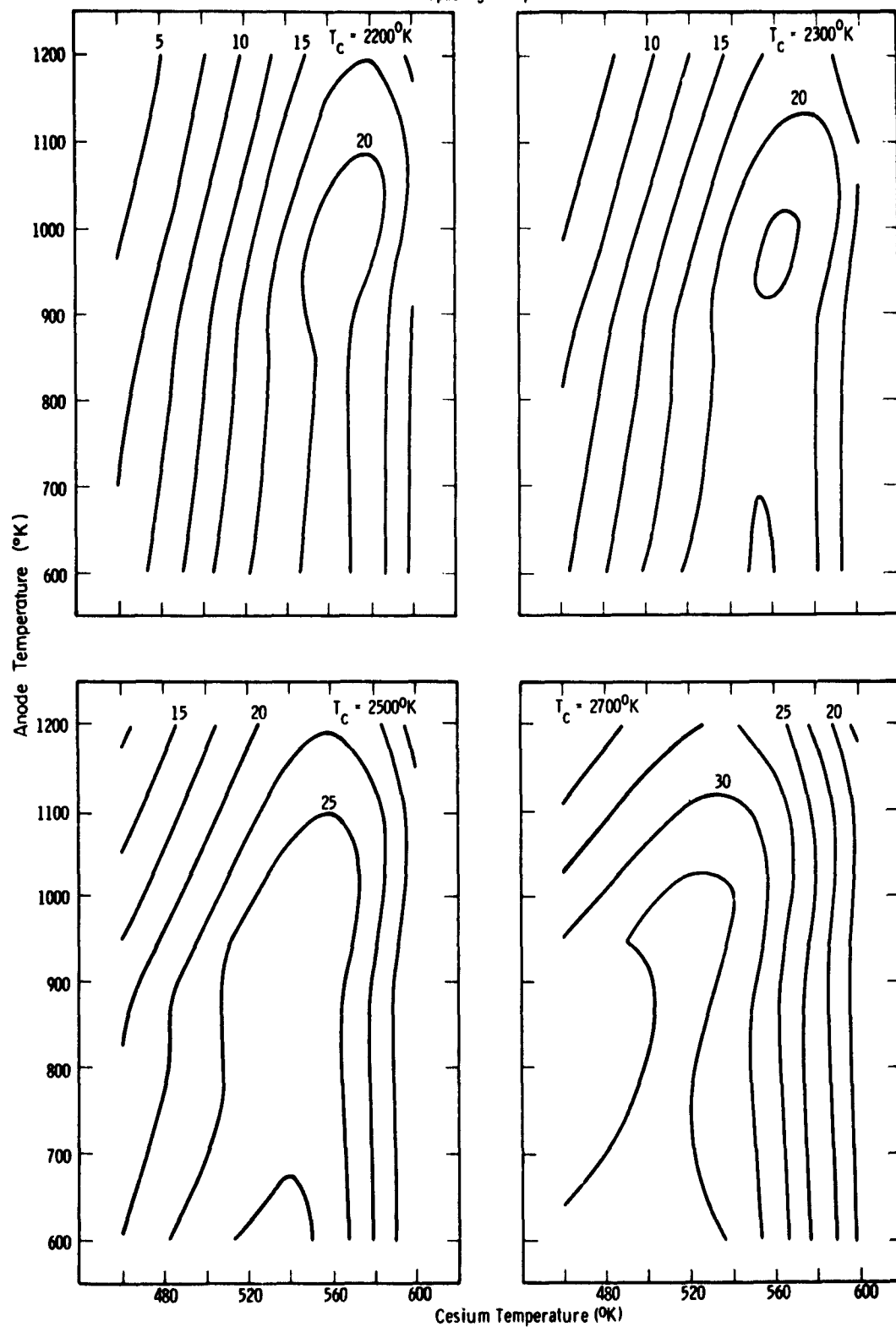
Spacing = 50 μ 

Fig. 121

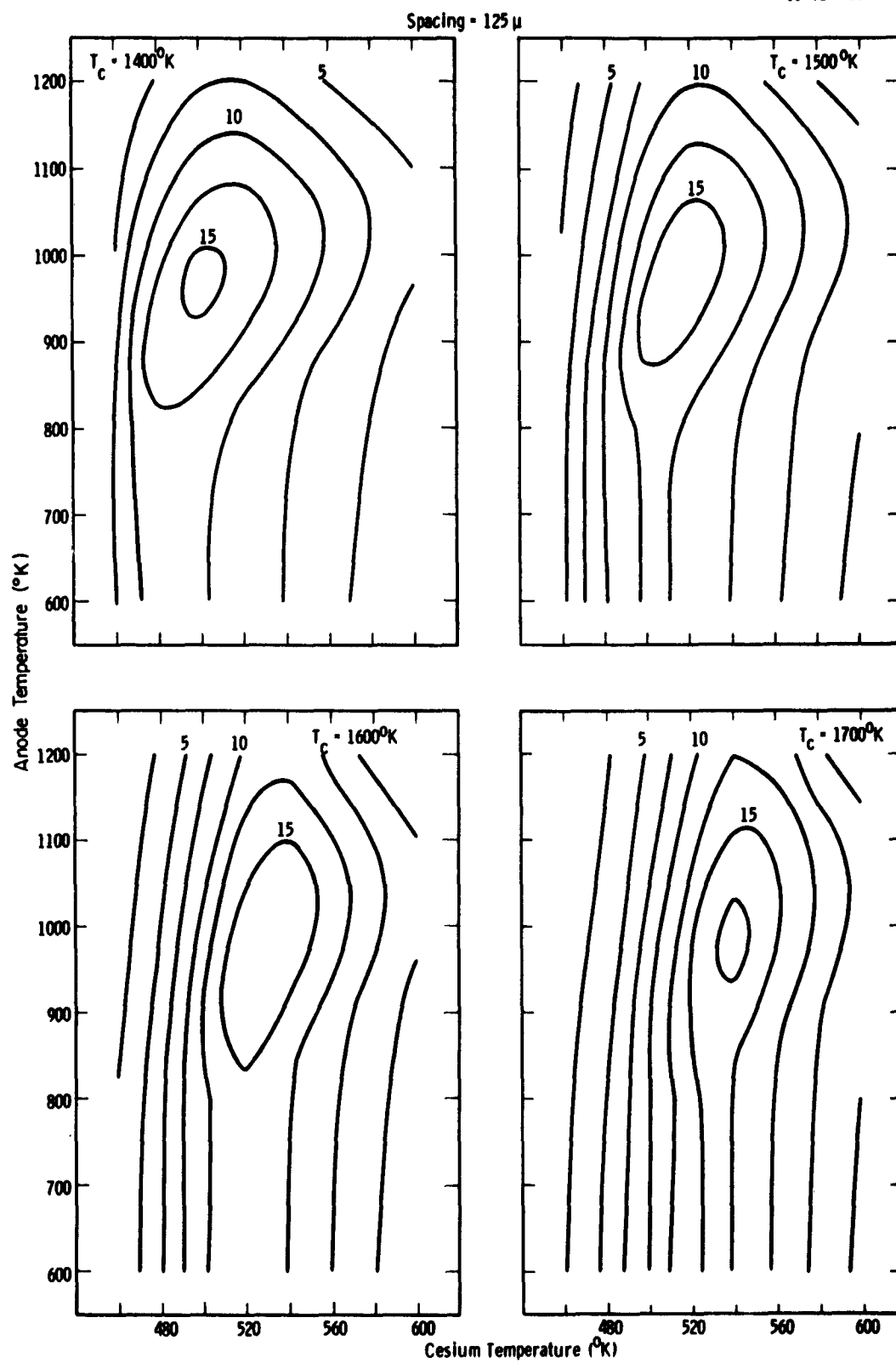


Fig. 12j

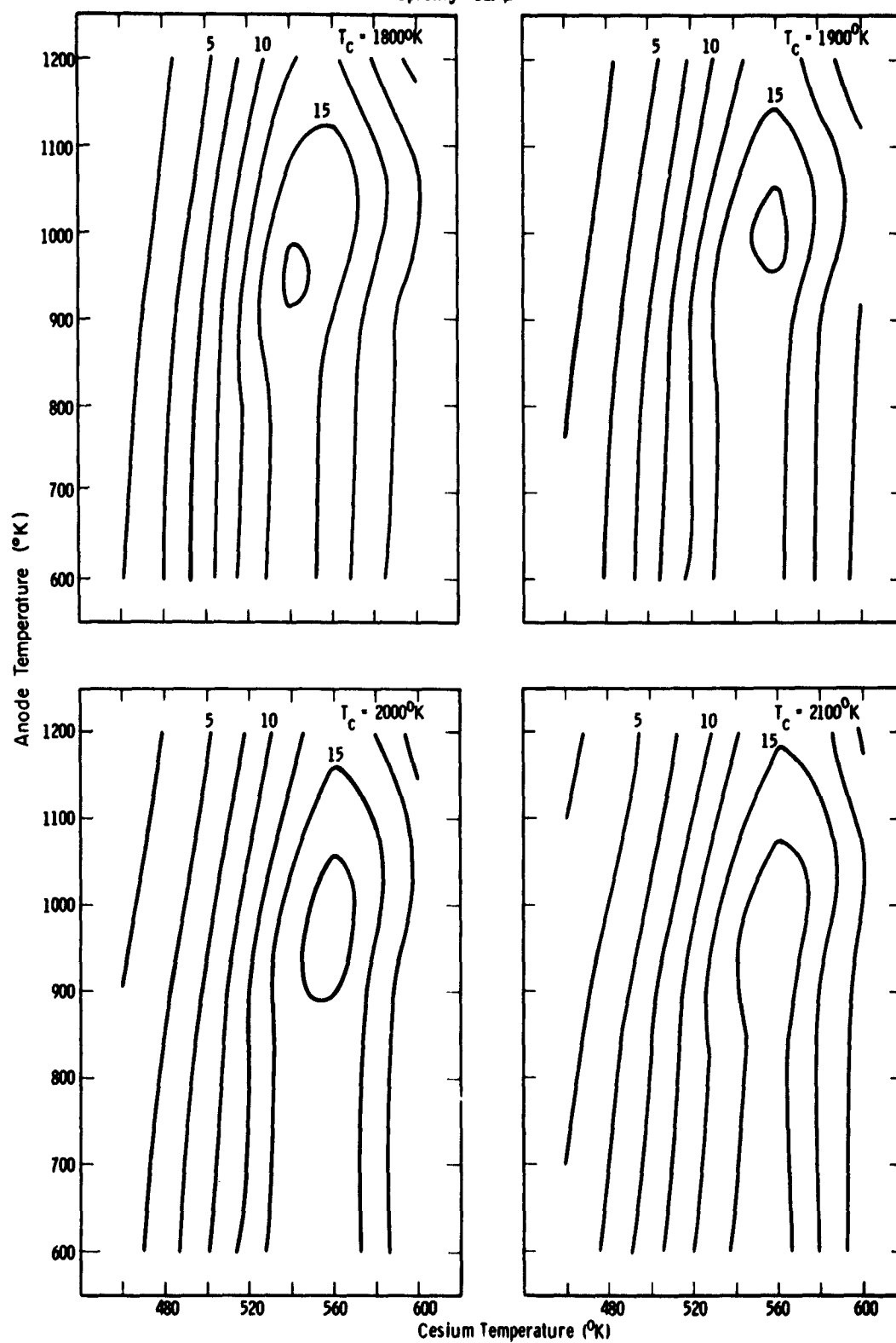
Spacing = 125 μ 

Fig. 12k

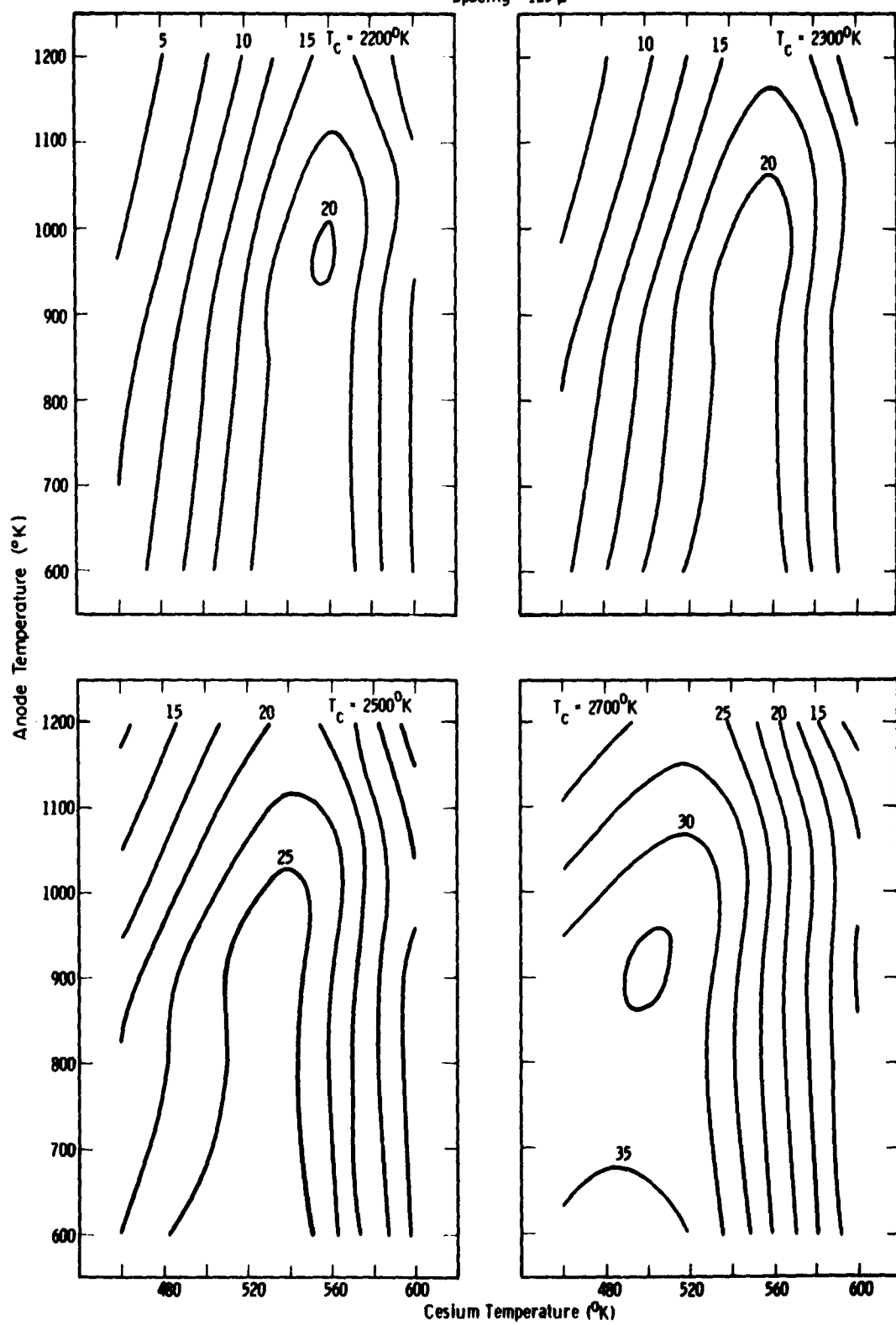
Spacing = 125 μ 

Fig. 121

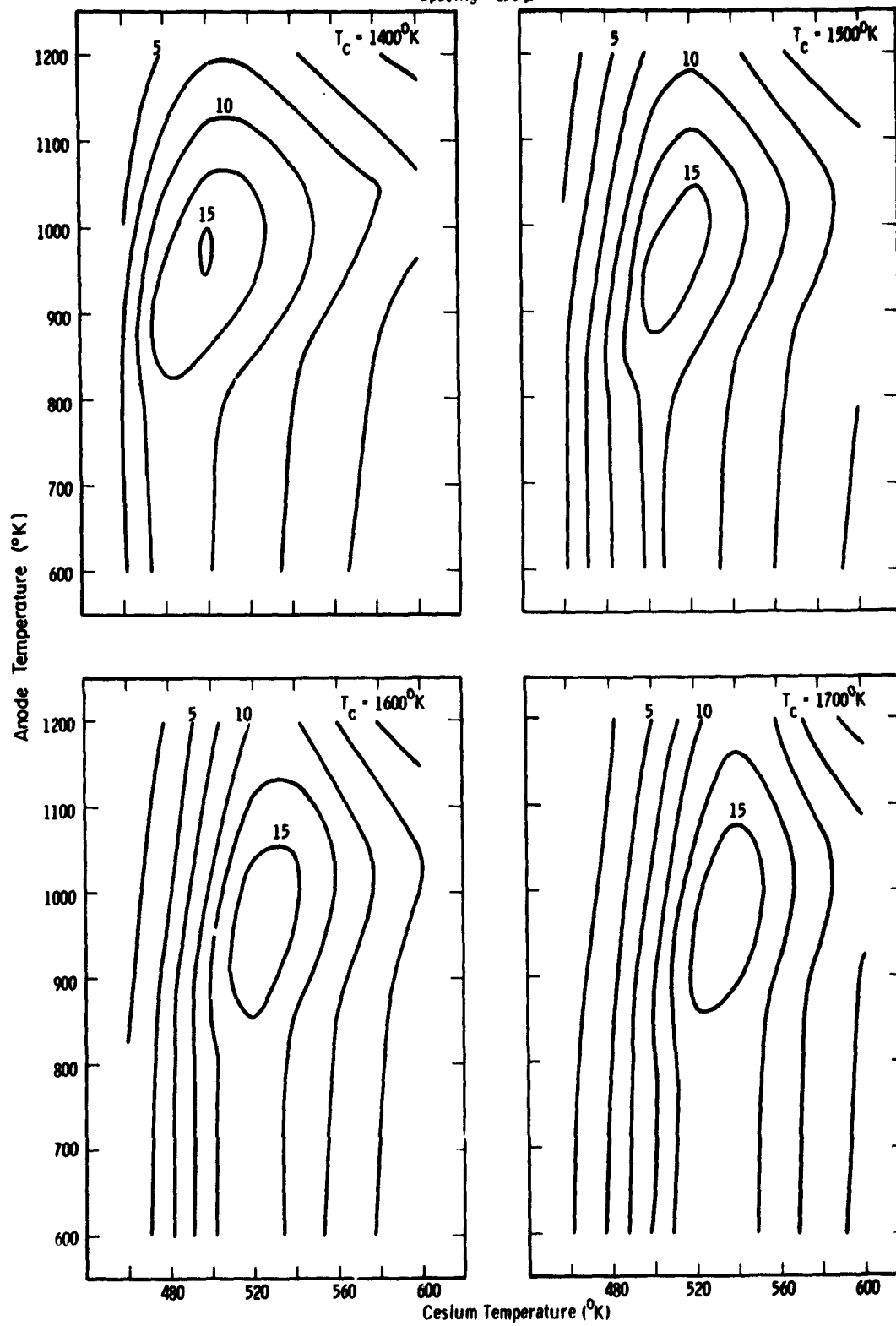
Spacing = 250 μ 

Fig. 12m

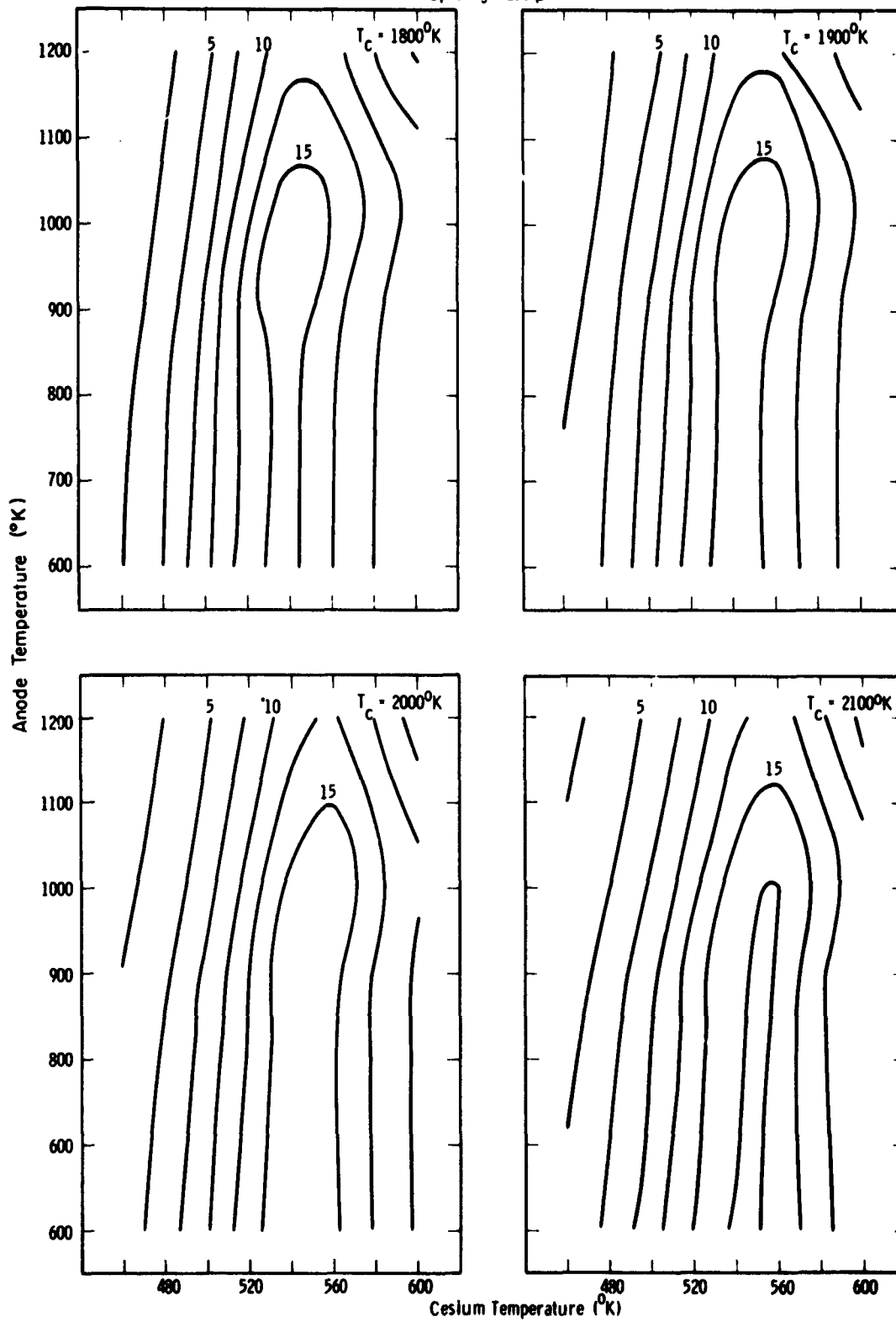
Spacing = 250 μ 

Fig. 12n

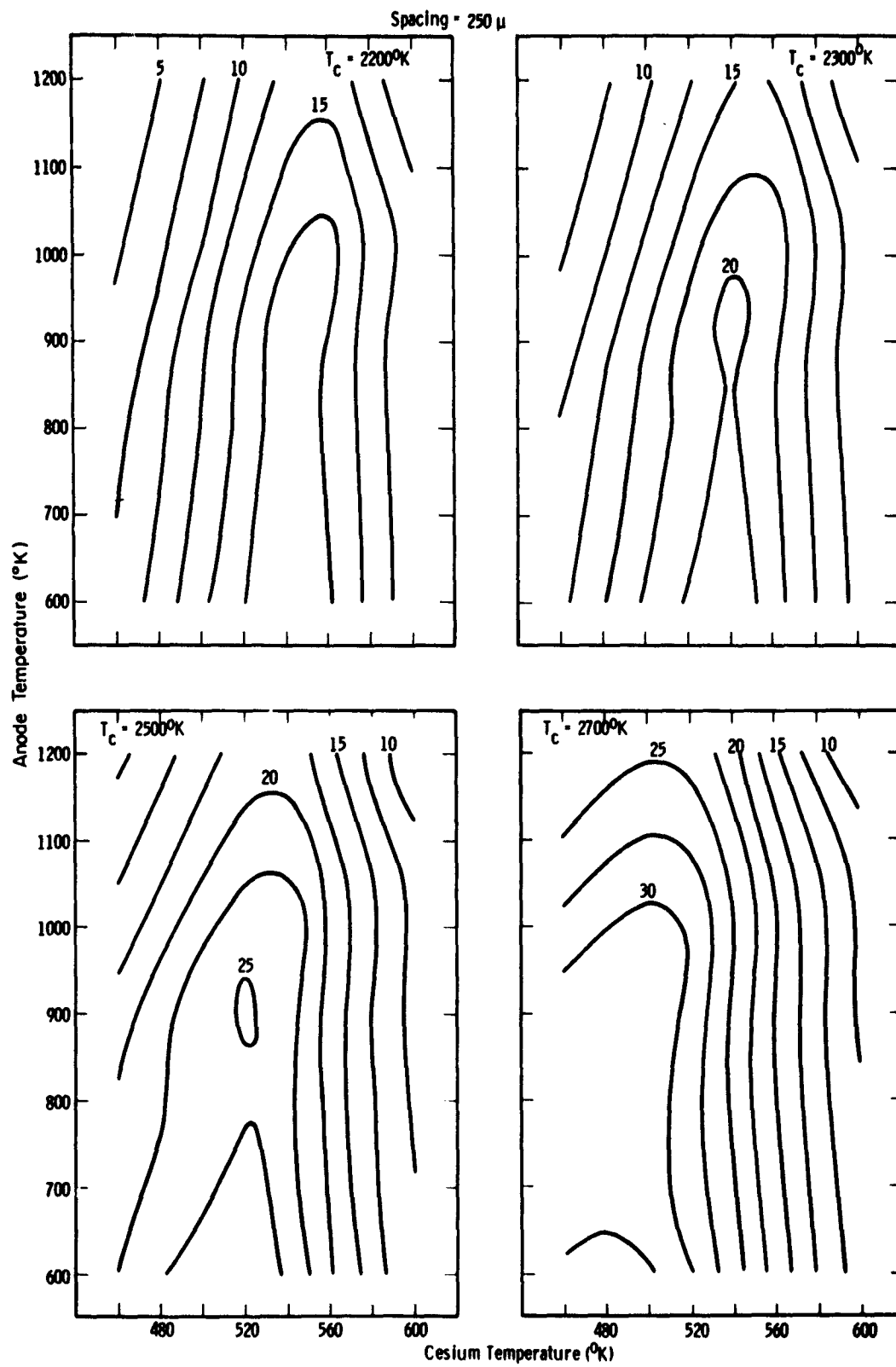


Fig. 12o

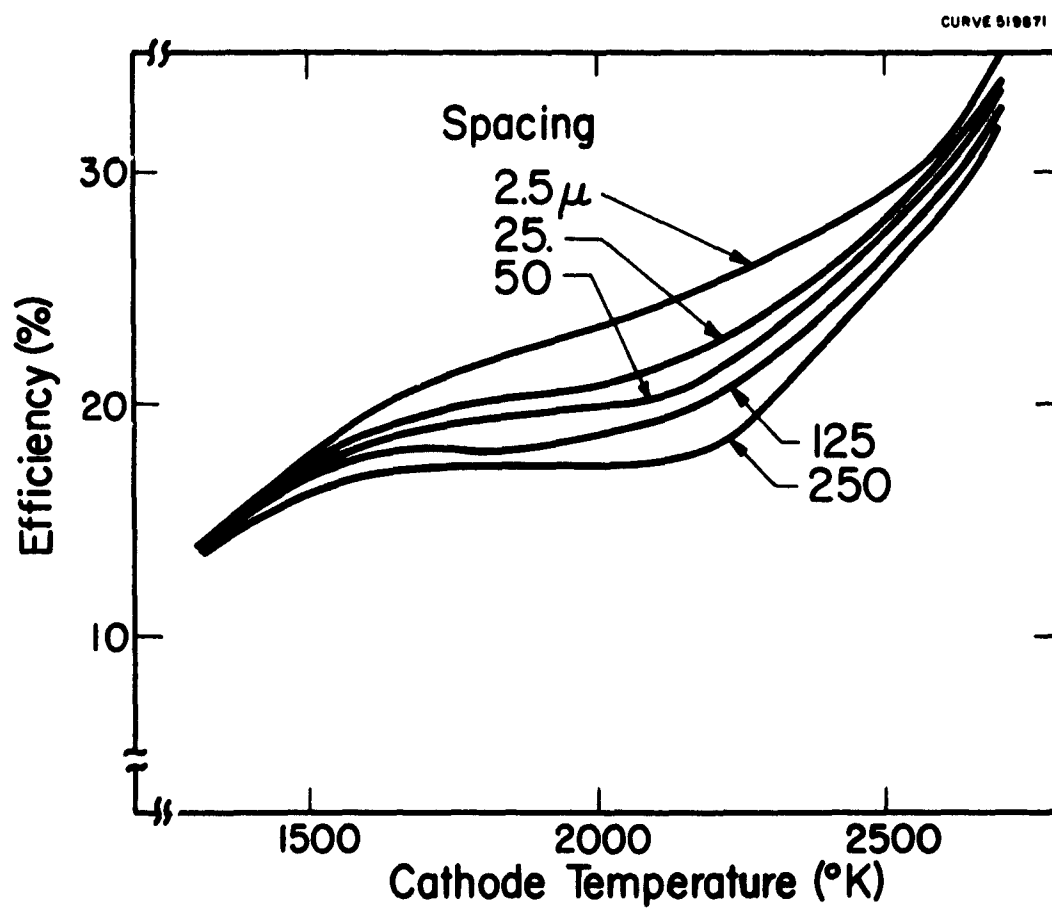


Fig. 13

Optimum efficiency as a function of cathode temperature

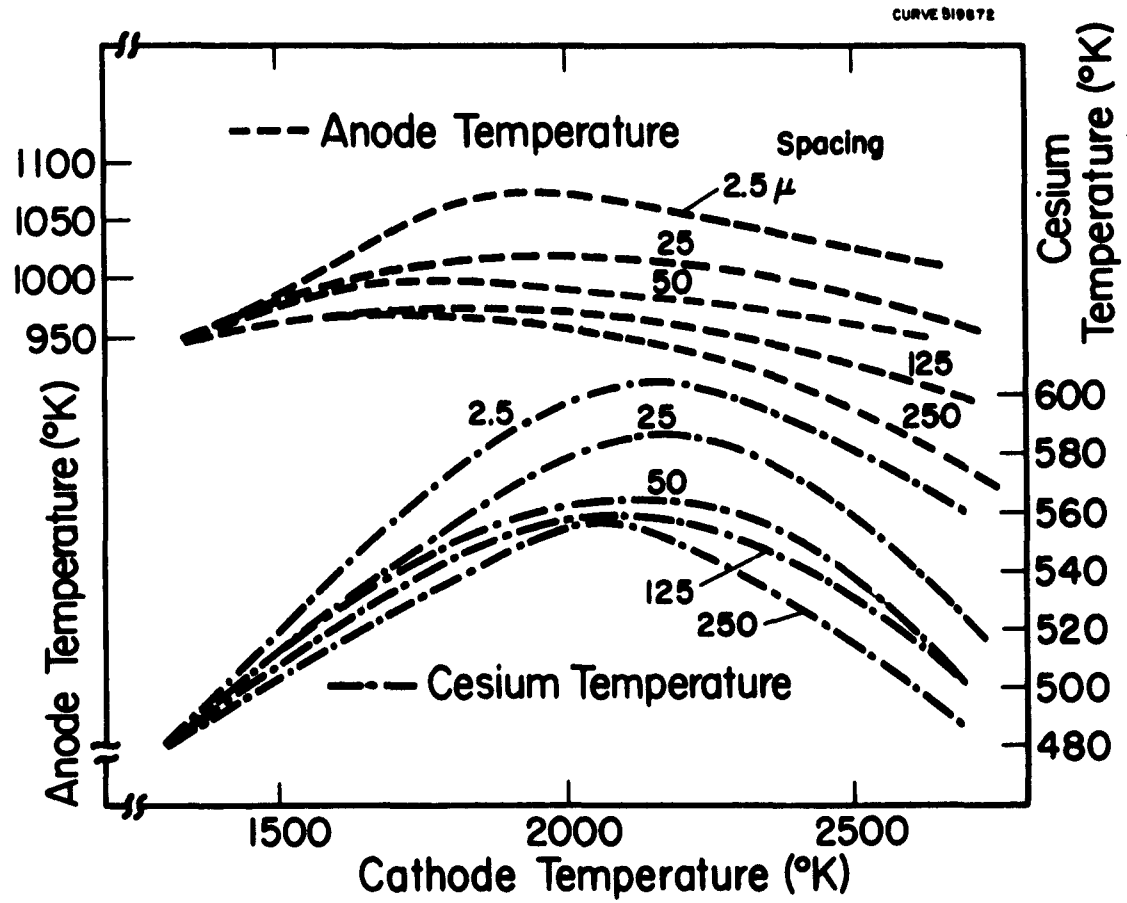


Fig. 14

Optimum anode and cesium temperatures as a function of cathode temperature